CHAPTER 6
TOPOGRAPHIC SURVEYING

1. INTRODUCTION

From the hydrographic point of view a Topographic Survey consists of a series of tasks carried out with the aim of determining the composition of those parts of the earth's surface which emerge from the water. It includes the coastal relief and the location of permanent natural or artificial objects and features.

Such information is partly obtained by determining the position of points on the ground, which allows their shape as well as details of the features to be depicted, enabling their location and description to be charted. Other sources of data include remote sensing processes from aerial photogrammetric information, other airborne sensors or satellite imagery products. In these cases it is necessary to create ground control points in order to adjust the information to the reference frame in use.

The term topography often has other applications, for example in oceanography it is used to depict seafloor surfaces or the boundaries of certain water mass characteristics. All these meanings share a common external description of surfaces covering a physical body.

This chapter deals with the methods applicable to the description of coastal features as part of hydrographic surveys, particularly with regards to the appearance of the ground and the location of detail. It includes coastlining and location fixes, generally related to the high water line for marine surveys, the information on these areas ranges from this line to the low water line, as well as conspicuous coastal features which allow the mariner to position himself relative to near shore dangers.

Except in harbours or coastal areas, where operations or projects are planned or expected to be undertaken, it is necessary to make detailed observations of coastal formations by topographic survey methods.

In some cases, much of the topographic surveying may be undertaken via photogrammetric processes. In these surveys, control is achieved by positioning details on the ground which may be identified in images. Additionally it is necessary to add information which may provide a proper interpretation of the structure of coastal features.

In coastal topographic surveys it is also essential to locate all aids to navigation within the surveying area; if required, the horizontal and vertical geodetic control network should be made denser. In all these cases, it is essential that the reference system for the topographic survey co-ordinates, the geodetic control and aids to navigation (reference stations, lights, beacons, etc.) is consistent with the reference system used for the rest of the hydrographic survey. This precaution is fundamental for the mariner, who positions himself with the use of the aids to navigation and other coastal details, to be able to rely on the charted depths at every fix.

This chapter will deal first with the methods applied to land surveying, then it will deal with remote sensing ranging from photogrammetric processes to satellite imagery.

Except for the restatement of some basic principles, which are deemed essential, it is assumed the reader has previously examined Chapter 2 (Positioning) where subjects related to co-ordinates on the spheroid and the plane, horizontal/vertical control methods and positioning equipment and methods are covered in more depth.

2. TOPOGRAPHY, COASTLINE DELINEATION AND AIDS TO NAVIGATION POSITIONING

2.1 Specifications

2.1.1 All tasks shall assume, as a minimum, the specifications stated in publication S-44 (IHO Standards for Hydrographic Surveying), particularly those relating to Chapter 2.

2.1.2 In S-44 Table 1, errors with regard to positions for other important details and coastal features are expected to be below the following limits:

TABLE 6.1 (TABLE 1 IN S-44)

	SPECIAL ORDER	ORDERS 1a and 1b	ORDER 2
Positioning of fixed aids to navigation and topography significant to navigation. (95% Confidence level)	2 m	2 m	5 m
Positioning of the coastline and topography less significant to navigation. (95% Confidence level)	10 m	20 m	20 m
Mean position of floating aids to navigation. (95% Confidence level)	10 m	10 m	20 m

2.1.3 Thorough checks must be conducted to confirm that the reference system used to show all the control point co-ordinates is the same. Verification should include an analysis of records and whenever doubts arise, field checking should be included.

2.1.4 To check positioning accuracies, a strict routine for cross checking between physically obtained control point details and the supplied co-ordinates should be instituted. This will avoid the situation of co-ordinates from measured closed circuits returning to the same control point being exclusively used; instead, other ways of ensuring the expected consistency should be included. Therefore, at least one connection that ensures the transfer of co-ordinates from one control point to another should be included in the applied measurements.

2.1.5 When satellite services (GNSS) are used for altimetric purposes, it should be ensured that, besides the accuracy of the process being undertaken, corrections between heights above the reference spheroid used and the mean sea level are sufficiently accurate to meet the requirements of S-44. The main purpose of this precaution is to meet the requirements directly associated with sea levels, water intakes or artificial outlets, surveying for coastal projects, ground control for photogrammetry, harbour surveys, etc.

Exceptions to these requirements are surveys intended to show the coastline from the sea, the sea-level positioning for conspicuous objects or the heighting of lights, signals and beacons where errors up ± 0.3 m are allowed for groups of signals (leading lines) and up to ± 0.5 m for an isolated signal or object. In the case of ground control points intended to define the coastline shape, the error tolerance can be ± 0.5 m for Special Order and ± 1 m for Orders 1 or 2, when the ground slope is below 10%. On steeper slopes error tolerance can be up to ± 1 m ±·0.8 iH, where **H** is the horizontal error, which is shown in Table 6.1 and **i** is the slope (elevation angle tangent).

2.1.6 The principle methods of coastlining are:

a. Real Time Kinematic with GNSS (RTK trough GPS, etc.);
b. Resection fixes (EDOM, sextant, theodolite, etc.);
c. Traverses (EODM, Total Stations, level and tachstaff, tachymetry or sextant and 10' pole)*;
d. Intersection (EODM, theodolite or sextant);
e. Air photography;
f. Existing maps.

(*) *In traverses with sextant and 10' pole, the horizontal angles are measured by sextant (see 5.3.1 at Chapter 2) as well as the distances with a special rod, where an angle is converted into a distance (parallactic method, through the measure between two separate marks of a known distance apart).*

2.1.7 The methods used will depend upon the scale of the survey, the time and the equipment available; i.e. existing maps, where small details can be shown, could well be used for scales of 1:50000 or smaller (1:100000). Similarly air photography can be used, but it is likely that such images will be reduced and interpreted as necessary at the National Hydrographic Office (NHO).

Photogrammetric restitution is also a suitable method (derived from aerial information), but it is advisable to complement this process with ground data collected during the field reconnaissance.

2.2 Positioning methods and Accuracies

2.2.1 GNSS (See 6.1 at Chapter 2)

Methods using single navigation systems are only applicable for cases for which, as shown in Table 6.1, errors of ± 20 m are acceptable. Using particular caution, including an experimental calculation for corrections to points known before and after surveying for periods over 2 hours between sunrise and sunset, it could be applied to cases which, according to the Table above, require ± 10 m accuracies as long as the calculation of such corrections are consistent with the given limits.

Methods using the observable codes in differential mode (DGPS, etc.) with reference stations at geodetic control points may be used for cases requiring ± 5 m for the highest accuracies. In cases with more accurate requirements (i.e. ± 2 m Table 6.1), the processes used should be phase measurement of carrier waves L_1, L_1/L_2, etc.

In these cases, the following possible vector errors should be considered:

TABLE 6.2		
VECTOR LENGTH	L_1	L_1/L_2
Up to 10 Km	± 1 cm ± 1 ppm	± 1 cm ± 1 ppm
10 to 40 Km	± 1 cm ± 2 ppm	
40 to 200 Km	NOT APPLICABLE	
Above 200 Km		± 2 cm ± 2 ppm (*)

(*) *With suitable time periods, special equipment and software, errors may be below ± 1 cm ± 1 ppm.*

Regarding Table 6.2, it should be noted that upon the expected GNSS development from 2005, consideration should be given for updating to allow provision for the additional band L5 and the full operational reception compatible of GPS, GLONASS and GALILEO.

Likewise, the increasing potential of operating using real-time kinematic (RTK) mode suggests that its use may exceed present surveying capabilities and its use for some ground control positioning may be expected. For the present (2004), such techniques may be considered to have errors of ± 5 cm ±5 ppm.

Moreover, within GNSS development, not withstanding the above, new differential services, in addition to those already existing, are planned to come into operation:

- Ground - Based Augmentation Systems (GBASs) with transmissions from earth stations near airports as well as other intensively used sites;

- Satellite - Based Augmentation Systems (SBASs) with satellites receiving differential correction signals from different stations and then transmitting adjusted corrections. One of the most complete networks scheduled to become fully operational by 2005 is the so-called WAAS (Wide Area Augmentation System) sponsored by USFAA (US Federal Aviation Association).

Some of these services are operating with different characteristics, though they are expected to increase in number and introduce greater capabilities. This exploitation has generated the possibility of conducting more surveys without the need of establishing reference stations. Nevertheless, it is not advisable to be over optimistic with its application if there is no relatively near earth station contributing to the system. Another method is to implement active station networks, the reception of which is centralized and transmits precise ephemeris calculations which are applicable to a particular region.

Returning to coded differential equipment with base stations operating on control points, there are some which, by means of a so-called "sub-metric" treatment, may achieve errors in the order of 10 cm ± 10 ppm without strictly using the L phase of carriers and allow base-rover distances as much as 10 Km.

There is a wide variety of equipment on offer but very few fulfil such error limits. It is, therefore, advisable to check the procedures with a test by stationing them at several distances on the existing control points in order to obtain a reliable assessment.

For the remainder of this chapter, it is assumed that the equipment in use is measuring the phases of carrier wave(s) (L1 or L1/2) within the limitations stated in Table 2 and RTK mode error (± 5 cm ± 5 ppm) as mentioned.

Ideally, to carry out a topographic survey, all the points should be surveyed from base stations with control marks. Wherever existing control points are not sufficient it should be expedient to increase the density of them. Fig. 1 illustrates such a plan, i.e. from existing network marks, new control points are generated by GNSS vectors using geodetic receivers in a static relative mode. To make corrections to geodetic heights (above the spheroid), in order to obtain heights above mean sea level or others associated with it (see Chapter 2), it is necessary to tie in altimetric control points.

It is desirable that photogrammetric ground control points and aid to navigation signals are calculated, as a minimum, from two control points. Faster methods such as stop and go or real-time kinematic (RTK) modes may be applied both to these types of control points and to surveyed ground features, as long as they meet the requirements in Table 6.1.

If, while surveying, the need arises for the generation of additional control points, they should be obtained from two previously determined control points.

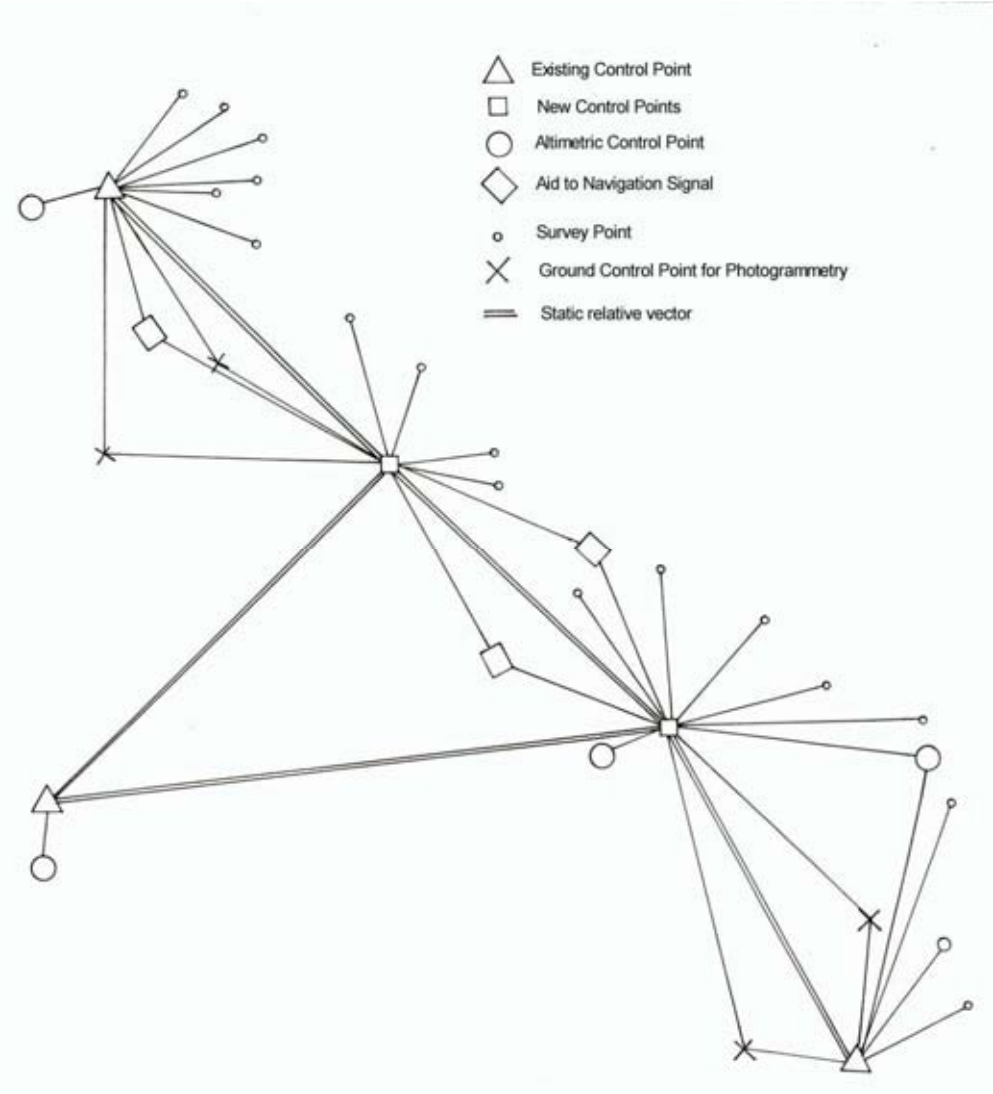

Fig. 6.1

The ease of creating new control points as well as the cost of building and preserving bench marks, or other marks, is setting the trend for minimum monumentation. In such cases, illustrations such as Fig. 6.2 may be chosen.

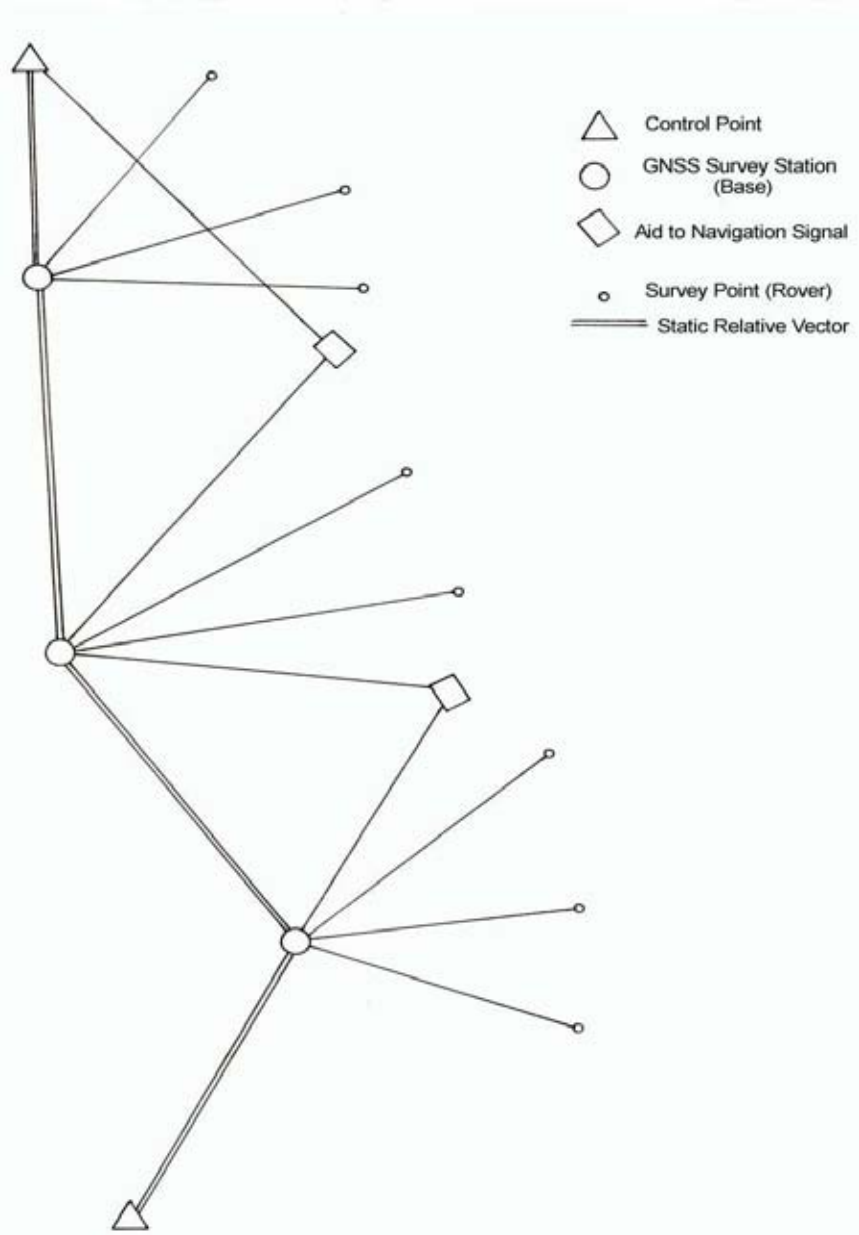

Fig. 6.2

Besides serving as a base for rover receiver reference, GNSS survey stations are connected to each other by static relative vector measurements thus forming, as a minimum, a traverse between control points without generating additional monumentation. In most cases, these traverses will have been measured with the same instruments as used to survey ground features.

2.2.2 Triangulation (See 3.2.1 at Chapter 2)

It is a technique based on principal angular measurements. Before the middle of the 20th century, it was the most common method for establishing geodetic control networks and for sole calculation of conspicuous points, marks and other aids to navigation or photogrammetric ground control points. Since the 1960s Electronic Distance Measuring equipment (EDM) or Electro Optical Distance Measurement (EODM) has superseded the above methods. More recently they have been replaced by satellite methods, particularly since a permanent global coverage was established in the 1990´s

The earliest form of triangulation for hydrographic purposes consisted of a series of observations as in Fig. 6.3, with a relatively small number of measured sides (baselines) and a large number of angular measurements, which are showed here with the observed directions. Such a diagram provides a great deal of redundancy; each double-diagonal quadrilateral has three angular verifications created by adding or subtracting values. Nevertheless the network scale is still determined by the baselines.

In old unconnected geodetic controls, position and orientation were established from astronomic observations of latitude, longitude and azimuth in a datum. Now days, if marks are use from these kinds of networks, it is usually necessary to re-observe and recalculate via GNSS in order to convert co-ordinates into a universal system like WGS 84 (see 2.2.3 at Chapter 2).

In general it should be noted that distances from the baselines could be measured within accuracies ranging from 1ppm to 3ppm, directions from ± 0.5" to ± 2", and transition from a base to another (that is, the contrast between the base transfer by triangle resolution and the other measured base) could normally be checked within 20 ppm and 40 ppm.

These limitations should be taken into account when trying to adjust an old triangulation network to a present framework via GNSS observations, with distances of 200 or 300 km there can be differences of several meters (2 or 3). Besides tolerating differences of these orders, it is necessary to have a sufficient number of well-distributed connections to common datums and of datum conversion algorithms in order to absorb the distortions typical of the old networks (see Chapter 2)

Not withstanding the above statement, densification by GNSS of datums with fixed co-ordinates computed from old triangulations should be avoided; such cases often lead to distortions and inaccuracies in the final results. If unavoidable due to the need to keep the co-ordinates of an old datum, it will be necessary to adopt very particular computation strategies and the limitations of the values obtained must be stated at an early stage.

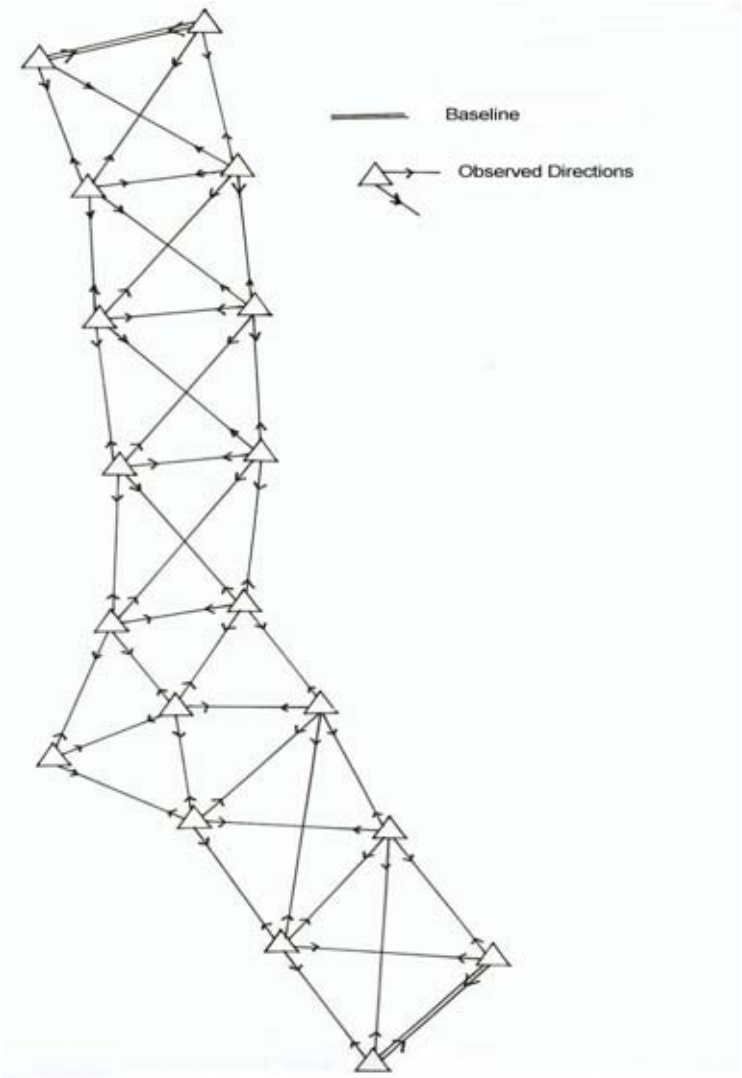

Fig. 6.3

A control network with the characteristics as in Fig. 6.3 had, in general, sides with lengths ranging from 15 to 25 km, 18 km on average, with triangle closure errors from ± 1" to ± 2"; this was termed first-order triangulation. The following densifications had shorter sides (10 to 15 km) with closure errors from ± 2" to ± 4"; they were designated second-order triangulation. There were also third-order and fourth-order triangulations with shorter sides and higher tolerances, ± 5", for third-order triangulation, and ± 10", for fourth-order triangulation. Table 6.3 details typical values and aspects of these orders.

Table 6.3

TRIANGULATION MEASURES CHARACTERISICS					
ORDER	SIDES LENGHTS (Km)	TYPICAL THEODOLITE DIRECT READING ERROR (“) (*)	TYPICAL NUMBER OF REITERATIONS (*)	TYPICAL DIRECTION ERROR (“)	TRIANGLE CLOUSURE ERROR TOLERANCE (“)
1st.	15 to 25	0.1 to 0.2	9 to 18	0.1 to 0.5	1 to 2
2nd.	10 to 15	1”	6 to 9	1 to 2	2 to 4
3rd.	5 to 10	1” to 10”	4 to 6	2 to 3	5
4th	2 to 10	10”	2 to 4	5	10

(*) *See 5.3.2 at Chapter 2*

For each order of work, the co-ordinates of the higher orders were taken as fixed co-ordinates and generally the baselines and astronomical stations were exclusively for the highest two orders.

In lower order work, it was normal to select a few higher order points at a time, as in Fig. 6.4 left; though in some cases for control densification networks selection of a larger number of points with shorter side observations (Fig. 6.4, right) was carried out, particularly whenever triangulation towers had been removed. These towers were used to elevate the line of sight over trees, topographic features and other obstacles interfering with the observations. Obviously their removal prevented long sights from being conducted which led to this type of solution.

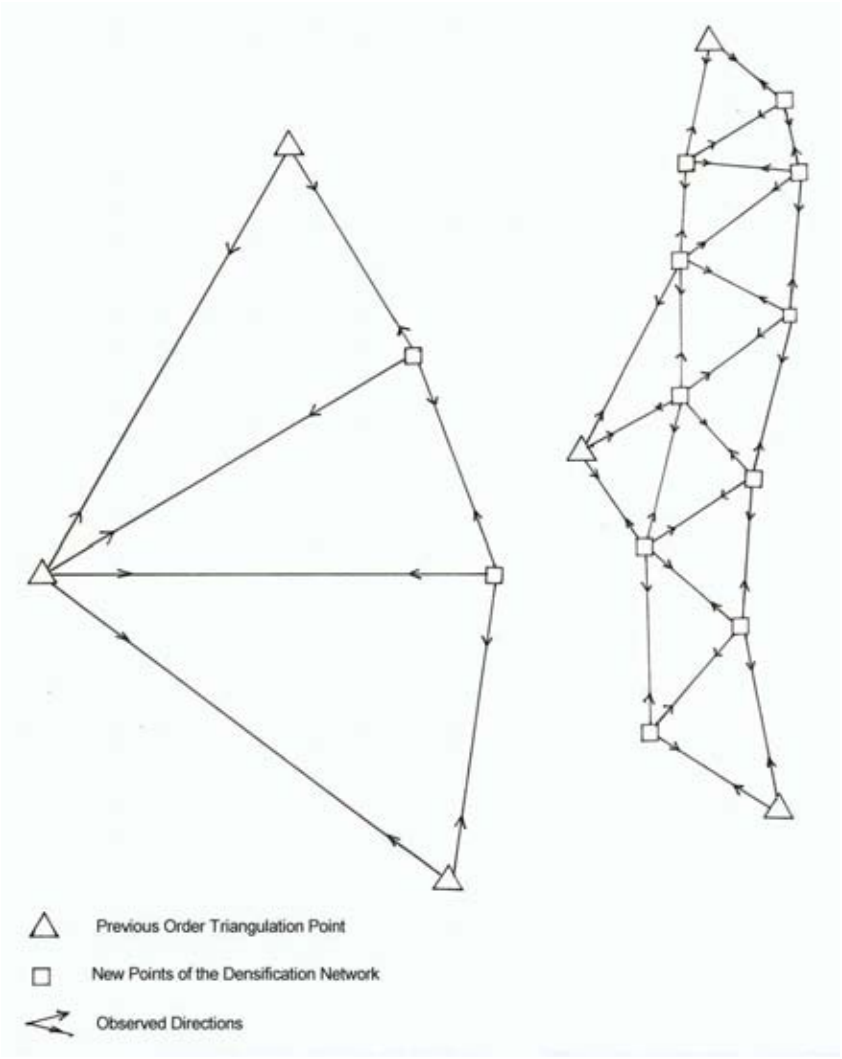

Fig. 6.4

In some cases, in hydrographic surveying, the term *triangulation* has been used to describe survey points with flare triangulation by intersection (see 2.2.4). These flares were dropped with parachutes vertically over the point to be located and, whilst burning, directions from control points would be simultaneously observed; this was conducted towards many coastal points requiring to be surveyed, as many were not visible. Balloons, luminous shots or mobile, elevated signals were also used for the same purposes.

The term triangulation has also been used when measuring angles to control points with a sextant, sometimes in combination with observations from such points. The exclusive use of observations from points to be calculated is treated as a resection in 2.2.4.

Although these survey techniques are becoming obsolete due to intensive use of other more responsive modern methods, they still are effective.

One of the typical problems of triangulation is the error propagation dependence on the figure shapes, on which the error results (positions) rely not only on the measurement error but also on the network geometry. This problem is dealt with for particular cases in 2.2.4 though it admits more complex generalisations. For example, a single chain of equilateral triangles is more rigid than a chain with unequal angles. Also, a two-diagonal square chain is more rigid than a chain with rectangles or trapeziums with similar diagonals.

2.2.3 Traverse (See 3.3.1 to 3.3.4 at Chapter 2)

Before the 1950-1960 decade, use of combined distances and directions was restricted to small areas but later, with the development of EDM and EODM equipment, larger networks with longer sides (5, 10, 15, 20, ... km) could be created. As stated at the beginning of 2.2.2, these techniques superseded triangulation.

For some time (about 1960) a new technique based on exclusive side measurement (trilateration) (See 3.2.2 at Chapter 2) was considered but it was quickly rejected, mainly due to a lack of internal checks. To clarify this concept, a single triangle has an angle closure condition while a trilateral of the same shape has no way of being checked; a quadrilateral with two diagonals and all its directions measured, as stated in 2.2.2, has four closure conditions whilst the same trilateration geometrical figure with its 6 sides measured has only one verification. This advantage with triangulation is limited since the method requires some sides being measured (baseline); however, trilateration can be conducted without observing any angles.

A combination of both techniques resulted in a suitable solution, although sometimes termed triangulateration, here it will be termed traverse, although often a traverse may be a simple succession of measured angles and distances.

One of the most important properties of traverses is that error propagation is independent from configuration; that is there is no requirement for complex network design involving suitable geometries or erecting towers to facilitate certain lines of sight. From the practical point of view with this kind of network, uniformity of control points with survey stations or aid to navigation requirements was possible.

In general, it is advisable to maintain a reasonable balance between the accuracies of both types of measurements (directions and distances) in order to improve the geometry independence in relation to the accuracy of results. One of the applicable rules is

$$\frac{\sigma DIST}{DIST} = \frac{\sigma ANG}{200000}$$

where $\sigma DIST$ is the distance standard deviation stated in the same unit as **DIST**, and σANG is the standard deviation of a measured direction stated in sexagesimal seconds. Then, for $\sigma ANG = \pm 1"$ the distances required are 5 ppm (1/200000) and for ± 4", 25 ppm (1/40000) is enough.

The required angular or distance errors must never be confused with the instrument reading or resolution capabilities. The observer limitations, the environmental conditions, the correction accuracies, the time when measurement were made, etc., must also be considered.

For example, for an inclined distance measurement with an angle of elevation of 20º and 5 km in length, with an elevation difference error of ± 0.5 m, the error in its horizontal projection is expected to be

$$0.5 \text{ m} \tan 20° = 0.18 \text{ m}$$

Thus, in spite of being measured with EODM equipment, whose error may be in the order of ± 1 cm ± 2 ppm, and with the inclined distance error of ± 2 cm, if used for transferring a horizontal position, the error is ± 18 cm.

A distance measured with EDM equipment must be corrected for environmental conditions (pressure, temperature, humidity).

Humidity is calculated according to pressure and temperature with dry and wet bulb observations, it is very important for measurements taken by microwaves. No measurement should be taken with EDM in an oversaturated atmosphere (rain, drizzle, fog); with EODM measurements humidity is not so important, although the luminous wavelength used should be considered. LASER radiations have an advantage since they are basically monochromatic, it is generally sufficient to obtain pressure and temperature data. For long distances (more than 5 km) it is recommended that the environmental parameters at both ends of the distances to be measured are obtained and then averaged.

Manufacturers usually provide the instructions for making the necessary corrections to their equipment. In EODM, the reflector prisms should be used with the equipment with which a calibration was conducted to avoid errors in measured distances, sometimes above 1 cm.

In distances above 5 km corrections for earth and ray curvature must be made. Such correction is:

$$+\frac{(1-k)^2}{24R^2} D^3$$

Where **k** is the refraction coefficient (rate between earth and ray radius). In mean conditions it is 0.25 for microwaves and 0.13 for luminous waves. It is sufficient to introduce its approximate mean value as earth radius.

$$R = 6371000\text{m}$$

Figure 6.5 illustrates **D** (measured distance) and **S** (reduced distance to reference surface) meanings. This is necessary for the above correction and the correction for point elevations, which is detailed below.

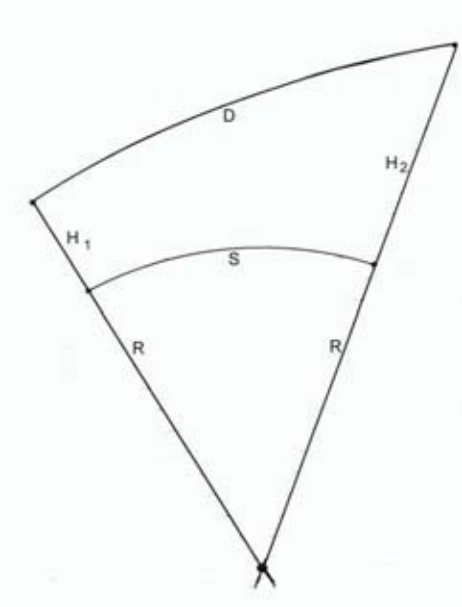

Fig. 6.5

It is important to note that the above correction for curvatures takes into account the geometric effect of both arcs as well as the physical influence produced as a consequence of ray propagation at a slightly lower level than that for mean environmental conditions at both ends.

Correction for ray elevation and inclination is more significant. The general expression is:

$$S = \sqrt{\frac{D^2 - (H_2 - H_1)^2}{(1 + \frac{H_1}{R})(1 + \frac{H_2}{R})}}$$

The way in which such elevations are obtained, especially their difference ΔH = (H2 - H1), affect the correction error. By simply considering the numerator:

$$S \approx \sqrt{D^2 - \Delta H^2}$$

we can deduce the influence:

$$dS \approx \frac{\Delta h}{\sqrt{D^2 - \Delta H^2}}\, d\Delta h = i d\Delta H$$

previously mentioned. Therefore, the elevation difference error must be multiplied by the slope, **i = tan α**, in order to obtain the influence produced on the corrected distance error.

In topographic surveys it is usual to make calculations in plane co-ordinates; for this purpose it is necessary to have previously applied corrections to the projection plane. The way in which this type of corrections may be calculated is detailed in 2.2.5.

The general and most correct way of calculating a traverse network on the representation plane is via a previous calculation of the co-ordinates for every new point commencing with the values of the known points and the uncorrected observations. It is necessary to average some results taken from different points starting with the additional redundant observations. When the provisional co-ordinates have been accepted, the above corrections should be applied and then observation equations are to be obtained, the unknown quantities of which are the corrections to the co-ordinates, in order to conduct a least squares adjustment.

If any observation exceeds tolerance levels (maximum admissible error) the original records should be checked, if no apparent cause is found regarding the error source re-measurement should be considered. If there is sufficient redundancy, the erroneous observation may be removed and a new adjustment conducted.

In some basic traverse circuits an approximate adjustment may be achieved by distributing the angle closure error first and then the co-ordinate closure error proportional to side length or some other logical criteria.

Angle closure errors in traverses must be below:

$$\pm\left(5''+2''\sqrt{n}\right)$$

where **n** is the number of angular stations making up the circuit. In secondary traverses, intended to increase the density of the control points, the error may extend to:

$$\pm\left(10''+10''\sqrt{n}\right)$$

When the purpose is limited to fixing co-ordinates of coastal details, larger tolerances may be permitted.

Co-ordinates closure errors should be no more than the values stated in Table 1 depending on the use of the network, noting that adjusted co-ordinates for intermediate points will have errors in the order of half the closure error. Nevertheless, for control networks, closure errors should not be greater then ±(0.2 m + 10 ppm) for primary horizontal control and ±(0.5 m + 100ppm) for secondary stations to meet the requirements in 2.1.2.

When errors are greater than a traverse tolerance, there are methods available to assist in locating the error source. For example, when an angle closure error is detected the grid bearing of the suspect side is calculated from all components of the co-ordinate closure error. However, if there is a large angle error, the angles should not be adjusted, on calculating the traverse in both directions, only at the affected point will the co-ordinate values roughly match.

When a network is accurately adjusted by least squares from provisional co-ordinates, the process enables, from the variance-covariance matrix, the calculation of adjusted co-ordinate errors. A similar calculation in a traverse may not be so clear since co-ordinate closure errors are more general. In such cases, the mid points may be permitted to have an error in the order of half the closure error, decreasing towards each end.

Traverse calculations in plane co-ordinates are very simple. The initial grid bearing is obtained from increases in **ΔE**, **ΔN**. Two control points whose co-ordinates are known in advance are represented as **P** and **Q** in Fig. 6. Then:

$$\operatorname{tg} B_{PQ} = \frac{E_Q - E_P}{N_Q - N_P} = \frac{\Delta E_{PQ}}{\Delta N_{PQ}}$$

where ΔE_{PQ} and ΔN_{PQ} signs (+/-) also define the quadrant.

If true azimuth referred to true north, rather than grid north as the referred available orientation, with grid declination γ (the definition of which is given in Annex A), this be should be taken into account. From this point forward only plane orientations (grid bearing) will be considered. Moreover, if a Transverse Mercator projection is used, it is assumed that corrections to observations (distances and directions) for the plane of representation have been made according to specifications in 2.2.5.

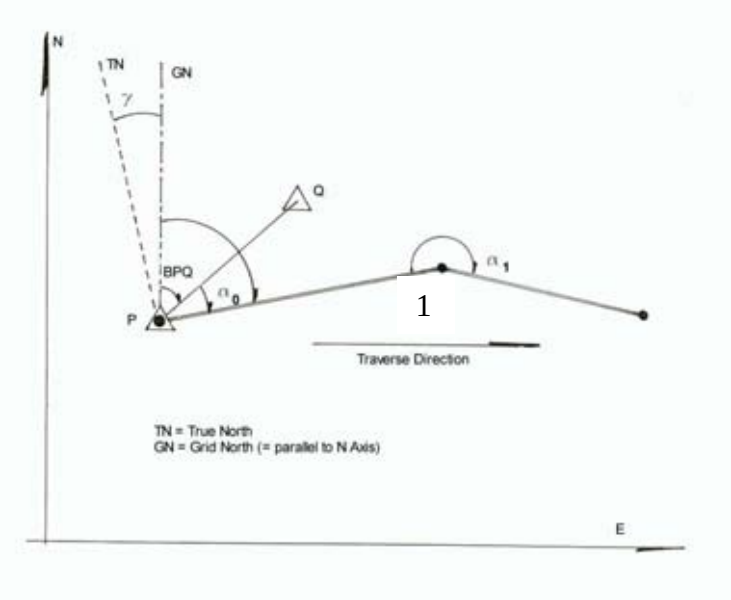

Fig. 6.6

Returning to computing a traverse, the grid azimuth of the first side is obtained by simply adding the first angle:

$$B_{P1} = B_{PQ} + \alpha_0$$

$$B_{12} = B_{P1} + \alpha_1 \pm 180°$$

And using the following general form of bearing transfer:
The sign + is used in case the previous addition ($B_{P1} + \alpha_1$) is below 180º and the sign - when it is above. The latter is the most common case.

Increases in co-ordinates are obtained with the expressions for converting polar co-ordinates into plane co-ordinates:

$$\Delta N = S \cos B$$
$$\Delta E = S \sin B$$

It should be remembered that, in the cases of simple traverses, before making such conversions, it is normal to adjust an angle by distributing the closure error if it is below the given tolerance level. In more complex traverses, network calculations may be supplemented with the algorithms related to intersections or resections according to descriptions in 2.2.4 and 2.2.5. Adjustment requirements mentioned above should also be considered.

As regards adjustments, their respective methods will not be developed further, since such processes are expected to be developed at the NHO where appropriate software is available. It should be remembered, however, that good results may be achieved only if the data is checked in the field to ensure that closure errors or the calculation of point co-ordinates carried out by different methods show an acceptable consistency with the above specifications.

A simple traverse is deemed to be fully closed if it starts from a pair of control points and ends at another pair. There are then three possible closure errors available: one angle closure error and two co-ordinates closure errors. This case is illustrated at the top of Fig. 6.7; it allows an initial angular adjustment and a subsequent distribution of the differences in co-ordinates. There is a special case of a simple closed traverse which makes a circuit, starting and ending at the same point. Even though it may be properly checked as detailed above, it is not advisable to conduct such methods for the reasons set out in 2.1.5

A simple traverse is termed half closed when a direction to another control point has not been measured from the final point; this means that no known angle checking or its corresponding adjustment is permissible. Nevertheless, if co-ordinate closure errors are acceptable, a similar distribution as in the previous case may be carried out as illustrated in the second case of Fig. 6.7.

A simple traverse is deemed to be precariously closed when, although it starts and ends at control points, there is no final measured direction with an orientation. The only check is to confirm that the measured distance between the control points P and R generated from the traverse is fairly consistent with the distance calculated from their known co-ordinates; this illustrated in the third case in Fig. 6.7. The simplest way of calculating the distance is by giving it an arbitrary or approximate orientation for the initial calculation and by then rotating the orientation and adjusting the length according to the differences to the end point.

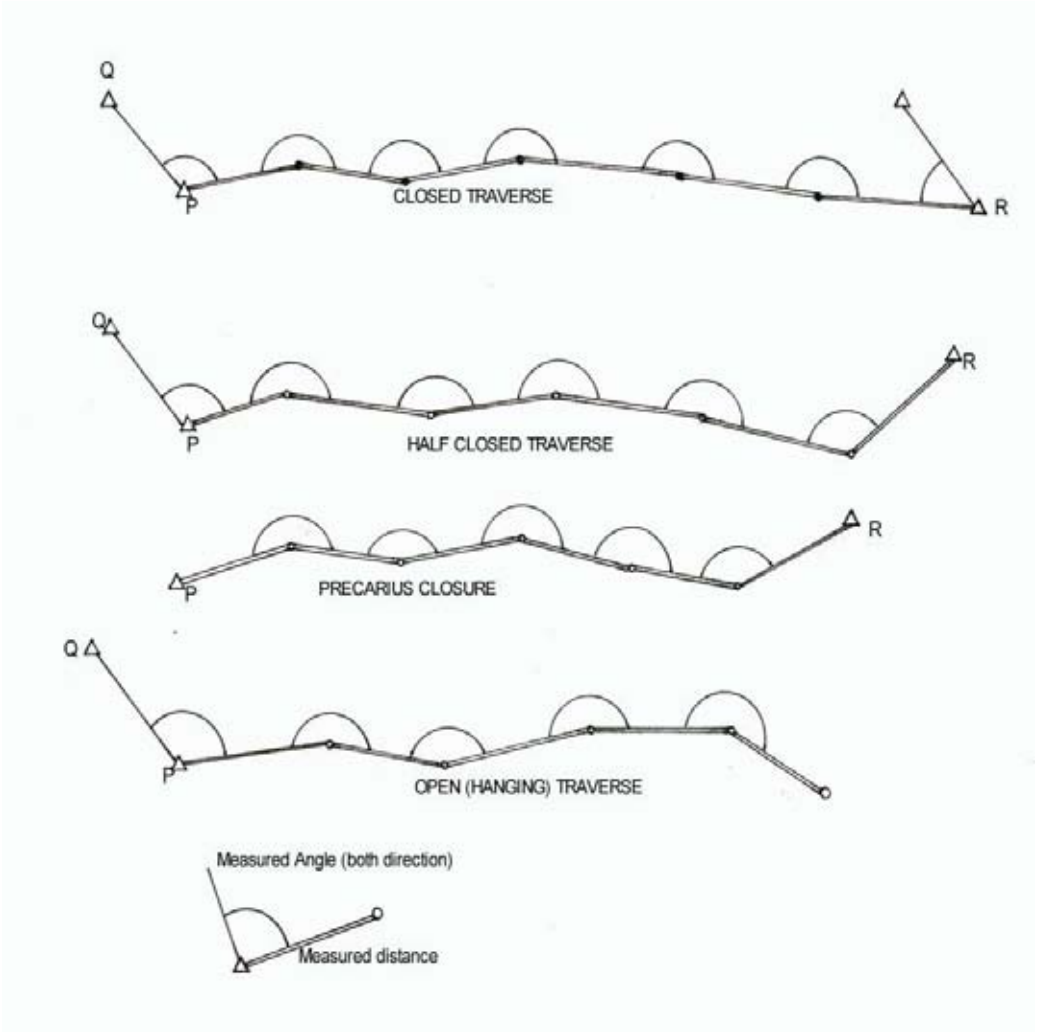

Fig. 6.7

A simple traverse is deemed to be an open, not closed, or hanging traverse only if it starts from known points but ends at new unknown marks, thus no closure verification or adjustment can be made; this is not a recommended configuration. When it is the only choice, extreme caution should be exercised and the temporary nature of subsequent results should be clearly stated.

Traverses are closely associated with trigonometric levelling operations. These consist of a series of measurements taken to determine differences in elevations by vertical angles. (See 4.2 at Chapter 2)

The most precise way of obtaining a trigonometric difference of elevation consists in measuring the direct distance between the points and the vertical angles reciprocally and simultaneously from both stations:

$$\Delta H_{12} = \frac{i_1 + s_1}{2} - \frac{i_2 + s_2}{2} + D \sin\left(\frac{\alpha_1 - \alpha_2}{2}\right)$$

where (see Fig. 6.8):

i_1 = theodolite height above bench mark in point 1;
s_1 = signal (target) height above bench mark in point 2;
i_2, s_2 = theodolite and signal heights above bench mark in point 2;
D = slant and elevated distance (see Fig. 6.5);
ΔH_{12} = difference of elevations between benchmarks 1 and 2.

The elevation angles (α) are positive when they are above the horizon and they are negative when below the horizon. In Fig. 6.8 α_1 is the positive angle and α_2 is the negative angle. It is necessary for both to be simultaneously measured in order for a correct adjustment of ray curvature, which changes throughout the day.

A trigonometric difference of elevation obtained under these conditions may have an error of

$$\pm 0.01 \text{ m} \cdot \text{K}$$

where **K** is the distance expressed in kilometres, which is an error of 1 cm/Km.

If slant distance (**D**) has not been measured and ground distance reduced to the reference level, commonly the mean sea level, is available, which is the case of triangulation or intersection (see Fig. 5), the formula to be applied is:

$$\Delta H_{12} = \frac{i_1 + s_1}{2} - \frac{i_2 + s_2}{2} + S\left(1 + \frac{Hm}{R}\right)\text{tg}\left(\frac{\alpha_1 - \alpha_2}{2}\right)$$

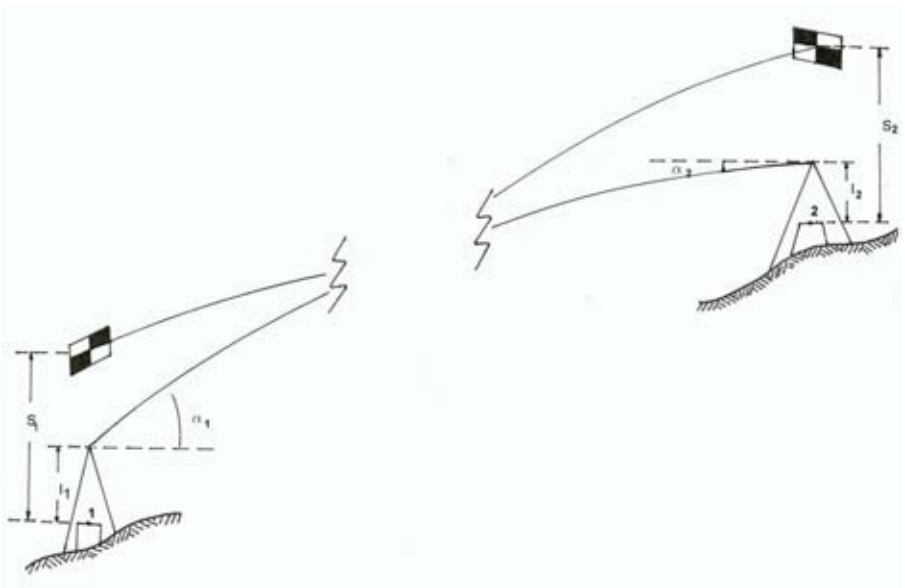

Fig. 6.8

If the elevation angle is known only at point 1, the formulae to be applied are:

$$\Delta H_{12} = i_1 - s_2 + D\sin\alpha_1 + \frac{(1-k)}{2R}D^2$$

$$\Delta H_{12} = i_1 - s_2 + S\left(1+\frac{Hm}{R}\right)tg\alpha_1 + \frac{(1-k)}{2R}S^2$$

In the last three formulae, **R** is the terrestrial mean radius, in principle 6371 Km, but a more correct value relative to latitude and azimuth may be used for the adopted spheroid. The same is valid for the formula above to transfer **D** to **S** (See Fig.6.5)

$$S = \sqrt{\frac{D^2 - \Delta H^2}{\left(1+\frac{H_1}{R}\right)\left(1+\frac{H_2}{R}\right)}}$$

$$Hm = \frac{H_1 + H_2}{2}$$

Hm is the mean elevation

If only $\mathbf{H_1}$ is available, it may be calculated as:

$$H_m = H_1 + \frac{\Delta H_{12}}{2}$$

Where $\mathbf{\Delta H_{12}}$ is obtained by an iterative process which improves the value $\mathbf{H_2}$.

Coefficient **k** has the above stated meaning and it can be considered to have a value of:

$$k = 0.13 \pm 0.05$$

then the error of a non-reciprocal trigonometric difference of elevation may be:

$$\pm (0.01 \text{ m K} + 0.004 \text{ m K}^2)$$

The use of trigonometric levelling is ideal both for reducing the sides due to differences of elevations and height and for other altimetric requirements to overcome possible accuracies.

2.2.4 Intersection and Resection

The most general form of intersection is when directions are observed from two control points into a mark, whose co-ordinates are required. Directions in orientation mean that directions are measured from the same stations to other known points, it then being possible to obtain the grid bearings of both directions. In some very special cases these are astronomic or gyroscopic orientations; in such cases it is required to go from the true azimuth to the grid bearing by applying the grid declination shown as $\boldsymbol{\gamma}$ in Fig. 6.6.

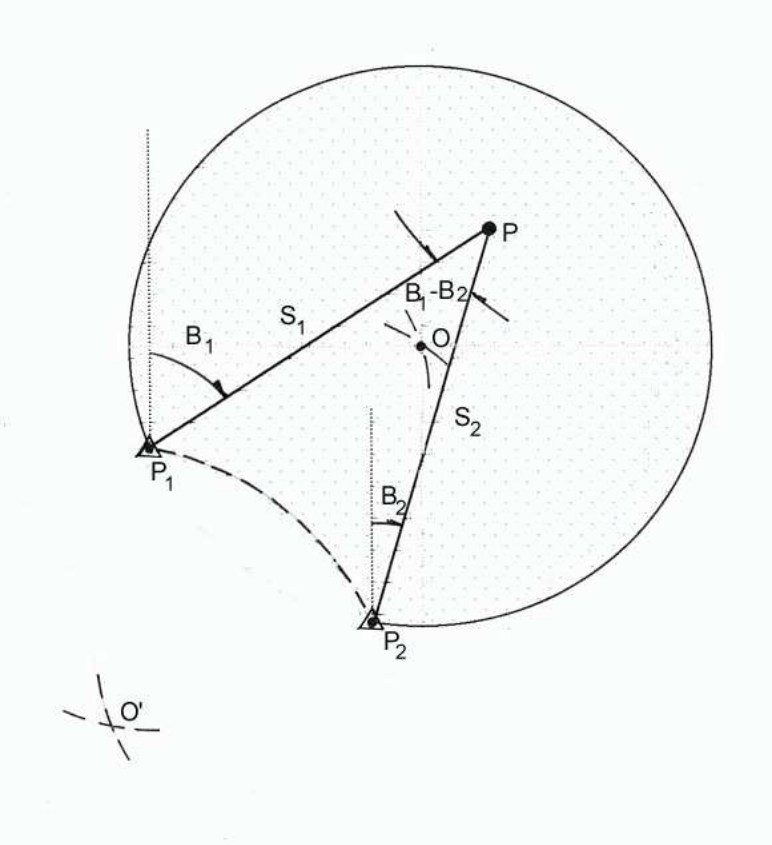

Fig. 6.9

Fig. 6.9 shows a typical intersection example. It should be made clear that in some cases, especially in short distances, reciprocal directions between known points (P_1 - P_2; P_2 - P_1) are used as the origin of plane orientations (B_1; B_2) to the point intended to be determined (P).

Besides grid bearing errors arising mainly from angular errors, distances (P_1 - P ; P_2 - P) and the angle between these directions, which is equal to the difference (B_1 - B_2), contribute to the errors in the co-ordinates of P. The simplest rule is that the angle should range between 30º and 150º. The area for this condition is shaded in Fig. 6.9 and corresponds to the limits of two circles centred at O and O' which are obtained as the vertices of two equilateral triangles with a common side P_1P_2.

Outside this area, errors largely increase to reach indetermination for B_1 - B_2 when equal to O° or 180°.

Another intersection case is shown when distances are measured from P_1 and P_2 to the point to be determined (P). These distances (S_1; S_2) define two symmetrical solutions as regards axis P_1 - P_2. To solve this ambiguity it must be known if P is on the left side of P_1 to P_2 (this is the case in the figure), or on the right side (a symmetrical case). An alternative solution is to note, when seen from P, which is the known point on the right or on the left (in the case of Figure 6.9, P_1, is on the right and P_2 on the left).

Algorithms to make corrections to the plane and obtain the co-ordinates of P, taking into account the cases stated, are shown in 2.2.5.

In cases of intersection, directions (straight lines) or distances (arcs), the best solutions are obtained when the crossing angle (B_1 - B_2) tends to 90°. In these cases the error ellipse tends to be a circle. Strictly speaking, taking into account that errors in measured directions and distances increase their influence with distance and such ideal solutions slightly differ from the 90º rule, its use, however, is a good way to quickly examining the suitability of the set up.

The most common resection case is when three known control points are observed from a new point, as in Fig. 6.10. This case is usually known as Pothenot-Snellius resection.

In this case, indetermination occurs when the circumference of a circle passes through the three known points. The same angles (α, β) to the control points can be measured to any point located on that line. It is relatively easy to avoid this situation by plotting on a chart the known control points and seeing if they lie on a circle centred on the unknown point. Another method is to check the addition:

$$\alpha + \beta + \omega$$

If it is near 180° such situation must be avoided.

The algorithm to solve this case, including corrections to compute on the projection plane, is shown in 2.2.5.

Resections have been very frequently used by hydrographers, both in topographic surveying by theodolite and hydrographic surveying by sextant. The advantage being that it was only necessary to put signals on the control points, the surveyor then being free to carry out his tasks without the assistance from ashore.

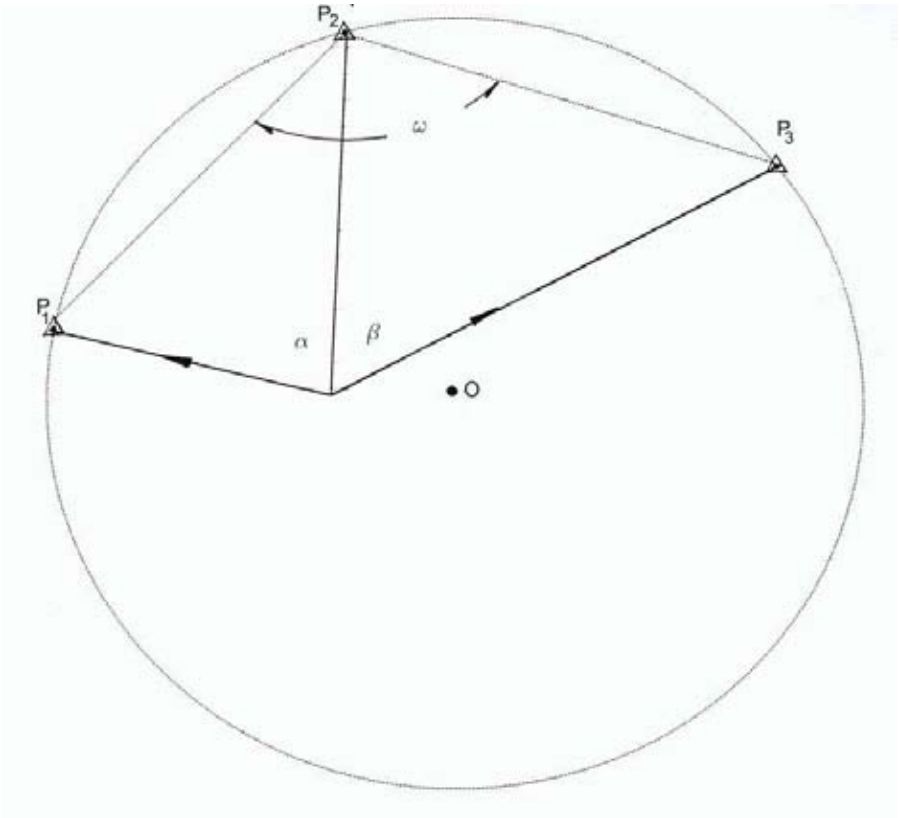

Fig. 6.10

It is possible to present multiple resections as generally given in Fig. 6.11.

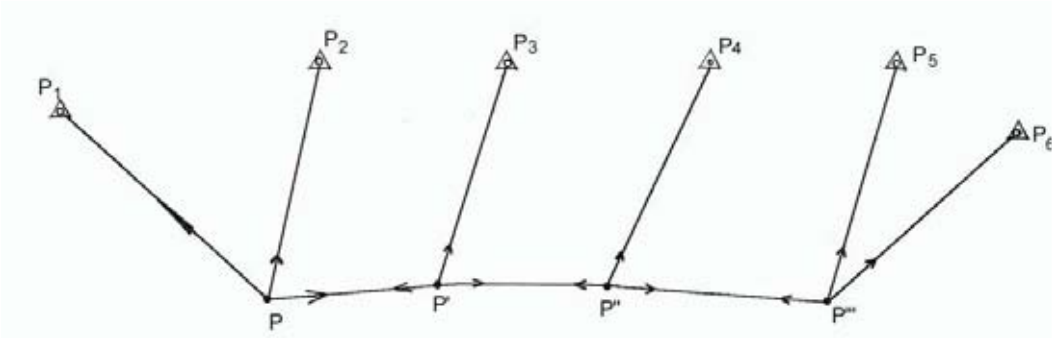

Fig. 6.11

That is from new points P, P', P'', P''', ... directions to known points P1, P2 ... P6 are seen. In such cases it should be noted that in the first and last points, two known control points are seen; at the intermediate points, besides reciprocal directions, a sight to one of those known points is sufficient.

Where there are only 2 new points and 4 control points are seen, it is known as Marek solution. If only the two control points seen from two new points are used, it is called Hansen solution. These particular cases are illustrated in Fig. 6.12.

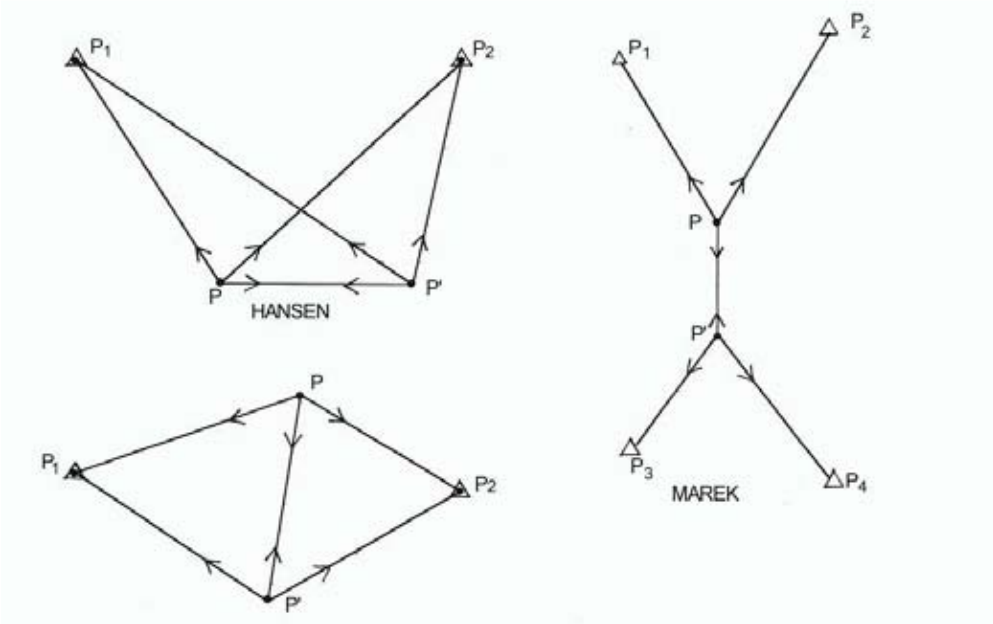

Fig. 6.12

Even though these multiple resection cases may be used whenever required, they are not recommended due to their limited opportunities for checking. A simple solution to apply is by incorporating additional sights to provide redundancy and the opportunity to check.

Therefore more than three directions to known points should be seen from every new point, or that new points will be interconnected by reciprocal lines of sight, as shown in Fig. 6.13; even though every new point is determined by directions to three known points, reciprocal lines of sight between new points include them in calculations of adjacent points.

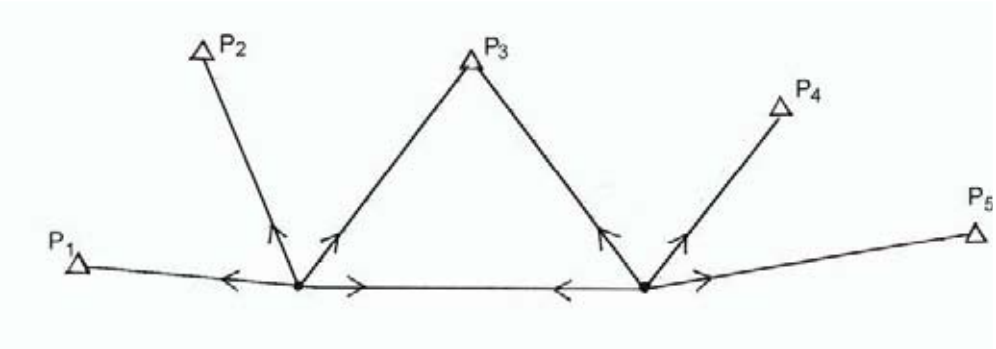

Fig. 6.13

Configurations originally close to indetermination can be improved in this way.

Solutions of this kind require some type of adjustment, whether rigorously by least squares or by iterative average of several positive solutions by trying to give more strength to cases further away from the situation of indetermination.

2.2.5 Usual Algorithms

a) Corrections to projection plane (See ANNEX A)

One of the processes to be conducted for calculations with rectilinear figures on the representation plane to be correct is related to the corrections that must be applied to measured observations (distances and directions). In this section we shall deal with the Gauss Krüger projection, also known as Transverse Mercator, which is often used for topographic calculations.

ANNEX A deals with the nature of this projection for cases of "tangent cylinder", that is those in which distance deformation starts on the central meridian:

$$m = \frac{ds'}{ds} = 1 + \frac{x^2}{2R^2} + \ldots$$

where **x** is the east co-ordinate referred to the central meridian:

$$x = E - X_0$$

when a false easting value $\mathbf{X_0}$ is used.

If this coefficient is applied between two points 1 and 2 (not infinitely near) a relationship:

$$\frac{S'}{S} = 1 + \frac{x_1^2 + x_1 x_2 + x_2^2}{6R^2}$$

is obtained. It should be noted that if a point is on one side of the central meridian and the other point on the other side, the product $\mathbf{x_1 \cdot x_2}$ will be negative.

Also that **R** (mean terrestrial radius) must be calculated for mean latitude of the working area and the representation system includes a coefficient (**K**) in order to contract distances over the central meridian, as in the case of UTM representation (where K = 0.9996, see ANNEX A). The coefficient for reducing distances (to obtain the plane value by multiplying it by the geodetic value over the spheroid) must be affected by the same value:

or

$$\frac{S'}{S} = K\left(1 + \frac{x_1^2 + x_1 x_2 + x_2^2}{6R^2}\right)$$

$$S' = K\left(1 + \frac{x_1^2 + x_1 x_2 + x_2^2}{6R^2}\right)S$$

Measured directions also require the application of a correction. This need arises from the fact that geodetic lines (on the spheroid) on being transferred to the plane, are represented by a slight concavity towards the central meridian.

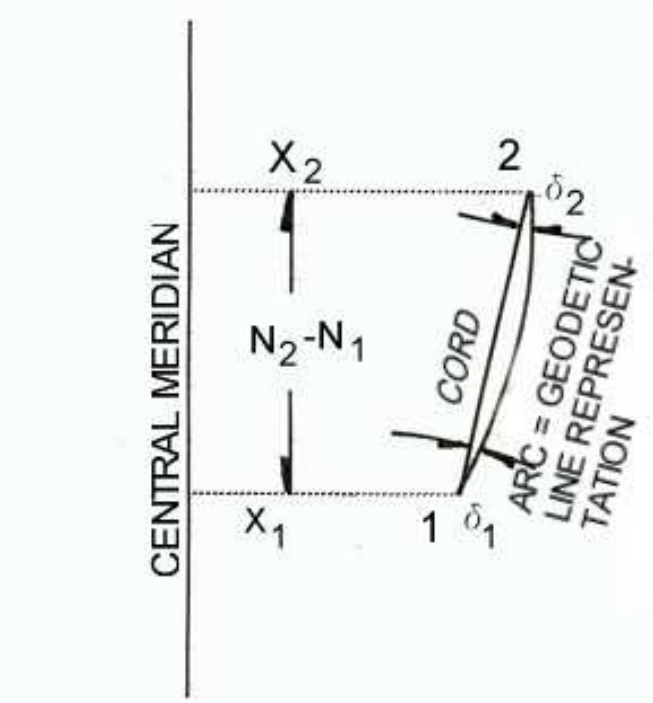

Fig. 6.14

Fig. 6.14 shows such curvature and the corrections which should be applied to pass from the arc, corresponding to the geodetic line, to the cord, corresponding to the side of a rectilinear figure on the plane. On accepting the correction sign to pass from the arc to the cord, we may see that:

$$(\delta_2 - \delta_1) = \frac{\rho''}{2R^2}(x_1 + x_2)(N_2 - N_1)$$

since absolute value addition for such corrections must be equivalent to the quadrilateral spherical excess the surface of which is 1/2 ($x_1 + x_2$) ($N_2 - N_1$) and **ρ"** is the typical constant to pass from radians to sexagesimal seconds (ρ" = 206265").

As arc curvature increases with **x** values, naturally the **x** of the known station point carries more weight than that of the observed point. Then:

$$\delta_1 = \frac{\rho''}{6R^2}(2x_1 + x_2)(N_1 - N_2)$$

$$\delta_2 = \frac{\rho''}{6R^2}(2x_2 + x_1)(N_2 - N_1)$$

and the difference between them leads to the first expression ($\delta_2 - \delta_1$).

In general terms, if there is a need to reduce a series of directions to points Pi measured from a point Po, the corrections (along with their sign) are:

$$\delta_i = \frac{\rho''}{6R^2}(2x_0 + x_i)(N_0 - N_i)$$

It should be noted that westward of the central meridian **x** values are negative; thus the correction sign generating a change in concavity is automatically modified. On the assumption that the direction between the known station and the observed point are on different sides of the meridian, the change in the **x** sign will decrease the **δ** value. This is logical since the geodetic line will have a curvature inversion in order to keep above concavity.

For calculations of corrections for both distances and directions, it is normal to make a preliminary calculation of the mark's co-ordinates and ignore any deformations. Corrections are estimated using these provisional co-ordinates and then the final calculation is undertaken. In some cases provisional co-ordinates are used for adjustment; however this will not be dealt with further.

b) Intersection of Directions.

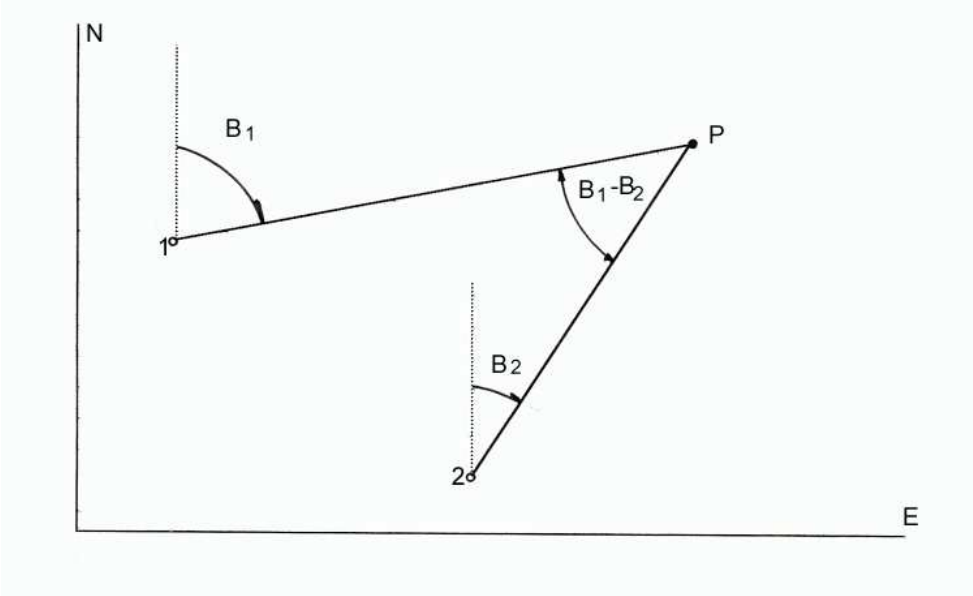

Fig. 6.15

Figure 6.15 shows an intersection of two directions, of which the grid bearings B_1 and B_2, are known. It may be the case that they have been obtained from line of sight observations 1 – 2 and 2 - 1.

There are several solutions and software to solve this problem. One of them is:

$$N = N_1 + \frac{\left[(N_1 - N_2)\sin B_2 - (E_1 - E_2)\cos B_2\right]}{\sin(B_1 - B_2)}\cos B_1$$

$$E = E_1 + \frac{\left[(N_1 - N_2)\sin B_2 - (E_1 - E_2)\cos B_2\right]}{\sin(B_1 - B_2)}\sin B_1$$

c) Intersection of Distances

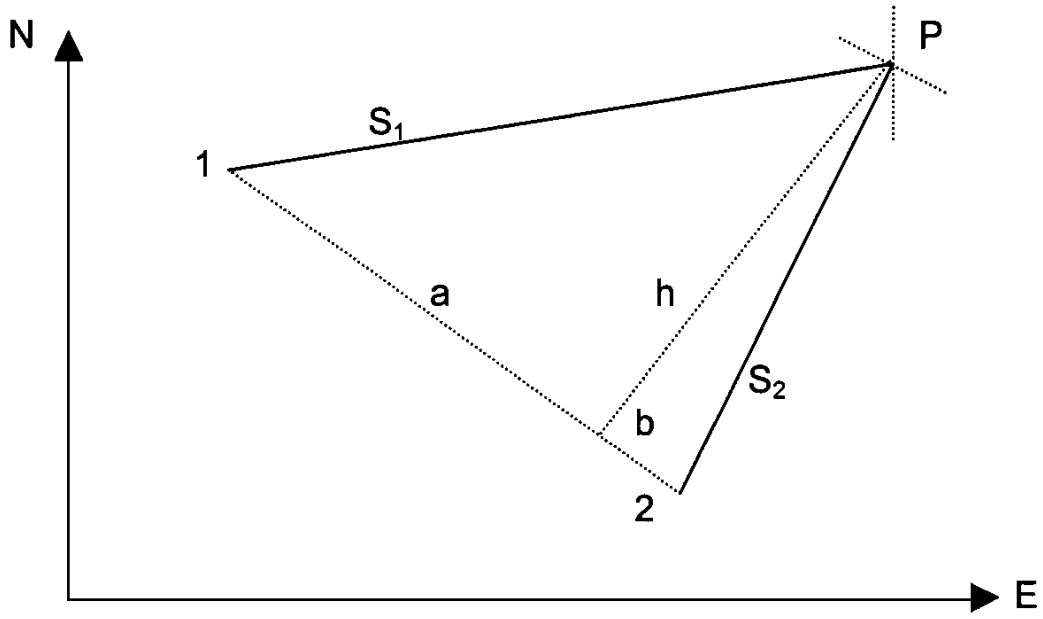

Fig. 6.16

This case is illustrated in Fig. 6.16, it has two mathematical solutions; therefore it is important to make it clear whether point P is on the left (this is the case in the figure), or on the right of line 1-2.

One solution is by applying the following calculations:

$$S_{12} = +\sqrt{(N_2 - N_1)^2 + (E_2 - E_1)^2}$$

$$\sin B_{12} = \frac{E_2 - E_1}{S_{12}}$$

$$\cos B_{12} = \frac{N_2 - N_1}{S_{12}}$$

$$a = \frac{1}{2}\left(S_{12} - \frac{S_2^2 - S_1^2}{S_{12}} \right)$$

$$b = \frac{1}{2}\left(S_{12} + \frac{S_2^2 - S_1^2}{S_{12}} \right)$$

$$h = +\sqrt{S_1^2 - a^2} = \sqrt{S_1^2 - b^2}$$

$$N = N_1 + a\cos B_{12} \mp h\sin B_{12}$$

$$E = E_1 + a\sin B_{12} \pm h\cos B_{12}$$

The lower sign is for the case when P is on the left of 1-2 and the upper sign is when it is on the right.

d) Resection

As stated in 2.2.4 above a resection occurs when directions or angles are measured:

from a point, the calculation of which is required, to three known control points. This situation, as well as nomenclature to be applied in the algorithm, is shown in Fig. 6.17.

Before proceeding, it should be noted that there are many graphical, numerical and mechanical solutions with which to obtain the station point position.

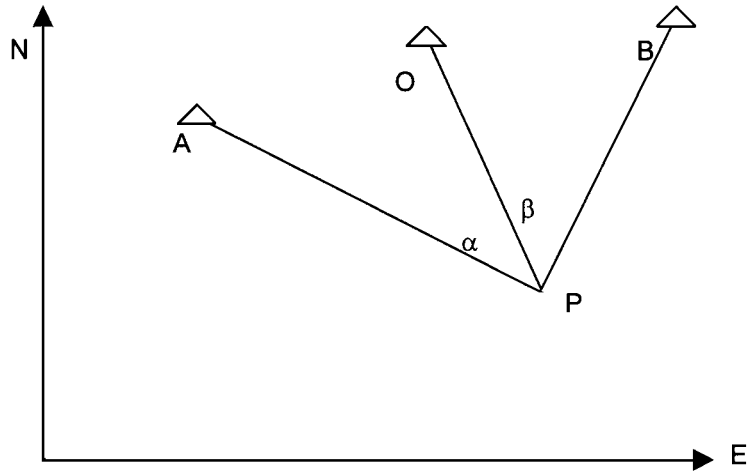

Fig. 6.17

With such numerical solutions it is essential that a method is available to detect cases close to indetermination as indicated in Fig.6.10.

E

Fig. 6.18

The use of two auxiliary points 1 and 2 constitute the base for the algorithm, proposed below, is shown in Fig. 6.18.

The formulae to calculate the co-ordinates for these points can be obtained simply from:
When points 1 and 2 are too close to each other (for example less than a tenth of distances

$$N_1 = N_A - (E_0 - E_A)\cot g\alpha$$
$$E_1 = E_A + (N_0 - N_A)\cot g\alpha$$
$$N_2 = N_B - (E_B - E_0)\cot g\beta$$
$$E_2 = E_B + (N_B - N_0)\cot g\beta$$

AO or OB) it can be assumed that the network is close to indetermination.

Calculation for N and E co-ordinates of point P can be achieved by:

$$N = N_1 + \overline{10}.\cos .(\vec{12} - \vec{10}).\cos .\vec{12}$$
$$E = E_1 + \overline{10}.\cos .(\vec{12} - \vec{10}).\sin .\vec{12}$$

Where

$\overline{10}$ = The distance from 1 to 0 = $\sqrt{(N_0 - N_1)^2 + (E_0 - E_1)^2}$

$\vec{12}$ = Grid bearing from 1 to 2 [tg $\vec{12}$ = $(E_2 - E_1) / (N_2 - N_1)$]

$\vec{10}$ = Grid bearing from 1 to 0 [tg $\vec{10}$ = $(E_0 - E_1) / (N_0 - N_1)$]

When calculating orientations ($\vec{12}$, $\vec{10}$) it is necessary for quadrants to be discriminated with signs ΔE and ΔN. For this purpose you may make use of the usual subroutines to pass from plane coordinates to polar coordinates.

Another way of solving the last part of the calculation is to obtain the coordinates of P such as the perpendicular base from 0 to segment 12 making use of the subroutines available in Computer-Assisted Design (CAD) programmes

Some checking calculations may be established though the most complete method is to calculate grid bearings from P to the known points (A, O, B) and then check

$$\alpha = \vec{PO} - \vec{PA}$$
$$\beta = \vec{PB} - \vec{PO}$$

2.2.6 Levelling and its Errors

Trigonometric levelling and the possible errors have been discussed in 2.2.3 (traverse). It should be noted that in the case of intersections a similar operation can be undertaken with the algorithms and the resultant calculations. It is also be possible to apply them for surveys using polar co-ordinates or EODM tachymetry, when it is particularly useful to have total stations which store (horizontal and vertical) ranges and directions to surveyed points. On processing such information and when ranges over 100 m are used, it is important to verify that the software application includes corrections for refraction and earth curvatures.

Direct levelling (with spirit or self aligning levels) is generally more precise. In the case of geodetic levelling, which requires the use of levels of higher sensitivity and stadia graduated on INVAR plates (an alloy of nickel and steel with a coefficient of expansion below 1 x 10^{-6} 1/°C) and other precautionary measures, error propagation may be below:

$$1\ mm\sqrt{K}$$

where **K** is the track distance expressed in Km.

If common topographic levels, wooden or plastic centimetre-graduated stadia with joints or couplings and instrument-stadia distances below 100 m, with equidistant stations (within 3 m), are used, you may attain accuracies of the order of:

$$7mm\sqrt{K}$$

for which it is assumed that every section between bench marks is measured in both directions with a tolerance of the order of:

$$\pm 3mm\sqrt{K} \quad \text{(geodetic) and } \pm 10mm\sqrt{k} \quad \text{(topographic)}$$

for both cases, without bias to any intermediate or even less accurate solution which may be adopted.

In hydrographic surveying, the highest accuracies are required to tie-in permanent tide stations followed by temporary tide stations, which are generally established during the survey, the calculation of levels for harbour facilities and standards for engineering works associated with water behaviour.

In an extensive hydrographic survey (more than 50 km) with no available local levelling datums, it is expedient to provide, as a minimum, a direct levelling line to which the tide stations can be related and leave a reference mark from which future trigonometric levelling can be conducted. When applying these provisions, the specifications in 2.1.6 should be considered and an analysis of the stability of the relationship of the tide station and mean sea levels is necessary.

When using satellite methods (GNSS) for altimetric purposes, the provisions in 2.1.6 and Chapter 2 need to be noted particularly the requirement for modelling corrections to pass from heights above the spheroid to values associated with sea level used in hydrographic surveys. Regardless of preset correction diagrams that may exist, it is necessary to adjust them to altimetric points as described in 2.2.1, including the provisions in Fig. 1, in connection with the relationship between altimetric marks. In other words, use of GNSS techniques for altimetric purposes should be limited to point interpolation rather than extrapolation. This concept is likely to evolve in the future but in 2004 there remains no likelihood of

confidence in general correction models and still less in places where there is no guarantee that local observations have been carried out to create them.

2.3 Coastal and Harbour Ground Surveys

2.3.1 Application of Direct Topographic Methods

In general, coastal surveys which are a part of hydrographic surveys are mostly carried out by photogrammetry or other remote-sensing processes. In such cases the surveyor's main task, when processing information, consists of obtaining a proper interpretation of coastal features, that coastline delimitation poses no difficulty and that data on the ground control points are adequately provided. He must also ensure that aids to navigation signals and stations have their horizontal and vertical positions properly determined.

However, there are cases in which all this information must be obtained by direct topographic survey methods, i.e. by field observations and measurements. These cases are generally related to the need to represent certain areas on large scales (1:5000, 1:2000, 1:1000 ...). This often occurs in areas where there is a port infrastructure or where a harbour project, landing, water intake or other engineering works are being carried out or extended to occupy the inter-tidal zone and extending into the near shore strip.

The limited extent of such places as well as the required high degree of detail may require that such surveys are carried out by topographic measurements in the field.

2.3.2 Density of points to be surveyed

Firstly the required degree of detail must be established. The usual method is to set a scale according to the essential representational needs of the final product, in order to properly obtain the shape it may be necessary to survey a point every square centimetre. Nevertheless such a distribution shall not necessarily be strictly homogeneous. Priority should be given to sites where there is a significant change in slope or where there are outstanding characteristics: hillocks, holes, saddles, ridges, talwegs, etc.

Generally the survey of points on near-perpendicular lines to the shoreline provides much more useful information for good representation of shape than any other type of distribution.

For details which must be surveyed to allow representation of natural or artificial features, more or less independently of relief, the quantity of points should be adequate enough to be able to plot them at the intended scale, straight sections probably only require the surveying of turning points and if orthogonal, simplification may be greater still.

2.3.3 Applicable Methods

Satellite techniques (GNSS) are ideal for surveying horizontal positions. If they are intended to be extended to planimetric and altimetric positions, the provisions detailed in 2.2.1 should be observed. Generally the process is more advantageous when the density of the points to be surveyed is low (i.e. more than 50 or 100 m between them for scales of 1:5000, 1:10000, etc.). Ground-permitting, this process may be achieved by placing the rover station in a vehicle. The opportunity of processing information in a fully automated manner would rapidly improve the achievement of results.

EODM tachymetry is a particularly appropriate method for cases where, from a few stations, points with distances of 1000 m and above may be surveyed. Use of total stations with its capacity to store distances, directions (horizontal and vertical), attributes of surveyed points, etc., makes it possible to quickly

process the information and generate the appropriate survey sheets which can be completed with additional data if required.

Stadia method tachymetry is ideally suitable for sites where the survey of a large number of points very close to each other (50, 20, 10 m) is required at relatively short distances (below 200 m) from every station. Reading of graticule lines is made on generally centimetre-graduated stadia.

Ground distance is obtained as **K.m**, where **K** is the stadia constant, usually 100, and "**m**" is the difference of stadia line readings. If an elevation angle α has been measured, the horizontal equipment ground distance to the stadia is:

$$K \bullet m \cos^2 \alpha$$

and the relative elevation to the surveyed point equals:

$$\Delta H_{12} = i_1 - S_2 + K \cdot m \cdot \frac{1}{2} \sin 2\alpha_1$$

where $\mathbf{i_1}$, $\mathbf{S_2}$ and $\boldsymbol{\alpha_1}$ have the meanings given in 2.2.3 for trigonometric levelling.

In the case of lines with too great an incline of sight ($\alpha > 10°$), this method is not recommended for height transfer since the distance error (of the order 0.2%) and the sight's probable lack of verticality introduce considerable altimetric errors (this is less frequent in EODM tachymetry).

With special stadia having divisions of 5 cm or 10 cm, the survey ranges may extend to 500 m and above, although it is not advisable in the case of lines with too great an incline of sight for the above reasons.

All these procedures allow calculation, from the above formulae, of the 3 horizontal and vertical co-ordinates of the mark. In some cases these co-ordinates and orientations may be obtained by resection complemented with inverse trigonometric levelling, based on the adequacy of the formulae given in 2.2.3

In flat areas direct levelling is a simple and precise method of surveying. If necessary stadimetric distances (K.m) may also be used as well as horizontal directions which may be measured by some other instruments.

In relatively flat locations, for constructions with some orthogonal shapes measurement of perpendicular distances may be made using tapes and an optical square. Simple though it may be, it proves to be a useful method to be applied in some places such as docks, piers, moorings and other port buildings. This type of survey is usually be complemented with direct levelling in order to determine platform or floor elevations.

2.3.4 Relief Representation

Although the trend is to generate databases which provide a variety of applications for information through a Geographic Information System (GIS), implying the availability of a Digital Terrain Model (DTM), planimetric and altimetric measurements are frequently requested to be represented by contour lines. For this purpose, selection of a contour interval should be made at not less than four times the estimated error of elevations.

An alternative method of selecting the contour interval is by scales. In the case of very broken ground, the scale denominator thousandth part may be measured in metres (example: 5 m for 1:5000), but in the case of flat and featureless terrain, the values may decrease to a tenth part (0.5 m in the former example).

Both criteria should be harmonised and basically, the survey purpose as well as relief fluctuation in the area should be taken into account.

Several software packages are available for drawing contour lines from discreetly surveyed points. Some of them have proved to be very capable but it is expedient to adjust their drawing algorithms by incorporating some interpretation rules for the relief before the final version.

Fig. 6.19 shows how drainage lines tend to stress the contour line curvature while ridges tending to separate the water movement on the surface are gentler. These trends generally undergo changes and contours collectively representing the relief must keep some agreement.

The concepts mentioned above are valid for application in ground shape; however, not all of them are valid for seafloor application.

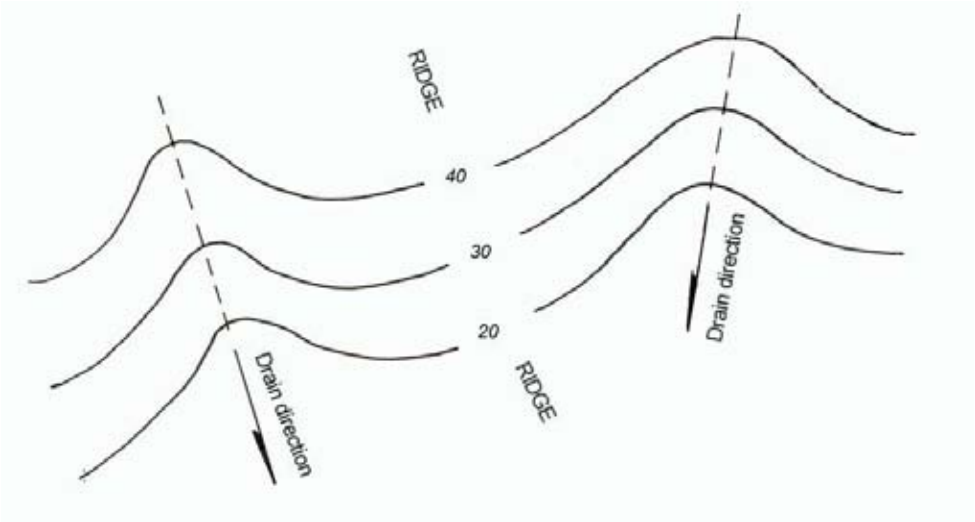

Fig. 6.19

With some geomorphological knowledge, the criteria may be generally improved for a better relief interpretation.

3. REMOTE SENSING

Some techniques for obtaining information through remote sensors, which capture the ground radiation, will be described in this section. This information is stored and then processed, thus generating products that provide topographic data.

If ground radiations originate from the reflected solar energy, sensors are called passive; if they are generated from reflected emission of devices associated with the sensor, sensors are called active.

The range of frequencies and wavelengths of electromagnetic waves for remote sensing is shown in Table 6.4:

Table 6.4

NAME	FREQUENCY (Hz)		WAVELENGHT (m)
Microwaves	3×10^{9} to 3×10^{11}		10^{-1} to 10^{-3}
Thermal Infrared	3×10^{13} to 3×10^{12}		10^{-5} to 10^{-4}
Medium and near infrared	$4{,}3 \times 10^{14}$ to 3×10^{13}		0.7×10^{-6} to 10^{-5}
Visible Light	... 4.6×10^{14} .... 5.4×10^{14} .... 6.6×10^{14} ...	Red Green Blue	... 0.65×10^{-6} .... 0.55×10^{-6} .... 0.45×10^{-6} ...
Ultra Violet	3×10^{15} to 3×10^{16}		10^{-7} a 10^{-8}

Radio waves have the lowest frequency whilst x, gamma and cosmic rays have the highest. They also have other applications.

Among the passive sensors uses, which use visible light radiations and their close proximities, is the Photogrammetry. Since this technique began to be applied with light sensitive films, it has been used in hydrographic surveying since the beginning of the 20th century, it remains one of the most efficient ways of obtaining good information of the relief, especially for large scales (1:20000, 1:10000, 1:5000, ...)

From the 1970s and more intensively from the 1990s, remote sensing applications were extended from active and passive airborne and satellites sensors to other imagery processes. Satellite methods have not generally the same capacity as photogrammetry in the ground shape interpretation. However, they have additional capabilities for detecting the surface properties of soil and water covered areas. They also offer impressive updating capabilities, frequently at relatively low costs.

In photogrammetry, as well in other imagery processes, it is necessary to undertake ground control operations in order to achieve correct scale results and obtain good referenced positions. Ground control consists of locating, in the field, identifiable points based on the information provided by the sensors.

3.1 **Photogrammetry** (See 3.4 at Chapter 2)

Strictly speaking, photogrammetry is the technique that allows objects to be described in three dimensions from overlapped photographic images, taken from adjacent places. For hydrographic surveys, aerial photography with vertical axis through a metric camera is more useful.

3D description is achieved by stereoscopic viewing of virtual models and the measurements are taken with the use of specific instruments to achieve topographic representation. Of course, this technique requires ground control points obtained via field topographic methods or densification through an aerial photogrammetric process, also called aerotriangulation.

There are other products which are not 3D but may be considered to be part of photogrammetry. Among these are photo-plots, which can be obtained by simple assembling photographic images adjusted by rectification (scale and inclination).

3.1.1 Principles and applications of aerial photographs

The objective of aerial photographs is to provide information to obtain true ground representation including relief. This can be done through photogrammetric restitution or stereo compilation. Nevertheless, as previously stated in the concept of photogrammetry, there are other 2 D products which can be obtained from aerial photographs.

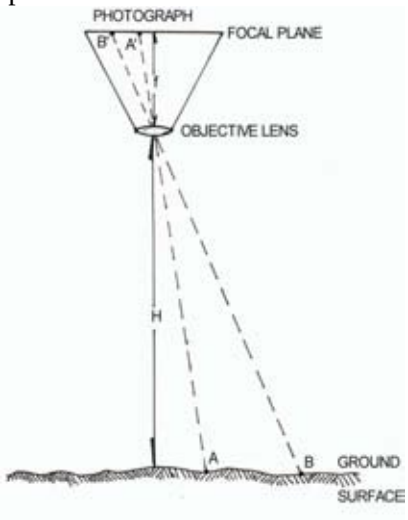

Fig. 6.20

To explain this it is necessary to take into account the basic expression for the aerial photograph scale:

$$S = \frac{A'B'}{AB} = \frac{f}{H}$$

Where the ratio among the focal length **f** and the flight altitude **H** is directly related to the image scale (see Fig. 6.20 for a camera with vertical axis).

Although objective lenses might be considered as a centred optical system with two nodes, the scheme is simplified with only one optical centre similar to a thin lens. That simplification is enough for the approximate calculation of the flight scale. See also that, as H>>f, it is assumed that the image is formed in the focal plane.

A change in the flight height causes a change in scale; a lack of verticality in the camera axis produces a change in the scale in different points of the camera. For example, a rectangle ABCD on the ground can be represented as a trapezium A´B´C´D´ on the photographic image where the scale of segments A´B´ is shorter than in C´D´ (See Fig.6.21).

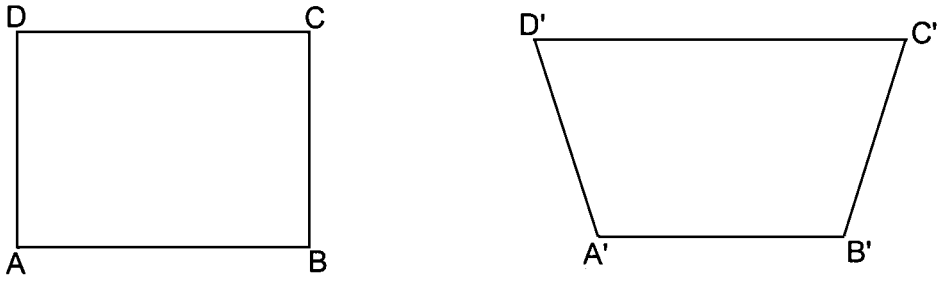

Fig. 6.21

Moreover, if there are features in the relief with significant vertical characteristics, the scale introduces other changes on each photograph. This can only be resolved by a 3D treatment like restitution. An adjustment of the change in the flight height and the axis orientation is possible by rectification through a 2D photographic process. Note that this adjustment is only possible on flat surfaces.

Special devices can fulfil the process of rectification mentioned above by using rectifiers provided with a camera, which project the image onto a board. The set allows a series of combined movements which enables the projected image to change and to include slopes according to focusing conditions. The current way to rectify is by making the projection of four well-distributed points coincide with their well-marked locations, as in Fig. 6.21. There are also equivalent 2D numerical procedures for solving this problem.

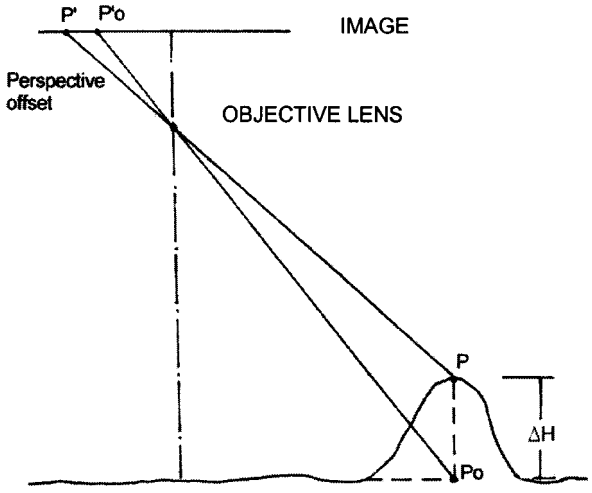

Fig. 6.22

The limits for these processes rest with the image of a point with a certain difference in elevation relative to the surrounding area, which experiences a perspective offset on the image (see Fig 6.22). Note that, apart from the difference in elevation $\Delta \boldsymbol{H}$ *(Delta H)*, the distance of the elevated point from the camera vertical axis increases the offset, in other words, points near the vertical axis of the camera do not display significant offset effects.

An alternative way to generate photographic images free from this effect is to combine the photographic process with the 3D treatment, the product is called orthophotograph.

The best way to present ground photographic images is through an orthophotomosaic, which is an assembly of images forming a uniform-scale mosaic. The next in quality is the rectified mosaic adjusted as mentioned; the coarsest method is by assembling raw photographic images and accepting an approximate scale as a function of the average flight height.

The type of photo-plot should always be specified so that caution can be exercised with respect to the validity of the product metric.

3.1.2 Aerial photograph acquisition elements

Extraterrestrial solar radiation has a maximum range of wavelengths from 0.4 micrometers to 0.8 micrometers (1 micrometer= 10^{-6}m), which is between infrared and blue (see Table 6.4). The radiation changes when passing through the atmosphere, the soil reflection also impacts on the light spectrum received by the camera. Thus, the film and the emulsion must be carefully selected.

Among the black and white films (scale or tints of greys) orthochromatic emulsions are especially useful between 0.4 and 0.55 micrometers, panchromatic ones between 0.3 and 0.65 micrometers, with an additional increase in wavelengths of 0.6 and 0.9 micrometers. The most useful in aerial photogrammetry is the panchromatic emulsion. There are several types of three layer colour films, but they are more useful for photo interpretation, described later (3.1.8), than for photogrammetry.

There are a series of specifications regarding density, speed, resolving power, granularity and base stability which must be determined in order to achieve the best result in the prevailing conditions to meet the needs for the final product. The objective and filters to be used should be addressed in the analysis.

The objective lens is composed of an optical system where a good distortion correction is particularly required.

The image format commonly used is 23 cm x 23 cm with the focal distances (f) (see 3.1.1) detailed in Table 6.5:

Table 6.5

Camera Type	**f (mm)**
Super Wide Angle	85
Wide Angle	153
Intermediate angle	210
Normal Angle	305
Narrow Angle	610

Cameras with a shorter focal distance (f) require a better distortion rectification whilst the images are also more affected by atmospheric refraction. The Wide Angle is the most commonly used type of camera.

For photogrammetric purposes, an aerial camera must have a good determination of f, a rigorous correction of the distortion or other optical and mechanical conditions which can be checked by calibration. The camera is termed a metric camera if these conditions have been met. These cameras have an accurate system for ensuring verticality of the axis and assure the flatness of the film. They also have a proper dwell time control and allow an overlapping control between consecutive photographs (end lap), etc.

Although digital cameras generally enable high quality images for photographs, their development for use in photogrammetry is advancing rapidly but presently (2004) only non metric cameras are available.

An important component for aerial photography is the aerial survey platform. Criteria include suitable space for the camera and its attachments, have sufficient endurance, are able to operate at the required flight heights and required speeds, satisfy permissible vibration limits, etc.

Among other requirements it must have GNSS positioning, often with a differential capacity, a requirement for positioning synchronisation with the camera and multiple antennas for platform inclination checking.

3.1.3 Flight planning

Initially it is necessary to define the flight scale, meaning the scale of the camera, which, as it was stated in 3.1.2, has a format of 23cmx23cm. If the type of camera is defined, the scale also determines the flight height H=f/S (see 3.1.1 Fig. 6.20).

Although the scale may be enlarged five times to obtain good photogrammetric products to meet the hydrographic requirements, the analysis of the required altimetry accuracy should be conducted. It should be noted that the deviation of the elevation obtained by restitution reaches 200ppmxH (200 parts per million of the flight height=H/5000). Sometimes, this can make it unachievable and the altimetry requirements must be met by other means.

Having defined the flight scale, flight strips must be studied. In the simplest situations, the coastal band can be covered by a set of rectilinear strips (see Fig. 6.23)

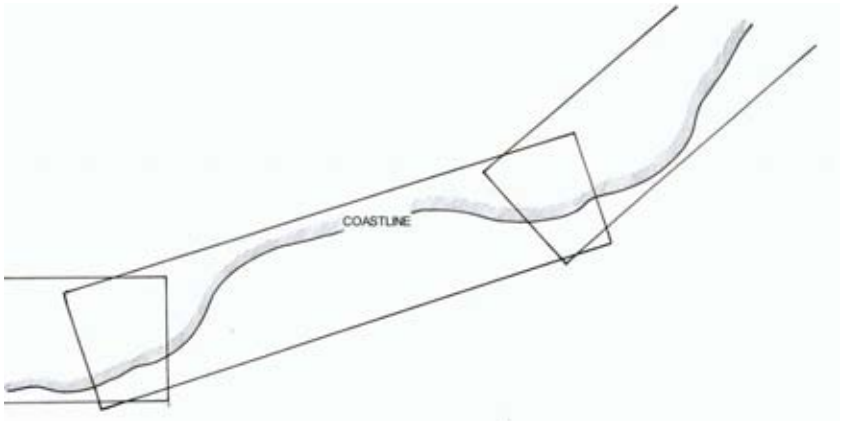

Fig. 6.23

When coastal features are extensive, wider inshore surveys are required. In this case, blocks of several strips must be planned (see Fig. 6.24).

Additionally end and side overlaps must be planned; generally, the end overlap is of 60% and the side overlap of 20%. When orthophotographs are required (see 3.1.1) or when ground features are so uneven that there is a possibility in gaps leaving some part of the information without stereoscopy, it may be necessary to enlarge the overlapping.

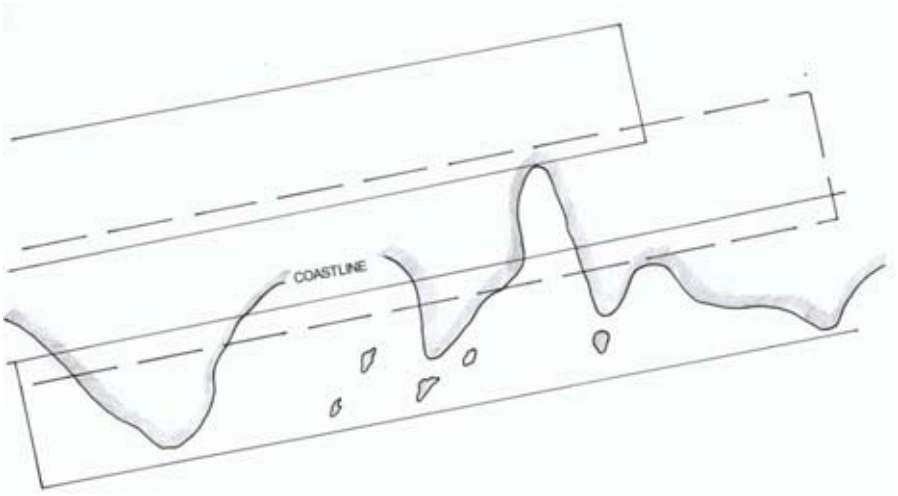

Fig. 6.24

The sun's altitude and angle during the flight should be considered, particularly in higher latitudes ($\varphi > 50^{o}$) in wintertime.

To ensure that shadows do not interfere or impact on image quality, the sun altitude angle should be greater than 30^{o}. The more uneven and cluttered the ground, the greater the elevation angle should be. The flight time may be limited by the time of the year and the latitude.

An additional limit for hydrographic surveys is that the flights should take place near low water to allow detection of features and dangers close to the foreshore in the inter-tidal zone.

The sky must be free of clouds below the flight height whilst many other meteorological conditions must be satisfied during the operation. All these limitations combine to make flight times longer and planning more complex.

The ground control and its densification by aerotriangulation must be considered when planning the flight. This provision is necessary to allow the opportunity of performing field tasks during the survey group's presents in the area.

The end overlap produces coverage as detailed in Fig. 6.25. If the overlap is of 60% or more there is a zone of 20% or more of triple overlap.

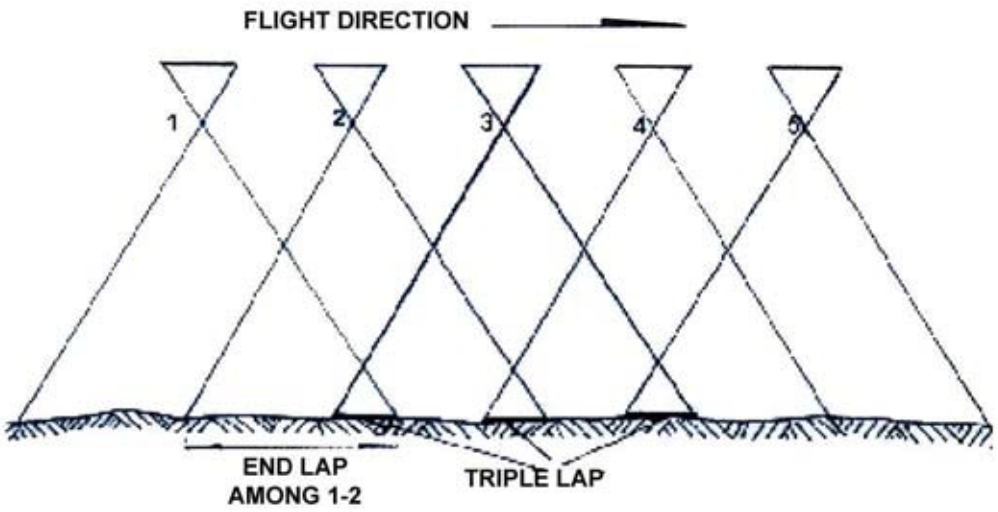

Fig. 6.25

In this zone, like in the side overlap (see fig 6.24), aerotriangulation can be carried out.

3.1.4 Restitution

The photogrammetric technique restitution is the basic process in the 3D treatment of the topographical information, generally aerial images are used. Restitution is carried on the optical, mechanical, analytical or digital adjoining photogram projection in the overlap zone, which allows stereoscopy observation.

In any version it is necessary to determine the relative and the absolute orientation of the model which replicates that part of the ground being surveyed.

A pair of photographs is oriented by intersecting five pairs of homologous rays corresponding to five ground points. This process is achieved by removing their parallaxes through motion projectors or by an equivalent digital process.

Prior knowledge of the co-ordinates of the selected points is not required; however it is expedient to choose them from the end overlap zone (see Fig. 6.26).

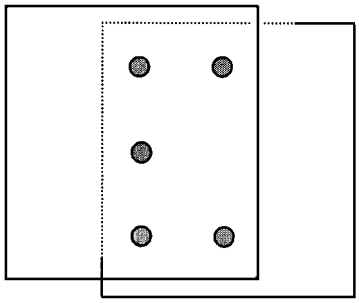

Fig. 6.26

Having done this, a 3D model is created, even though neither its position in the reference frame nor its scale has been defined. In other words, only a relative position of the photographs coincident with the cameras during the flight in an unknown scale and reference frame. It is possible to observe stereoscopically the entire model whilst holding the observed images location.

To assign a scale to this model and to express it in a reference frame compatible with the survey, at least 3D positions of two points (for example 1 and 2 from Fig.6.27) and the height of a third one must be known. However it is better to know the three co-ordinates of 1, 2, 3 and 4, which allows some verification.

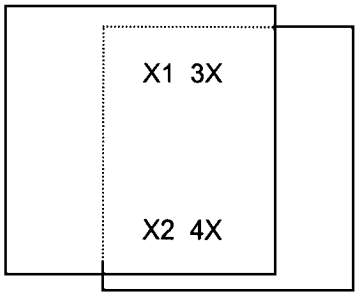

Fig. 6.27

Of course, this adjustment can be undertaken in an analogical way, by optical or mechanical means or numerically by analytical or digital stereo plotters.

With the models absolutely oriented, it is possible to obtain a topographic representation of the relief and description of features or infrastructures. The contour lines can be traced by analogical or digital means. In the latter case, it is possible to make a Digital Terrain Model (DTM) with a convenient density of stored points.

To obtain digital copies of the information, at present the simplest way is to scan aerial photographs through high-resolution scanners; however in the future, it will be available with information taken from digital cameras as mentioned at the end of 3.1.1.

3.1.5 Aerotriangulation

As has been described in 3.1.4, for the absolute orientation of a stereoscopic model in restitution, it is necessary to know the three sets co-ordinates of four points distributed as in Fig.6.27, although in principle the three sets of co-ordinates of 2 points and the vertical of a third point may be sufficient.

To achieve such control, whilst minimizing field work, an internal process has been developed by photogrammetry: aerotriangulation.

The first process in this technique consists in providing the ground control for the first model, determining its absolute orientation and then, passing to the second model adding a third image. Having completed all the movements in the third image projection, without modifying the previous during the process for the second model's relative orientation, it will be clear that absolute orientation has been transferred.

It is possible to repeat the process detailed above, however deformations could appear. Apart from the deviation, the effects due to terrestrial curvature and refraction of light rays must be considered. For this reason it is necessary to adjust the strip by adding ground control points.

Fig. 6.28

A strip with four start control points, four close control points and two intermediate pairs is shown in Fig. 6.28 (also see Fig. 6.23). The intermediate pairs should be present in six models in order to successfully solve for deformations and propagation of the deviation.

Both control points and tie points, to hold the restitution, must be present in the zone of triple superposition and when necessary with the side overlap.

Although the described distribution corresponds to analogical aerotriangulation processes, hydrographic experience shows that frequently a control is still valid in coastal surveying (see Fig. 6.23). This is also valid when strip adjustment is carried out through independent models using an analytic process. In this case, the normal method, after determining every relative orientation, is to note each model's co-ordinates and then to adjust them in numerical terms.

When there are several strips with side overlaps (see Fig. 6.24), block adjustment with independent models can be completed with certain advantages from the merged rigid set.

Points subjected to aerotriangulation are:

a. Ground control points;
b. Tie points;
c. Additional points for restitution control or items of detail requiring specific calculation.

Then, holding the co-ordinates of the ground control points fixed whilst taking into account their relation with tie points, a block adjustment can be undertaken. As a result, co-ordinates of the tie points and any additional points can be obtained and expressed in the ground control points' reference frame.

There are seven parameters for each transformation model in a normal process: one scale, three translation parameters and three orientation ones. Several software versions are available; the basic ones deal with the planimetric and altimetry processes separately. The more elaborated ones are based on 3D treatments with an important statistical analysis which tends to clean up the influence of out of tolerance deviations. With these kinds of blocks, the required amount of ground control points can be minimised. There is an integral utilisation for them and a strong linking between models to emphasise the set rigidity. With 5 + 0.2M ground control points, successful results can be achieved, M is the number of independent models that constitutes the block.

A block of independent models under adjustment is shown in Fig. 6.29. It must be remembered that apart from the number of ground control points, their distribution is important to assure an accurate and rigid network for the restitution.

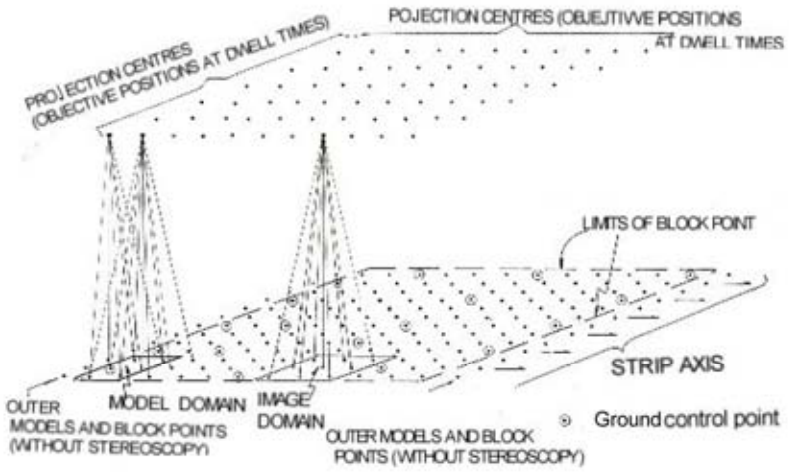

Fig. 6.29

For simplicity, only a few rays from the perspective centres to the points under aerotriangulation are shown. These perspective centres are associated with the objective position at the moments of exposure. The ground control points, of which some are coincident with tie points, but not in every case, are also indicated.

Fig. 6.29 is also useful to demonstrate the linking that can be achieved through intercepting homologous rays.

Even though they have been chosen by stereoscopy observation, the measuring of plane co-ordinates inside each image, without stereoscopic processing, sets up these rays. Through this method, at least nine points from the photogram are usually measured with a distribution as shown in Fig. 6.30. The stability of a block adjusted through this bundle block adjustment technique is higher than that achieved through strips or independent models. Occasionally, a first adjustment is conducted through independent models and then, with these provisional co-ordinates, the last adjustment is undertaken through bundle of homologous rays.

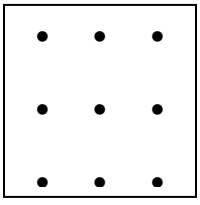

Fig. 6.30

In the block adjustments, by independent models or by bundle, apart from the three co-ordinates for each point being processed, co-ordinates for perspective centres are also created.

There are cameras which can be synchronised with GNSS systems. They have the capacity to receive differential corrections; the position of the centres can be introduced in the block adjustment. Thus, the number of ground control points can be reduced. Systems with three or more antennas are being developed in order to extend the capacity to the calculation for orientation.

There are other means to increase aerotriangulation capacity and whilst minimising ground works; the obtaining of images at smaller scales is among them. It has certain validity for horizontal co-ordinates but it is not capable, as yet, for solving altimetry requirements accurately. Some transversal strips at the same or smaller scale are also used. At the present time all these procedures for small photogrammetric scales (1:20000, 1:50000, 1:100000, ...) are avoided and replaced with the described technique of GNSS positioning through the projection centres with minimum ground control.

3.1.6 Ground control

One of the main tasks of topographic field surveying is the creation and marking of ground control points.

Although in 3.1.5 some guidance for selecting the points to allow aerotriangulation are given, it is necessary to consider the specified requirements of those responsible for restitution or the aerotriangulation processes. The objective of aerotriangulation is the control of the restitution described in 3.1.4

Selecting of control before the flight is theoretically possible, deciding on the positioning points which are to be photographed. However, the control is frequently selected after the flight by positioning identified points on the photographed images. This is a way of avoiding problems caused by the short life of artificial marks.

Apart from obtaining the values of the co-ordinates of the control points, their plots must be completed. An initial impression for that information can be acquired from photogram copies or on a photo-plot. Sometimes the feature is pricked through the image with details written down on the back. However, this is not always sufficient and it is necessary to add a description with graphs to clarify the chosen detail and to fix its position and the reference level for the vertical co-ordinate. This is important because sometimes the appropriate detail to fix the horizontal position has no well-defined level. For example, the corner of a building is a good point with which to refer a horizontal position but the ground level or both must be identifiable to give good vertical control.

In every case the description obtained in situ must be compatible with that which can be obtained by stereoscopic information. To do this it is useful to have a stereoscopy and accurate image copies to analyse this information or to observe it through a stereo plotter to provide the description to be used in aerotriangulation.

The accuracy in the position of ground control points must be carefully studied, taking into consideration the desired aerotriangulation results to control the restitution. A maximum deviation of 100ppm (100parts per million) of the flight height (that is H/10000) in the three co-ordinates can be accepted. In cases where difficulties arise, acceptable alternatives must be available and analysed.

Apart from the issues on the instructions for distribution of ground control points, accounting for the aerotriangulation adjustment, it is expedient to clarify that the provision of **x**, **y** and **z** co-ordinate points around the outside edge of the block are more useful; some internal points may be limited to the vertical **z** co-ordinate only.

3.1.7 Stereo plotter generalities. Digital processing.

A simplified scheme of a stereo plotter is shown in Fig. 6.3.1. It has two photogram supports (on film or in digital format) on which co-ordinates **x´y´** and **x´´y´´** can be read. It also has an observation device (represented by two eyepieces) which has two (optical, optical/mechanical, electronic) paths inside it to allow each eye to partially see each image, making the stereoscopic model available for measurements. The paths have floating marks with which to form a point which can be seen in 3D near the model. These marks can be moved on the model in the direction of the flight through the X control, transversal to the flight with the Y control and vertically via the Z control.

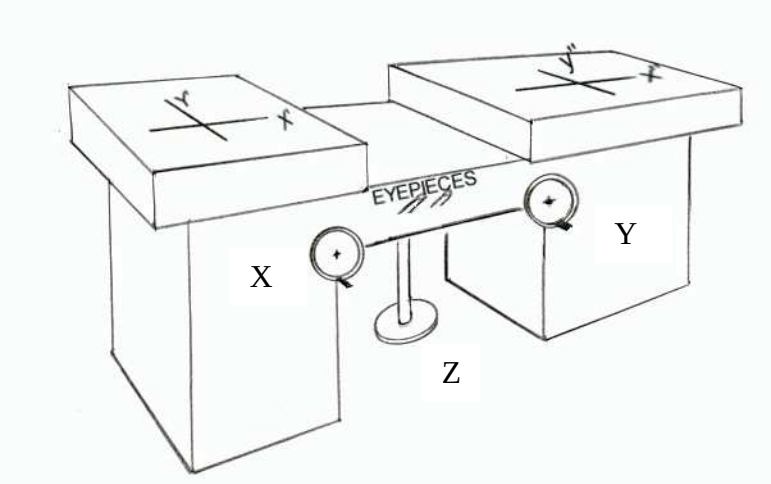

Fig. 6.31

As is indicated in Fig. 6.31, controls in **x** and **y** are operated through cranks and **z** through a pedal.

Through codifiers related to the movements in **x**, **y** and **z**, these co-ordinates can be registered. An independent model aerotriangulation process can then be applied to them. To conduct the process through ray bundles, it is necessary to have an instrument with codifiers to register photogram co-ordinates (**x´**, **y´**, **x´´** and **y´´**)

Apart from the required accuracy to distinguish 100ppm of the flight height (H/10000), an instrument suitable for aerotriangulation must have all the essentials to register and to codify.

Naturally, all the stated registration, codification elements and others related to orientation and inner equipment performance, should be connected to a computing system, particularly in analytical and digital versions (see 3.1.4).

In the new digital versions (soft or video plotters) a computer monitor is used to display the data required to carry out the observations detailed above (see Fig. 6.51). Both photograms are projected alternatively onto the monitor, the operator views one in each eye through special observation equipment (anaglyph, polarised lens or other electro-optical means), which create a stereoscopic image and therefore the ability to make the required measurements. Other peripherals are connected as indicated in Fig. 6.32. In a digital stereo plotter, the image is provided by a stereo camera (CCD = charge coupled device).

Fig. 6.32 shows a data flow diagram in a digital stereo photogrammetric system.

In electromechanical restitution devices the plotter gives the final output version of the work, additionally the plot was produced analogically without the aid of a computer process. In digital versions data output consists of files containing a precise format for future graphic manipulation (soft copy), such as a Geographic Information System (GIS). In these digital cases, the use of a plotter is a supplement providing a global overview of the aerophotogrammetry process.

The use of soft copy files is extremely convenient for hydrographic survey processing. The information from the photogrammetric process can be superposed, compared and made compatible with other data which is generated from the topographic field work, previous work or near shore bathymetric data.

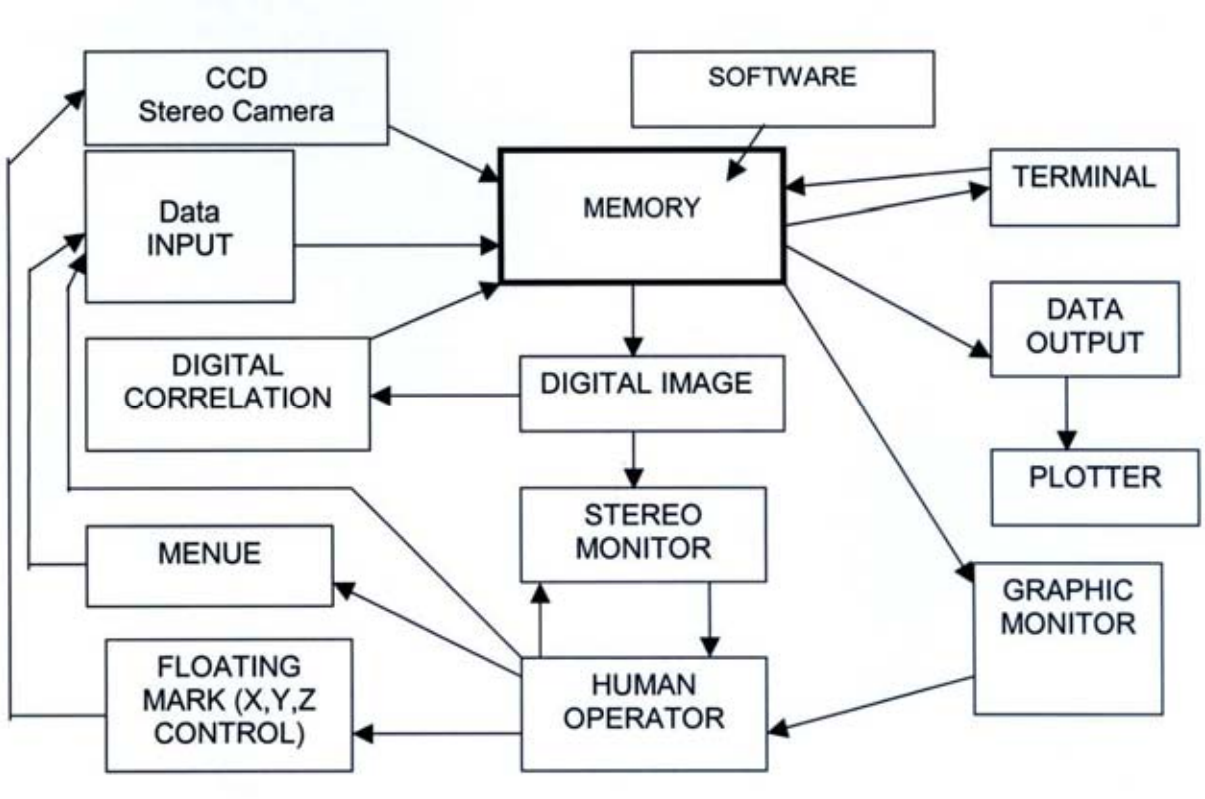

Fig. 6.32

3.1.8 Photo interpretation

Photo interpretation involves the examination of photographic images, sometimes supported by stereoscopic observation, which allows the identification of objects and features, as well as certain soil properties, vegetation, etc., in order to obtain a qualitative description of its character, use or behaviour.

In many cases, the relation between flight height and smooth topographic features is not sufficient for the relief to be viewed with sufficient detail to define the drain lines, as indicated in Fig.6.19. Nevertheless, it can be achieved through a minutely precise analysis of aerial photographs, thus, it is possible to detect the existence of temporary courses, separated by watersheds, whose features are clearer than in the relief interpretation. This is a typical example where photo interpretation can achieve more accurate descriptions than photogrammetry with small scale imagery, although this procedure should not be extrapolated.

Generally, image interpretation, photo interpretation being a particular case, can be undertaken more successfully by experts in their particular field. For example, a coastal engineer can make better conclusions regarding the behaviour of a beach than a surveyor, because he can analyse wave refractions and certain erosion processes.

In certain cases, very detailed contour lines can be traced assisted by images obtained from different periods, not only above the high waterline and the inter-tidal zone, but for the existence of permanent vegetation or the lines left by the flood tide currents before the backrush or the water image changes tonality with the depth.

An accurate combination between the calibration and the observation can be attained by comparison of some topographic or bathymetric measurements. This can produce excellent results. Nevertheless it is necessary to prove a strict correlation between the detected evidences, for example tone changes, and the measurements. If this is not verified, the basis for the interpretation must be revised. Sometimes, the behaviour of thematic phenomena is incorrectly interpreted as the presence of shoaler zones.

A photo interpreter's experience and the checking of doubtful details in the field allow photo interpretation to be a very useful procedure as a complement to topographic surveys.

3.2 Non-Photogrammetric Remote Sensing Imagery

In this section only non-photogrammetric systems and methods will be considered. As stated previously, the term "Remote Sensing" is applied to the detection of objects and the determination of their position and some properties without making actual physical contact with them. Although the term remote sensing covers all the techniques for making observations at distance, such as those based on acoustics, gravity and aero-magnetics, at the present time, the normal sense of the term has been restricted to that of the electromagnetic energy.

A generic remote sensing system is composed of four basic elements (Chuvieco, 1995) (Fig. 6.33):

Sensor system: sensor and platform (including the rocket vehicle which transports it until in the definitive operation orbit);

Scene: is the ground area covered within a certain time by the sensor;

Source of Energy: is the Sun (for the passive sensors) or generated by the sensor (for the active sensors).

System of Process, Sale, Interpreter and Final User: involves the reception-capture station, antenna, tracking system, sales, distribution agency, interaction with the client and finally the final user (i.e. government agency, defence, university, domestic service companies, etc.).

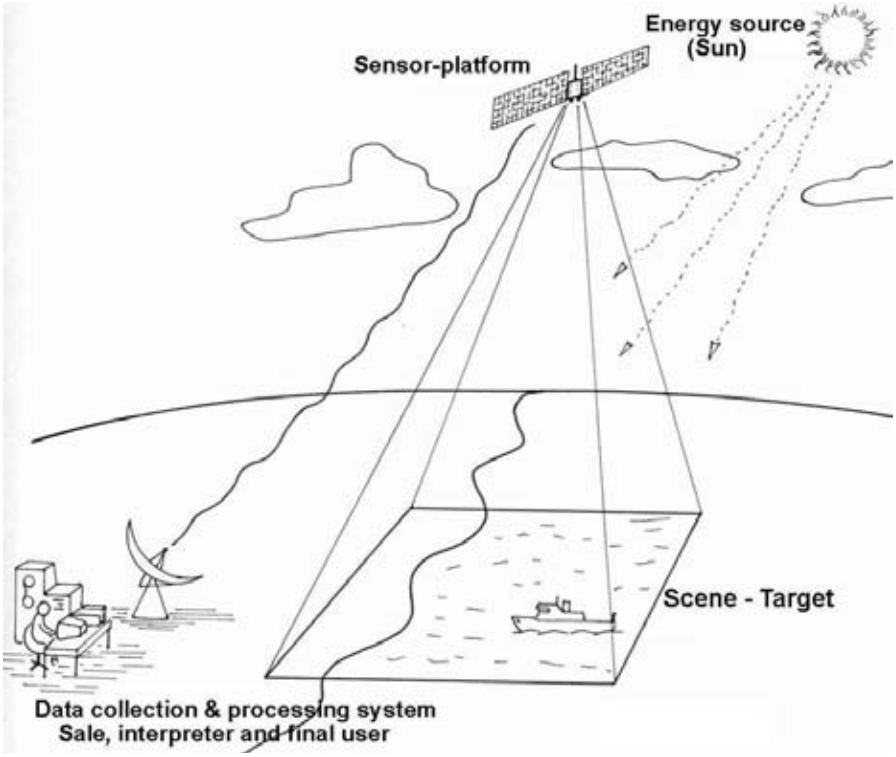

Fig. 6.33 "Remote sensing system (satellite passive sensor case)"

3.2.1 Satellite and sensors for Earth Resources Remote Sensing

The satellites employed in earth resources remote sensing use 2 types of **orbits** (Fig. 6.34):

a. **Equatorial geostationary orbit:** the satellite is at circa 36000 km distance and is over a fixed point on the Equator. These satellites only look at the Earth's surface in a particular way for a dedicated function; i.e. European meteorological satellite METEOSAT, the American GOES, etc.

b. **Cuasi-polar sun-synchronous orbit:** the satellite uses much lower orbits (700 to 1200 km) and it always passes over the Equator at the same time (sun-synchronous), moving a certain distance along the Equator and passing near the poles.
i.e. SPOT, LANDSAT, NOAA, METEOR, JERS, ERS, RADARSAT, etc.

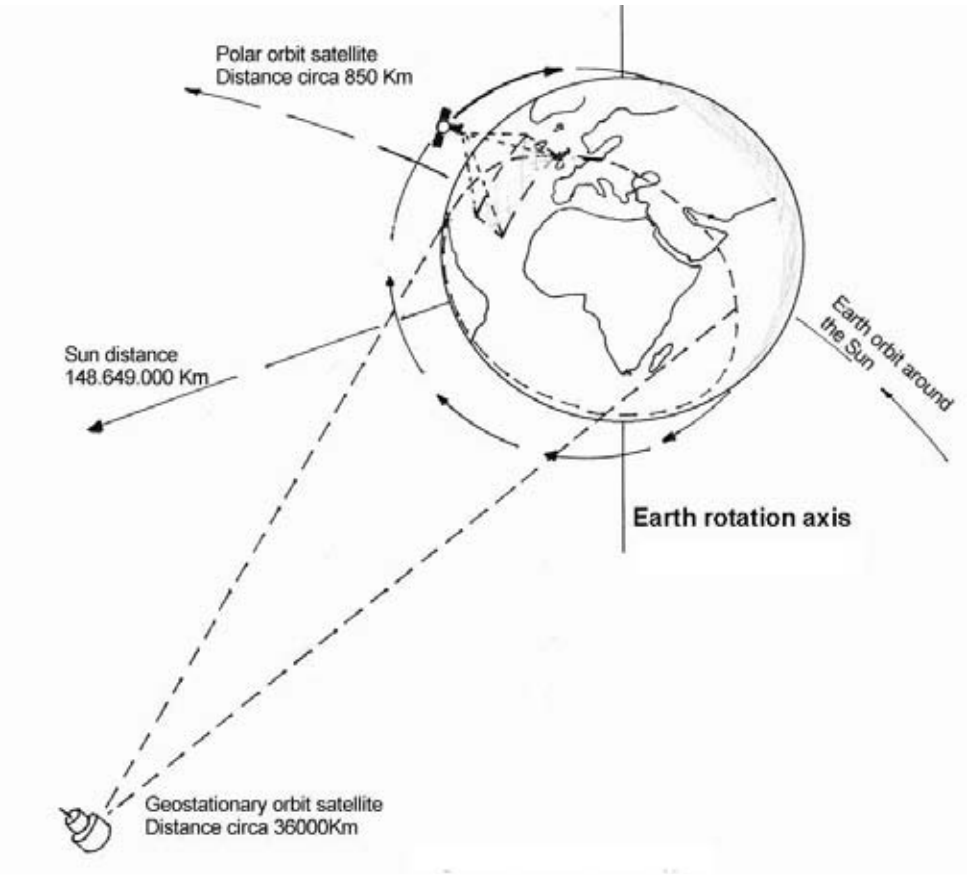

Fig. 6.34 "Main satellite orbits"

The **instrument-sensors** can be classified according to system methodology:

a) In the origin of the **energy source** used, they are divided into (Fig. 6.35):

Passive: the instruments capture the radiated energy emitted from the area of interest and generate a corresponding and measurable electric signal. The energy source is the Sun.
Examples: MSS and TM LANDSAT, AVHRR NOAA, HRV SPOT, MMRS SAC-C.

Active: the sensors emit an energy beam and register the backscattered proportion from the Earth's surface. They are able to obtain images in any meteorological or light conditions, since the energy source is self generated and independent of the Sun.
Examples: SAR ERS, JERS and RADARSAT.

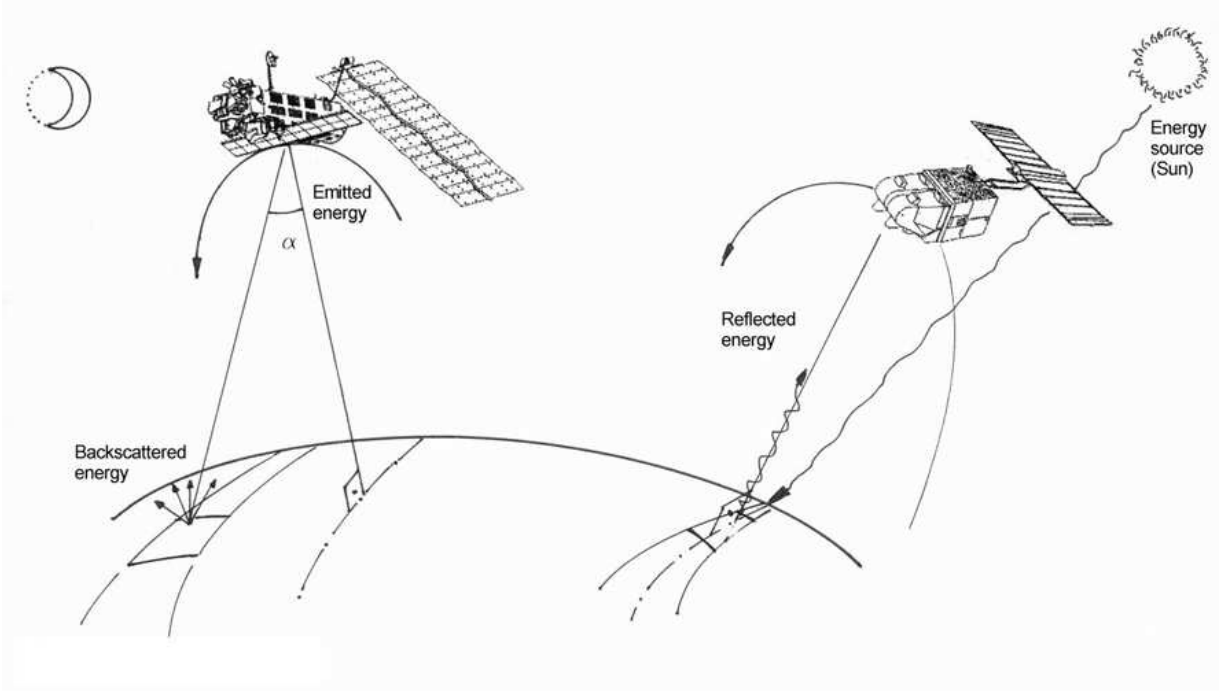

Fig. 6.35 "Passive and active sensors"

b) The useable sections of the **electromagnetic spectrum**:

Optic: this includes the visible spectrum of the human eye (0.4 μm – 0.7 μm) and the reflected or near infrared (0.7 μm – 3 μm).
Examples: MSS LANDSAT, HRV SPOT, MMRS SAC-C.

Thermal: corresponds to the thermal or emissive infrared (7 μm – 15 μm).
Examples: AVHRR NOAA, TM LANDSAT.

Microwave: the longer length waves (mm to cm) used mainly by the radars.
Examples: SAR ERS, JERS and RADARSAT.

Sources of electromagnetic radiation which may be used for remote sensing can be natural such as the sun, earth and atmosphere or artificial sources such as flash lamps, laser and microwave emitters.

The main natural energy source is the sun, whose radiated energy reaches a maximum (peak) at a wave length of 0.47 μm (green visible). On its way to the Earth, sun energy passes through the atmospheric layer and undergoes complex interactions, summarised in the effects of absorption, reflection, scattering and emission (Fig. 6.36):

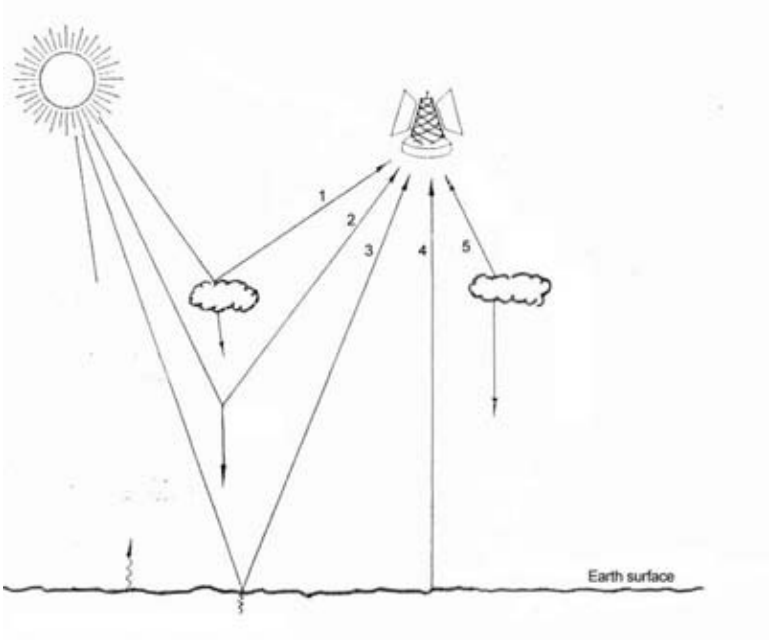

Fig. 6.36 "Radiation received by the sensors"

The different components are:

1. Radiation reflected by the atmosphere;
2. Radiation scattered by the atmosphere;
3. Radiation reflected by Earth surface;
4. Radiation emitted by Earth surface;
5. Radiation emitted by atmosphere.

Only a small part of the energy captured by the sensor is used to extract information regarding the Earth's resources: that reflected and/or emitted by the Earth's surface. The rest should be filtered to enable additional information to be extracted.

There are zones in the spectrum, which have a better electromagnetic radiation path; they are called "atmospheric windows" (Fig. 6.37). In these zones the absorption is lower, so the transmitted energy is higher. The main windows are:

0.4 – 0.7 μm in the visible;
3.5 – 5.5 μm and 8 - 14 μm in the thermal IR

The sensor captures and measures the electromagnetic energy coming from the area of interest in discrete spectrum bands. The measurement of the intensity of the transmitted energy from a target in each band is called spectral response or the "spectral signature" of this target.

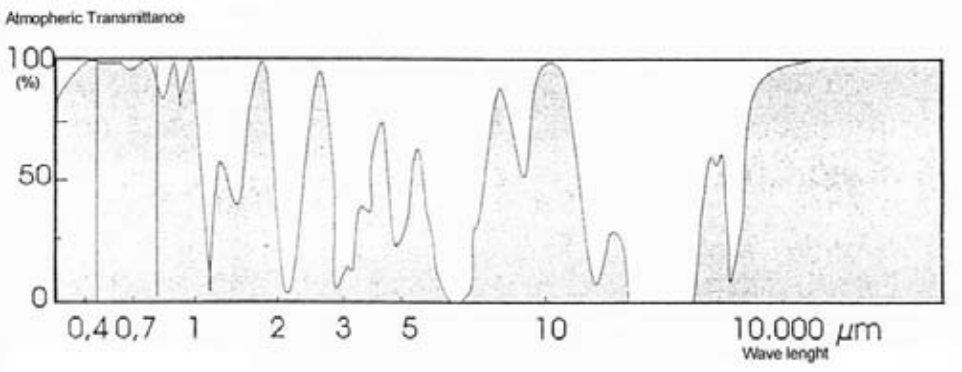

Fig. 6.37 "Atmospheric windows"

3.2.2 Main Remote Sensing Systems

The main remote sensing systems can be classified as follow:

PASSIVE SENSORS:

- Photographic systems
- Return Beam Vidicon Systems
- Opto-mechanical scanners
- Opto-electronical scanners

ACTIVE SENSORS:

- Radar systems

- **Photographic systems**

The photographic cameras were the first sensors able to receive multispectral pictures from space. They continue to be a method often used for remote sensing, particularly from air platforms. Their basis of operation is the impression of a scene onto photosensitive films via an optic system which allows control of the exposure conditions.

Most important characteristics are:

a. Film type: The most commonly utilised is the panchromatic film, on which the whole visible spectrum can be captured on a single emulsion. Radiation corresponding to the near or reflected infrared (IR) is captured in grey tones with the infrared film.

b. Number of objectives: Multiple observations can be carried out with two different constructions, incorporating several lens, each one of them with an appropriate filter, either in a single camera, which enable impressions of the same image in different bands of the spectrum, or by assembling several cameras on the same platform, each one with different filters and appropriate films. (See Fig. 6.38)

c. View angle: In vertical photography (the most often employed), the images are captured approximately orthogonal to the land surface (5° deviation being permitted) and in oblique photography, a viewing angle of less than 90° (used in studies of the relief, urban infrastructure, etc.).

d. Observation height: The height (**H**) is highly variable, depending whether it is air or space photography and the relationship with the focal distance (**f**) determines the scale (**S**) of the obtained photogramm (See 3.1.1).

$$S = f / H$$

An example of space photography can be cited in the panchromatic and IR pictures taken from the Space Shuttle during the European Spacelab Program (1983). Indeed, with the metric camera RMK 20/30 some stereoscopic pictures were obtained of several regions of the world, at a scale of 1: 820.000 at 250 km high with an approximate resolution of 20 to 30 m, these were used mainly for cartographic purposes (Konecny, 1986).

More recently, cameras like the MKF-6 (Fig. 6.38), on board the Soyuz space laboratory, have allowed the capture of pictures of high resolution and in 6 bands of the visible and near IR spectrum (Chuvieco, 1995). Also on board the Soyuz, cameras, as the KFA 1000, with focal distance of 1 m approximately and at 351 km of distance, achieved geometric resolutions from 5 to 10 m.

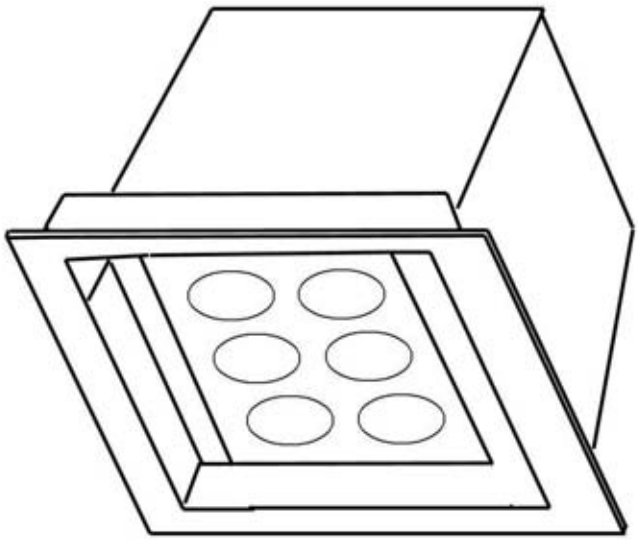

Fig. 6.38 "MKF-6 multispectral camera"

- **Return Beam Vidicon Systems**

Return Beam Vidicon (RBV) was a passive sensor similar to a television camera tube. This sensor failed early on the first ERTS (called LANDSAT after) and never came into routine use.

Two RBV cameras observed the whole surface in instantaneous form, using colour filters to provide multispectral bands centred in the blue-green, yellow-red and red-IR spectra in the first two LANDSAT satellites.

A forth RBV camera on Landsat-3 was a panchromatic (0.505 - 0.750 µm) version that provided four adjoining images at 30 m resolution.

This type of system has been used in TIROS and LANDSAT satellites, among others.

- **Opto – mechanical scanners systems**

These types of scanner are opto-mechanical instruments, where a mechanically driven optical element, generally a rotating or oscillating mirror, is used to deflect an optical beam to the detectors at right angles to the line of flight. The axis of rotation or oscillation of the mirror is parallel to the line of flight or orbit.

As examples, aircraft Daedalus scanner uses a rotating system and the LANDSAT satellite series utilises an oscillating system in their Multi Spectral Scanner (MSS) (Fig. 6.39).

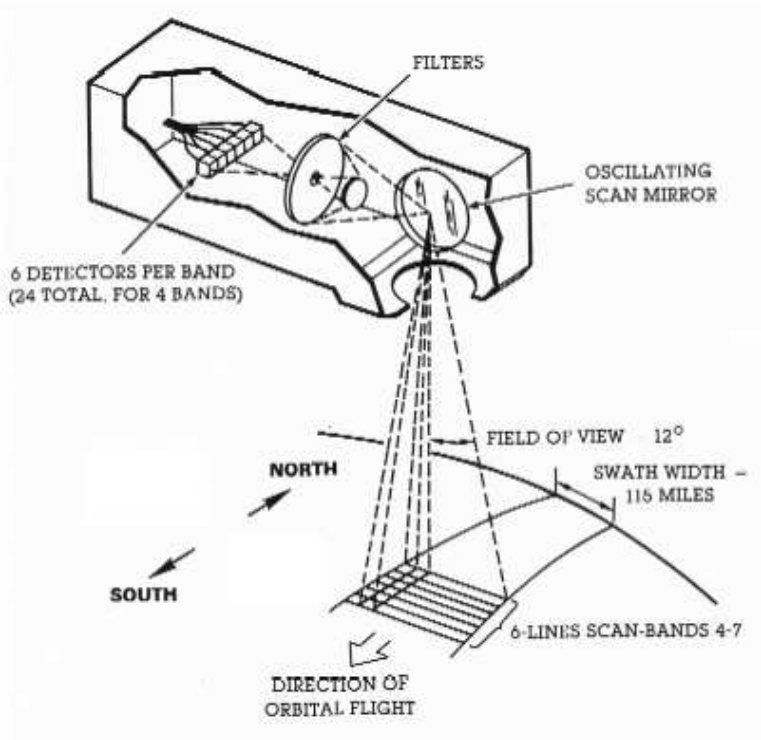

Fig. 6.39 "LANDSAT MSS (after NASA, 1997)"

MSS LANDSAT consists of a mobile mirror that oscillates perpendicularly to the flight direction. The received radiation passes to a set of detectors which amplify and convert it to an electric signal. This signal is converted to a numeric value which can be stored on board or transmitted to the network of reception ground antennas.

In summary, the sensor transforms an analogue signal, the received radiation, into a digital value, generating digital images. These radiation values can be translated, again, in radiation levels, knowing the calibration coefficients of the sensor and the conditions of acquisition.

The number and attributes of the detectors, which contain the scanning equipment, is fundamental in understanding the characteristics of the resulting image.

The signal sent by the optic system to these detectors is re-sampled at regular intervals, so only a numeric value is recorded at each certain distance. That interval marks the size of the minimum information unit acquired by the sensor; it is termed a "pixel" (picture element). The signal detected by each pixel has a direct relationship to the type of observed surface. If the signal originates from a homogeneous surface, the value of the pixel will correctly define it; in the case of a heterogeneous surface, the result will be an average of the characteristics of the area observed.

In many scanners, the received signal breaks down on board into several wavelengths, each one directed to a special type of detector sensitive to this energy range. These are known as multispectral scanners, because they are able to detect the same land surface utilising different spectrum bands.

The advantages of the multispectral scanners, in relation to the simple photographic sensors, are (Chuvieco, 1995):

a. They enable enlargement of the detected spectrum band to wavelengths longer than the visible one. The emulsions are limited to the range 0.4 to 0.9 μm, while the scanners can embrace from 0.4 to 12.6 μm, including the medium and thermal infrared;

b. Easier calibration and radiometric correction of data;

c. Ability to undertaken systematic and extensive coverage due their capacity to transmit data in real time;

d. Digital recording of the information, which improves their reliability and allows computer processing.

Disadvantages are the limited area resolution and the need for specific image processing systems.

Examples of these systems are the Advanced Very High Resolution Radiometer (AVHRR) in the satellites TIROS-NOAA and the Multi-Spectral Scanner (MSS) LANDSAT.

A more sophisticated multispectral imaging sensor, named the Thematic Mapper (TM), has been added to LANDSATs 4 to 7. Although similar in operational modes to the MSS, the TM consists of seven bands which have differential characteristics, adding bathymetric, geological and thermal capabilities with improved geometric resolution.

- **Opto – electronic scanners systems**

In the optic-electronic scanners, also called "pushbroom", the oscillating mirror is eliminated, due to a chain of detectors which cover the whole field of vision of the sensor. These detectors are energised by the orbital movement of the satellite, enabling them at each instant to survey a complete line, which moves simultaneously with the platform. The solid detectors which make-up an optical-electronic scanner are termed "Charge Couple Devices" (CCD) (Fig. 6.40).

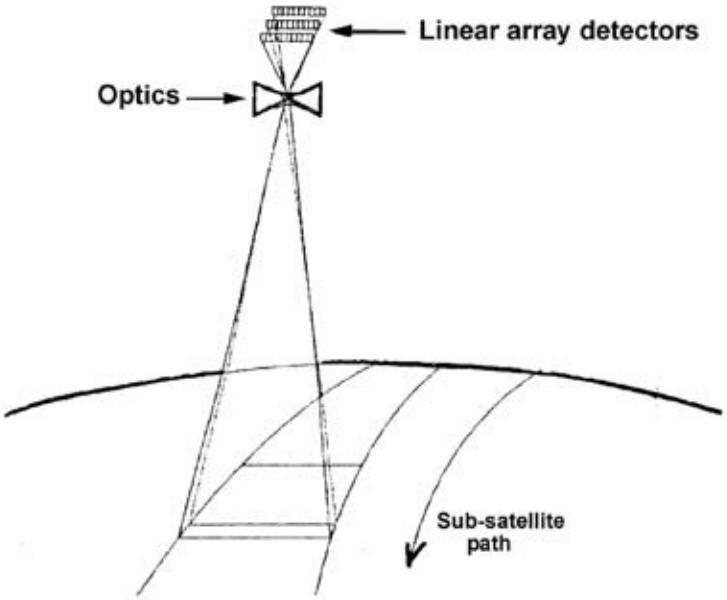

Fig. 6.40 "CCD system (after Chuvieco, 1995)"

With this type of sensor the space resolution of the system increases compared with conventional scanners, whilst eliminating the moving parts. It is also not necessary for the sensors to be interrogated by pixel, but rather by line, which in turn makes it more responsive for detection and emission of data.

Examples of this system are the High Resolution Visible (HRV) sensor of the French SPOT satellite, the German MOMS and the sensors of Indian IRS-1 and Japan MESSR MOS-1.

- **RADAR systems**

The RADAR (**RA**dio **D**etection **A**nd **R**anging) enables information about the topography, roughness, land cover and moisture of the scene to be acquired using an active radiometer of microwaves, which works in a spectral band between 0.1 cm and 1m. Due to their ability to operate in any atmospheric and light condition, they are increasingly used. There are important differences between how a radar image is formed and what is represented in that image compared to optical remote sensing imagery. To interpret radar imagery, it is necessary to understand the radar configuration, the energy associated with radar remote sensing, the way in which that energy interacts with surface targets and the way in which this interaction is represented in the image (Davidson, 1997).

The radar principle of operation is based on the emission of a pulse (beam) of microwaves (radio) toward the scene or target. The incident energy is backscattered by the scene towards the radar, which measures the intensity (detection) and the time lapsed between emission and reception (range) (Fig. 6.41).

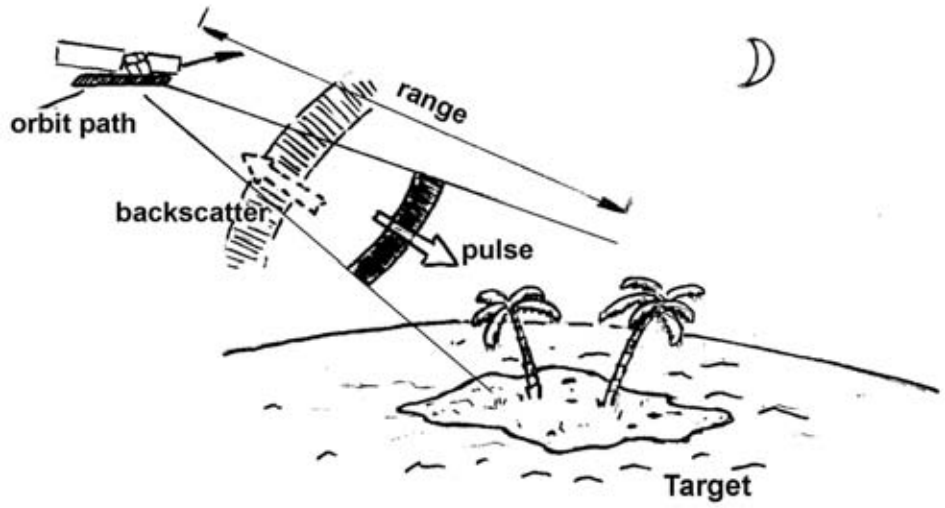

Fig. 6.41 "RADAR basic operation"

The **Synthetic Aperture Radar (SAR)** is the radar type most used in satellites. The principle is based on the Doppler effect, which affects the recorded observations when a relative motion between an object (target) and sensor is observed in the pulses from the terrestrial surface target caused by successive moments of the satellites orbit trajectory. The resulting resolution is equivalent to that which would be obtained with an antenna of similar length at the distance between the extreme points from which backscatter is received from the same target (Fig. 6.42).

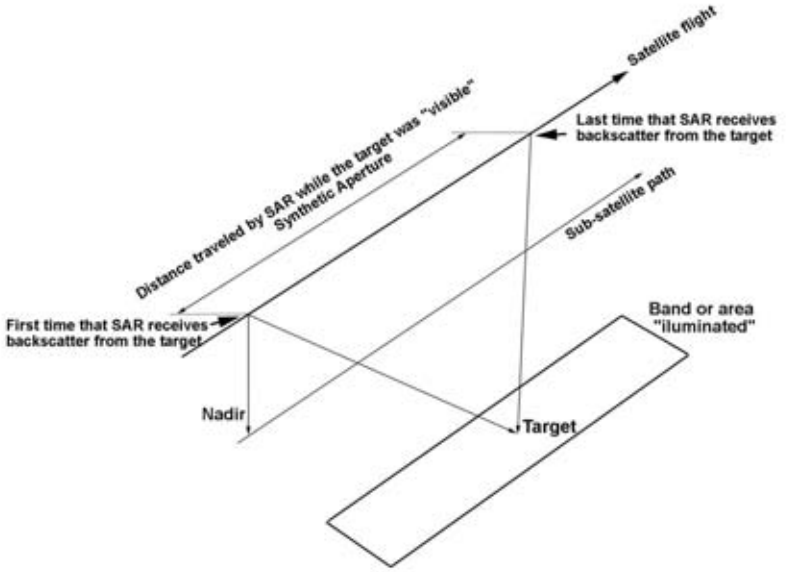

Fig. 6.42 "Synthetic Aperture Radar concept"

Examples of SAR natural resources sensors are the European ERS and ENVISAT, the Canadian RADARSAT and the Japan JERS.

3.2.3 Image Structure and Support

An image is generated from the energy captured by the sensor, which converts it to an analogical signal. Then it is processed and stored as a numeric value. The regular storing interval of the signal determines the images' unit of information. This minimum segment of data, represented by a single digital value, is termed a "pixel" (Picture Element), and, as was previously stated, it depends on the sensor geometric resolution. The pixel is characterised by a Digital Number (DN), resulting from the digital codification of the radiation detected for that range of the spectrum or band.

The numeric image is a geometric array (matrix), of two dimensions. In each pixel **Pij** (elementary point of the matrix) there are three associate values:

a. their line co-ordinate **Li**;
b. their column co-ordinate **Cj**;
c. the physical measure made by the receiver in that pixel in a range of wavelength: DNij.

A multispectral image is constituted by **k** arrays, called channels or bands. In this case, the image becomes a three-dimensional array, incorporating the band like third dimension. For example, an MSS LANDSAT multispectral image possesses four channels MSS_k, where k = 1, 2, 3, 4. (Fig. 6.43). The radiometric intensities of a channel are numeric recounts with values whose limits are between 0 and 255, allowing up to 256 possible values in general. These values are coded in bytes or 8 bits.

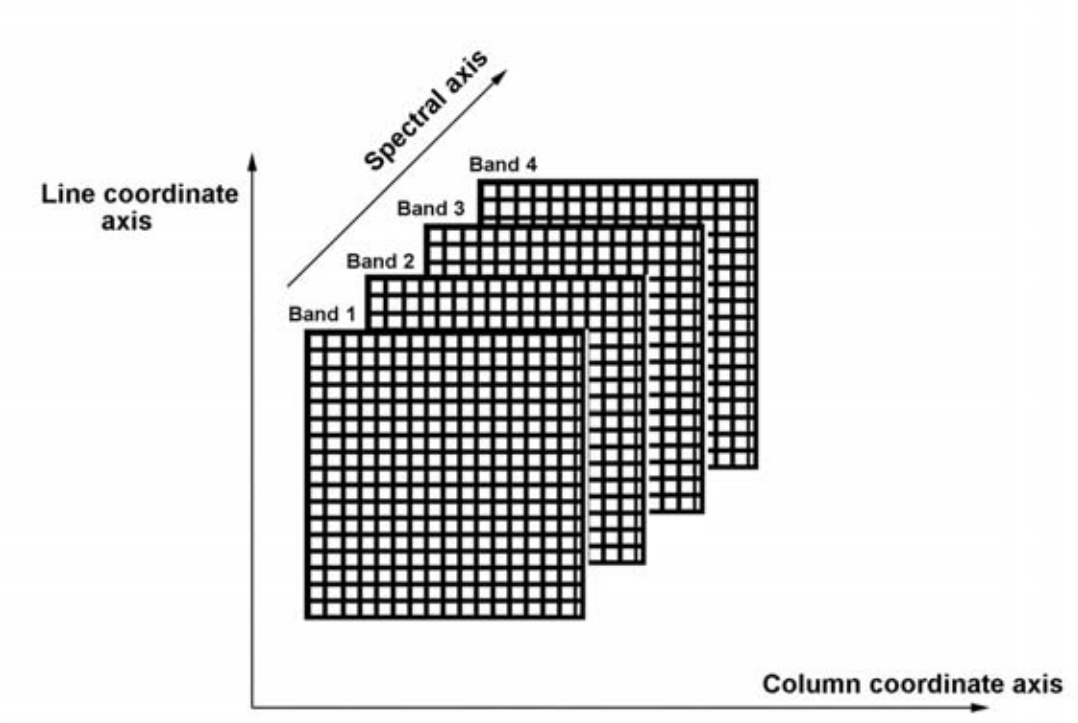

Fig. 6.43 "Multispectral image array structure"

The fundamental principle of visualization of a digital image is to associate a colour or a tone of grey to each radiometric value, conserving at the same time the matrix representation of the image. There are two visualization possibilities: the visualization of a single channel and the visualization of several channels in additive synthesis of colours.

In the case of unique channel visualization, a correspondence between intensity (DN) and tone of grey is defined, so that the minimum intensity (0) is assigned to black and the maximum intensity (255) to white, assigning the intermediate values to different tones of grey. The histogram of a numeric image is a graphic representation of the frequency of appearance of the different levels of radiometric intensity (DN); thus expressing the pixel distribution as a function of their radiometric intensity. The histogram allows one to know the distribution of the pixels in the image for the interval values from 0 to 255.

To improve a digital image it is possible to modify the correlation between numeric values and the range of grey or colour. The objective is to increase the global contrast of the image. It is done by replacing the original values, between the minimum and maximum levels, with new values distributed within the 255 levels, as a way of using all the available grey levels in the visualisation. This can be achieved by applying a lineal function (straight line), adapting the image according to the curve of the accumulated histogram or by other viable methods of distribution, the most common using exponentials, the lineal segments, etc.

For colour visualisation, the principle is the same as that for visualisation in black and white (B/W). The only differences being there is a colour associated with each channel numeric value and no grey intensity. Thus there should be a proper palette of colours defined.

There are conventions for the channel colour combination. For instance, the MSS LANDSAT normalised False Colour Composite (FCC) image assigns the blue colour to the green band (centred at 0.55 μm), green to the red visible band (0.65 μm) and red to the near-photo IR band (0.75 μm).

There are alternatives for the **image recording format**. In general, the image contains a "header" file, which indicates the recording format, the sensor type, geographical location of the area, date, solar position, data of corrections and calibration of the image. The more frequent recording formats are:

BSQ (Band Sequential): DN follows a sequential order, leaving the origin (line 1, column 1) until the final pixel of the first band; the succeeding bands then follow on.

BIL (Band Interleaved by Line): The DN are ordered by line. The first line of band one begins, then the first line of the second band and continuing on with the other bands. Once all the bands are completed, it passes to second line of the first band, the second line of the second band, etc.

BIP (Band Interleaved by Pixel): The format is similar to the previous method, except in this case the DN are ordered by pixel. The first pixel is recorded at the origin of each band, then the second pixel, and so forth until completing the image.

The **available image support**, requesting the negative or positive film or photographic page, varies according to the space programme. Negative film is the most versatile product, since it enables the generation of all the amplifications considered necessary at the desired scale. Positive film is very useful for photographic reproduction and impressions of the image. Paper is the most commonly issued analogue media as it guarantees the ability for a direct interpretation of high quality images; however the scale in which it is presented is rigid. LANDSAT TM image negative films (23x23cm) are offered at a scale of 1:500.000, while other programmes offer images at a scale of 1:1.000.000, additionally amplifications can be obtained in paper at scales of 1:250.000 and 1:100.000.

Presently magnetic Computer Compatible Tapes (CCT), Exabyte tapes and Compact-Disk Read Only Memory (CD-ROM) are the most useful digital media types.

3.2.4 Interpretation and Processing Fundamentals

Image interpretation refers to the techniques required to define, to recognise and to identify objects or phenomena in an image and to interpret their meaning. To conduct these tasks, it should be considered an essential part of preparation work to define the parameters and methods to be used.

The scale is one of first parameters to be defined and is linked to the previously mentioned objectives; the scale defines the minimum unit of information which should be included in the map, termed the Minimum Cartographic Unit (MCU). It is recommended that the MCU not be less than 4 mm^2 at scale of the map. Thus, the work scale should be related directly with the most suitable type of sensor to undertaken the project. In accordance with the International Cartographic Association guidance, the most suitable scale limits for the different sensors are:

LANDSAT – MSS	**1 : 200.000**
LANDSAT – TM	**1 : 100.000**
SPOT – HRV	**1 : 50.000**

To summarise image interpretation factors, the following should be considered:

- **Sensor-platform system**: The most appropriate sensor type depends on the objectives and the level of precision required for the project; i.e. global mapping (planispheres) will be carried out starting with sensors of low space resolution (NOAA AVHRR or SAC-C MMRS) while those requiring a larger scale will use sensors that offer greater spatial detail (LANDSAT TM or SPOT HRV). However, in other cases, the spatial resolution is secondary to time or spectral resolution; if the studied phenomenon is very dynamic in time, such as the detection of spills of oil in the sea, it would be suitable to use sensors of higher temporary resolution, whilst sacrificing space precision. In other projects, spectral dimension will be more important such as for studies of ocean colour starting from optic sensors.

- **Image capture date**: The most suitable moment to acquire images will be when the phenomenon to be studied has its highest discrimination ahead of others of similar spectral behaviour; i.e. riverside area mapping with large tidal amplitude and extended beaches, it will be most suitable to choose low tides due to having the highest quantity in detectable coastal details, thus image capture should be planned with an analysis of local tide predictions.

- **Image support**: Selection of media, on which the interpretation is carried out, depends on the techniques to be applied. If a visual analysis, then three main aspects should be considered: the material support of the image, the scale and the band number or selected combination of bands.

Photographic film or paper is ideal for analogical (visual) interpretation, while Exabyte, floppy disks, CCT or CD-ROM are best for digital processing. Additionally, the ideal number of bands for a project depends on the phenomenon being mapped or monitored.

- **Selection of the analysis method**: Image analysis methods can be visual or digital. Each has its own advantages and disadvantages. Visual treatment requires lower inversion than digital processing; however, computer processes presents lower unitary costs with larger areas, while visual interpretation follows linear costs.

In summary, when undertaking complex works the results of both methods are suitable, although digital methods are gaining in importance due to advances in image processing, via computer equipment (hardware) and programs (software).

Remote sensing **image visual interpretation** is based on the same skills used in classic air-photo interpretation. VIR and SAR images interpretation are similar in that the same interpretation key is used. When SAR images are employed, the unique properties of radar imagery must be remembered and incorporated into the interpretation process.

Main elements of visual interpretation used are:

- **Scale**: It is the relationship between lineal dimensions in the image and on the terrain (ground).

$$\mathbf{S = Image / Ground}$$

In general, scale (**S**) is expressed as a division with numerator equal to "**1**" and denominator "**D**":

$$\mathbf{S = 1 / D}$$

- **Shape and size**: Shape and size are linked directly with scale; shape refers to the spatial form of an object or area, shape can help to distinguish between natural and cultural features.

The size of a feature can be helpful in distinguishing features from each other in relative terms. The scale is one factor, which influences the size of an object or feature present on the image. Shape, size and scale are fundamental for the definition of the patterns.

- **Tone**: The tone refers to the energy intensity received by the sensor for a certain band of the spectrum. In a photographic product, pixels with dark tones indicate those areas where the sensor detected a low sign, while the clear areas are those of high radiation values. The tone is related closely with the spectral behaviour of the different land covers for the specific spectrum band in which it works.

In radar images, tone results from target backscatter, tonal variations are usually functions of the strength of the radar backscatter from the ground; i.e. smooth water surfaces appear dark because they act as a specular reflector with the energy being reflected away from the sensor.

- **Colour**: In VIR images the colour is a consequence of the selective reflectivity from the objects to different wavelengths. Those surfaces with high reflectivity in visible short wavelengths and lower in the rest appear with blue colour, while those which absorb short wavelengths and reflect long ones

appear with a red tint. If the sensor captures information in the bands of the blue, green and red spectrum, a composition in natural colour can be obtained.

SAR images are mono-band and so they are viewed in grey tones.

- **Texture**: Texture is the frequency of tonal or colour changes. It refers to the apparent roughness or softness of the image region, representing the space contrast between the elements from which it is composed.

The texture of the image comes from the relationship between the size of the objects and the resolution of the sensor. In general, texture is classified in thick, medium and fine texture. In SAR images, it may be classified as smooth, fine, grainy, linear, speckled and flecked.

Contrast is the relationship between clear and dark areas or the tone relationship between an object and the surrounding objects.

- **Shadow**: Usually shadow links the dimensions of the object (mainly its height) with the angle of incidence of the energy (Sun or waves beam).

In SAR images, shadows indicate relief type. Shadow length can be used to estimate height, while their projection indicates spatial form.

Finally, visual interpretation is carried out by evaluating all the above mentioned parameters and comparing the characteristics of the displayed objects with well known patterns (i.e. land cover, drainage net and urban infrastructure, etc.).

The process of identifying or helping to identify features through local and regional context is called association. For instance, terrain landscape and Antarctic Sea features tend to form associations through well-understood natural relationships and processes (i.e. floes, fractures and glacial landforms).

- **Pattern**: Pattern represents the orderly spatial arrangement or repetition of features. Spacing, density and orientation are indicative of pattern; for example river (or watershed) net is linked to relief, dendritic pattern is representative of an undulating area (hills, mountains), while meander patterns represent flat or plain areas.

3.2.5 Image pre-processing and complementary data

The satellite images, obtained by a third party, will have been processed by the acquiring institution in order to standardise the available products. A base treatment is conducted and, at the client's request, additional optional treatments improving the geometry and radiometry of the product can be completed, better adapting it to the objectives of its future application.

The process type and their denomination are characteristic of each system. In general, it is organised in a progressive hierarchy of corrections, such that each level includes all the previous ones whilst adding others.

For example, for HRV SPOT products, there are the following treatment levels (Fig. 6.44):

Level 1A: General basic level for all the images, where a calibration of sensors in each spectral band has been conducted. There is no geometric correction. These images are used in fine radiometric studies.

Level 1B: Systematic deformations caused by terrestrial rotation, panoramic effect, drift effect and incidence angle are corrected. There are corrections for geometric origin, but that may have influenced the radiometry, because a re-sampling is carried out.

Level 2: Geometric and localisation corrections are carried out using internal and external data. The internal data employees are: data of restored orbit, geometry of the instantaneous field of view (IFOV) and satellite altitude restitution auxiliary data. The external data are: parameters of the selected plane representation system, rectification medium altitude selected and ground control points (GCP) co-ordinates.

There are 2 sub-levels, in functions for the use and not of the GCP:

Level 2A: Two-dimensional corrections are carried out to transfer the scene to a certain cartographic projection (Mercator, Transverse Mercator, Lambert, etc. - see Chapter 2). Data from satellite altitude and geometry of the IFOV (instantaneous field of view) are used, without using GCP.

Level 2B: The geometric correction uses GCP, obtaining a higher precision than in Level 2A.

Level 3: The geometric deformations produced by the relief are considered. It requires data from the Digital Elevation Models (DEM). The absolute position precision is of the order of 0.5 pixels. As result, an orthomorphism is obtained.

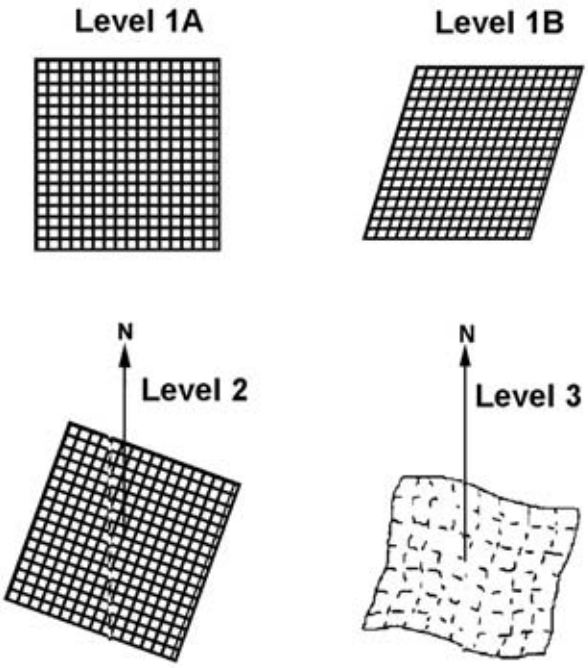

Fig. 6.44 "SPOT image processing levels (adapted from GDTA, 1993)"

Complementary data

Image processing requires complementary data to be used for its geometric corrections and preparation of the final cartographic product. The geo-codification can be conducted without the GCP but the resultant position is only relative, if a link to a reference system is required, the use of GCP will be required.

Ground control points (GCP) are points with previously known co-ordinates and clearly identifiable in the image. They are used to define the co-ordinate transformation equations from the image to the required geodetic reference system and cartographic projection. They can be obtained from cartographic documents (charts) or starting from topographical field tasks. In certain cases the land reflective signals (transponders) can be installed, which are easily detectable in the image, thus enabling the geo-codification in areas with few natural or artificial details.

Additional cartographic data (type of coasts, navigation obstacles, coastal details and urban, port and road infrastructure) can be used for the interpretation of the image or to enhance the final product. They can be obtained from digitalisation of existent charts, from geo-referenced databases (GIS) or from complementary surveys.

3.2.6 Image processing

Satellite images present geometric and radiometric distortions, which are dependent upon the sensor type, platform and the capture conditions. In hydrographic applications, information from multiple sources is very frequently used. Therefore, to standardise, and thus be able to compare and integrate the acquired data with other information, it should be normal procedure to rectify and to restore (rectification and restoration) the satellite images. The levelling and correction process depends on the evaluated images and on the application to which the final product is to be put. In some cases it can be enough just to correct the systematic errors and then co-register the images with other previously geo-referenced data; in other cases, the images will be corrected and re-sampled in a cartographic projection with a given scale. The complete correction of an image involves the initial processing of the raw image data to eliminate the geometric distortions, the radiometric calibration and the reduction of the actual data noise.

When images of diverse sources (i.e. LANDSAT TM, SPOT PAN, etc) are used, the processes of geometric correction, rectification, radiometric calibration and enhancement are prior requirements for the image fusion and they assure the compatibility on a pixel-by-pixel basis. The radiometric enhancement is as important as the geometric integrity in all aspects of mapping with images because the quality of the resulting final fused image depends on the precision of the geometric corrections in each participant image (Pohl, 1996). This should be given particular consideration given the frequent employment of mosaiced images to complete sectors of charts.

<u>Geometric treatments</u>

The geometric distortions can be classified as systematic (predictable and correctable) and accidental (random). The systematic errors are easily recoverable by applying formulae derived from modelling the sources of distortion. The accidental errors are corrected by applying polynomials with points of ground control (GCP) conveniently distributed in the image.

Geometric corrections can be grouped in following processes:

Co-registration (or registration simply): it is the adjustment of an image taking as a reference another image, using a polynomial transformation between common points in both. It is used when comparing two data sets, without utilising the cartographic projection (absolute position).

Geo-reference: it consists of the assignment of co-ordinates to the pixels of the image by means of the definition of the transformation equations.

Geo-codification: it involves the passage from image to map by means of the application of the transformation equations. The image becomes a chart, where each pixel has its corresponding geographical co-ordinate pair. The geo-codification is central to integrate images from diverse sources, achieving the integral compatibility of its data on a pixel-by-pixel basis.

Polynomial adjustment

Polynomial rectification is a relatively simple method of geometrically correcting the images. It consists of the transformation of the original image based on a group of appropriately distributed points with well-known co-ordinates. It is necessary that the points have co-ordinates in both systems: origin (**x** & **y**) and final (**X** & **Y**).

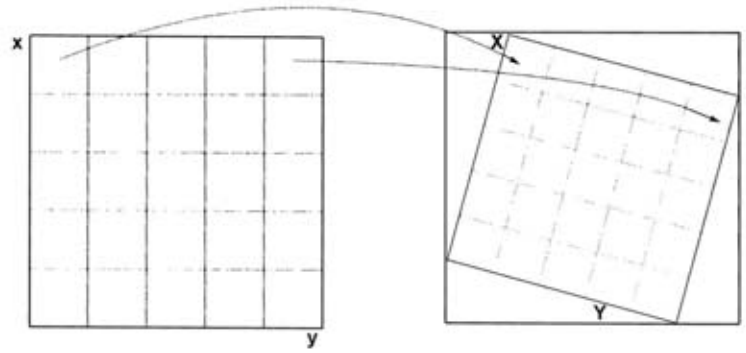

Fig. 6.45

The number of well-known points reflects the order of the polynomial in use; as the order increases, a higher number of points with well-known co-ordinates are required. A system of equations, whose coefficients are obtained by a least squares adjustment method, is produced.

A polynomial of first order (linear) requires 6 well-known co-ordinated points, it corrects for translation, rotation, scale, inclination, perspective and oblique distortions in the image (Fig. 6.46).

$$X = a_0 + a_1 x + a_2 y$$

$$Y = b_0 + b_1 x + b_2 y$$

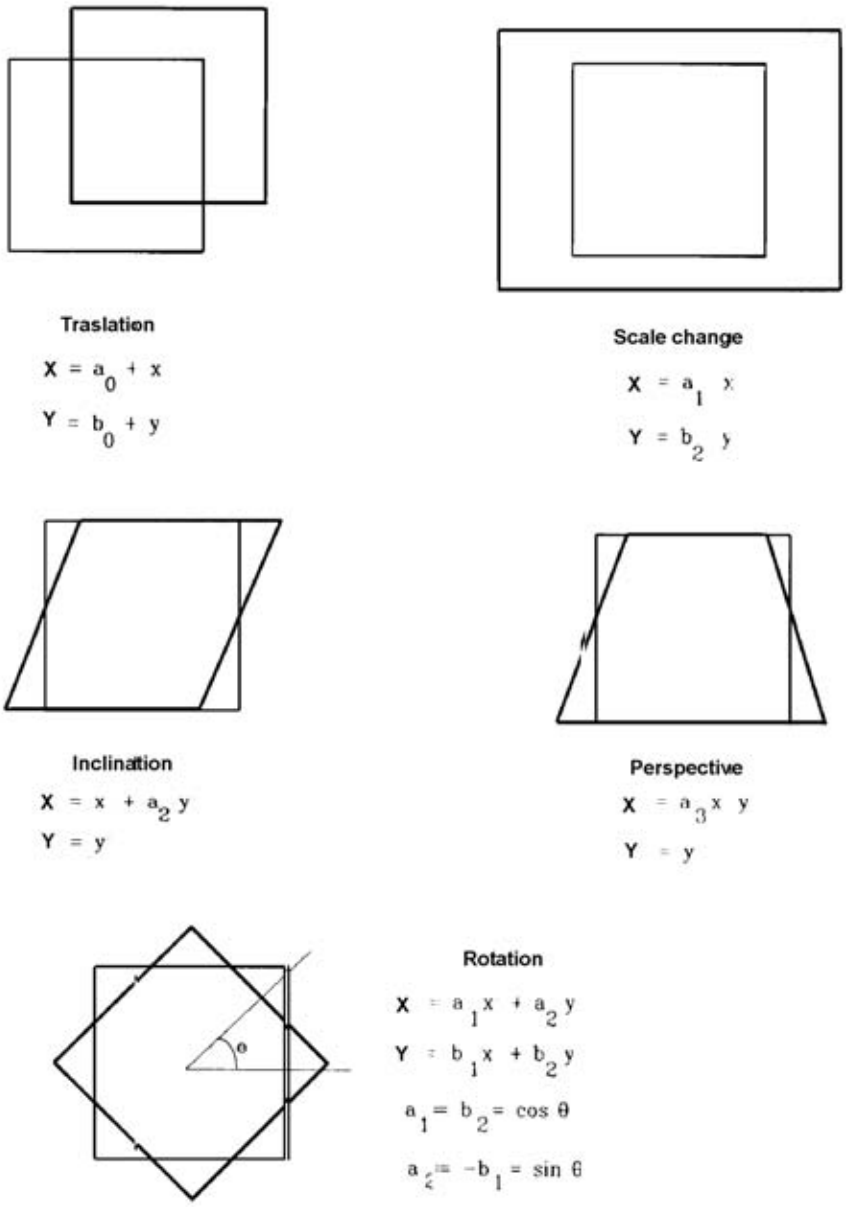

Fig. 6.46

A polynomial of second order requires 12 well-known co-ordinated points; it adds torsion and convexity parameters.

$$X = a_0 + a_1 x + a_2 y + a_3 x^2 + a_4 xy + a_5 y^2$$

$$Y = b_0 + b_1 x + b_2 y + b_3 x^2 + b_4 xy + b_5 y^2$$

Applying these equations, the original image can be transformed, resulting in an image shifted, rotated, scaled and warped.

The polynomial approach only locally corrects the image, since it depends on the distribution of points and their precision. In general it assures a correct image in flat featureless lands, but it is not very useful for very undulating areas.

The effectiveness of the adjustment comes from the evaluation of the residuals (deviations); the more often used indicator is the Root Medium Square error (RMS).

The assignment of the proper DN to the new position (**X** & **Y**) pixel can be made following different algorithms: nearest neighbour, bilinear interpolation and cubic convolution.

Nearest neighbour assigns to each pixel of the transformed image the DN of the nearest pixel in the original image. It is the quickest solution, but some linear features (roads, riversides, etc) can appear as fractured lines in the transformed image.

Bilinear interpolation calculates the measured average of the 4 nearest pixels. Here the distortion of the lineal features is smaller but the spatial contrast is diminished.

Cubic convolution considers the DN of the 16 nearest pixels. It produces a better transformed image but it requires considerably larger calculating capacity.

In summary, the choice of the method depends on the final use and objective of the project, on the available computer resources (hardware, software) and on the GCP availability. Also, image processing differs depending on whether the image comes from an optic (VIR) or from a microwave (SAR) system.

Geometric effects in VIR images

In general, optic images are more distorted by the process for obtaining the image itself than by the physical characteristics of the scene. For some sensors, such as the TM LANDSAT for example, the aspect (shape) and terrestrial rotation movement are important factors to consider during the correction of their images. In general such processes are undertaken by the supplier (see 3.3.5).

For the geo-codification, as described previously (see 3.3.4), object data of well-known co-ordinates (GCP) is a necessity and, in general, an adjustment by means of polynomials is beneficial.

Geometric effects in SAR images

SAR is a system very sensitive to the physical-chemical and geometric aspects of the target. SAR emits an energy beam that strikes the target surface sideways, creating a particular geometry with their images (Fig. 6.47) that can be summarised in the following terms:

- Altitude: distance between the satellite and the sub-satellite point on the surface of the Earth;
- Nadir: intersection of the vertical from the satellite with the terrestrial surface;
- Azimuth: direction, relative to North, of the trajectory of the satellite Nadir point on the terrestrial surface;
- Range vectors: vectors that connect the SAR to the ground, corresponding to each measured range sample at a single pulse transmission time;

- Slant range: the distance from the sensor to a target located in the range direction;
- Range direction: range vectors direction (perpendicular to azimuth);
- Ground range: the slant range projected onto the Earth's surface;
- Incidence angle: the angle between the radar range vector and the local vertical direction (Earth normal);
- Local incidence angle: angle between the radar range vector and the normal to the surface of each land element.

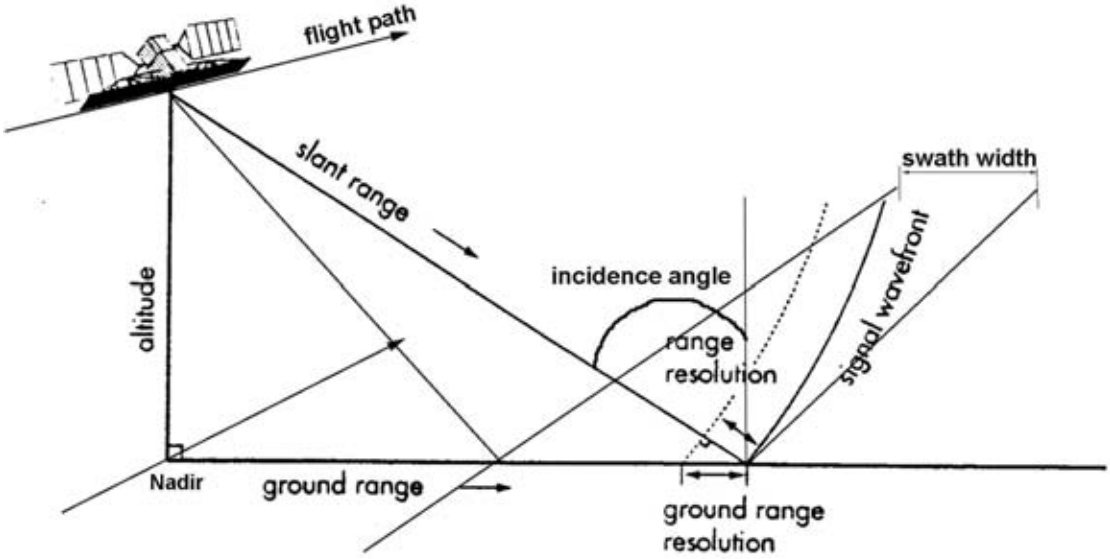

Fig. 6.47 "SAR imagery geometry (adapted after Raney 1992)"

The main parameter is the local incidence angle (Fig. 6.48). It can be seen that the geometry of signal-target interaction is a function of the land slope, which causes various distortions which differentiate it from a true orthogonal projection.

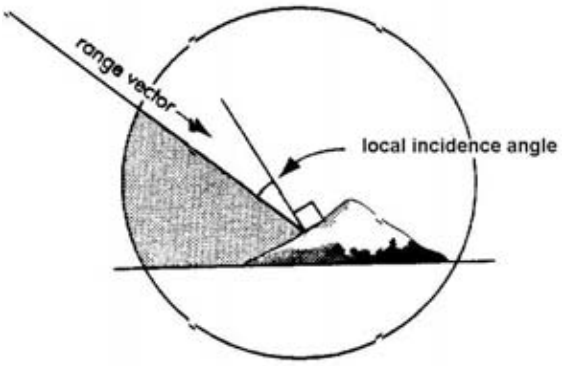

Fig. 6.48 "Local incidence angle (adapted after Raney 1992)"

Main distortions are called "foreshortening", "layover" and "shadow" effects (Fig. 6.49).

The effect “foreshortening” occurs when the local incidence angle is smaller than the angle of incidence but greater than zero. This distortion produces an effect which makes the viewed slope appear to be shortened and leaning towards the sensor.

In cases of small incidence angles or very abrupt relief, the radar signal returns from the peak of the mountain before that from the base, producing the effect of “layover”. In these cases the local incidence angle is larger than the angle of incidence.

The “Shadow” occurs on the slopes which are not illuminated by the radar signal. These areas appear very dark (without information) in the images.

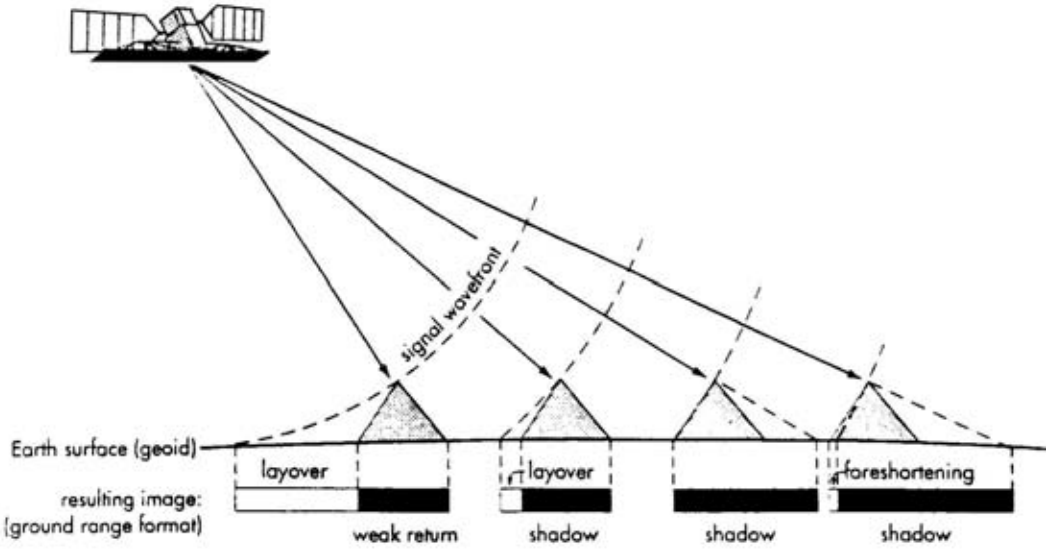

Fig. 6.49 "Distortions due to the relief (adapted after Lillesand and Kiefer 1987)"

Radiometric treatments

These techniques are useful to improve the radiometry, so that the features of interest appear clearer and more understandable to the interpreter. They are additional methods to those previously mentioned and they help in the interpretation of topographical features.

A common method involves the manipulation of the statistic of the image, represented by its histogram, which details the spectral frequency for each band of the image.

To improve the interpretation of the image, the association between the numeric values and range of grey or colour is modified with the intention of increasing the global contrast in the image (histogram stretching). This is equivalent to altering the current digital values for minimum (MIN) and maximum (MAX) with new values distributed within the 255 levels to make use of all the levels of grey possible.

The distribution can be conducted in several ways, the most frequent being a lineal distribution, which involves the values between MIN and MAX being redistributed in a straight line between 0 to 255 (Fig. 6.50).

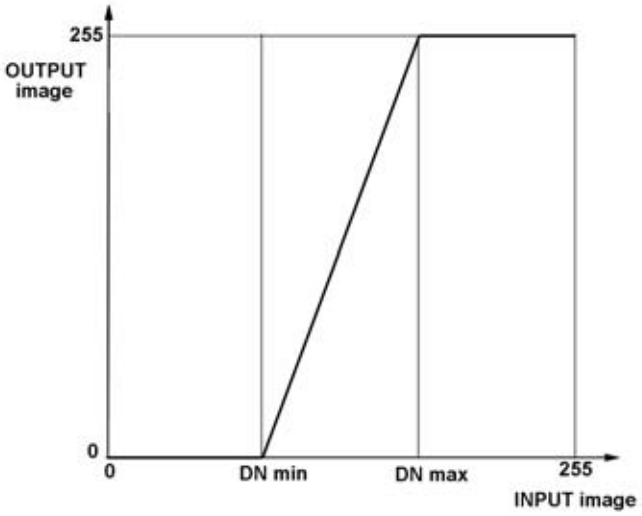

Fig. 6.50

Another means for assisting in the interpretation of the images is the application of spatial filters. The spatial filters are used to select or to mask a range of values, inside the total DN scale. These filters suppress certain frequencies, depending on the filter type. The low-pass filter reduces the range of DN in an area, reducing details and smoothing the general aspect of the image. The high-pass filter enhances the gradients of DN, i.e. the edges, which are used to better detect roads, railroads, riversides, etc.

The ideal filter is one which smoothes homogeneous areas whilst at the same time preserves limits and texture; it should maintain the arithmetic average and diminish the standard deviation.

In SAR images, adaptive filters are examples of high-pass filters and are employed to minimise effects of speckle. There have been numerous algorithms developed in recent times: Lee, Kuan, Frost and Gamma MAP.
In summary, filters are important for enhancing features and they can contribute to topographical interpretation, if they are used carefully and with discretion.

Radiometric distortions in VIR images

The sources of radiometric distortions are the atmosphere (due to dispersion and absorption effects), the sensor (effect of "striping") and the solar illumination. These effects are described in detail by Lillesand and Kiefer (1994) and Richards (1986).

Among the different components of the atmosphere, the effect of water vapour in form of haze can be reduced by applying a modification of the histogram.

A frequent problem is the presence of cloud which reduces the detectable data in optic images. Areas covered by clouds present a centre with high DN (white, near 255) with diffused and grey borders. Their corresponding shadows are also detected with very low DN. Resolution is via the application of diverse methods (thresholding and density slicing) and masks but they require a careful control, since some artefacts can be produced.

In general, radiometric distortions created by the sensor are small compared with the atmospheric influences. The most important of these distortions are those generated by the detectors, which manifest

in the form of strips (striping). It is a recurrent effect, which can be removed after the interpretation or processing of the image (Crippen, 1989).

The correction for the different solar illuminations requires a ratio between bands (band rationing). This correction is not usually applied, since the solar illumination produces an effect which facilitates the visual interpretation for cartographic updating.

Radiometric distortions in SAR images

SAR images present their own characteristics, which require particular treatments and calibration. These characteristics are related to speckle, the process based on multiple views, the range of DN and radiometric specific corrections.

The "**speckle**" is a characteristic phenomenon of radar images; it is produced by interference of the coherent beam by various individual reflectors. The backscattered energy represented in a pixel is formed from the contributions of a large number of individual reflectors, such tree and vegetation foliage. Interference of the returning waves to the SAR produces variations in the grey level of the neighbouring pixels, creating a grainy appearance to the image. Speckle occurs in active systems which use coherent waves and it limits the radiometric resolution of SAR images (Hoeckman, 1990, Schumann, 1994).

Since it is a random effect, it cannot be totally eliminated. The impact can be diminished using various procedures, which reduce the spatial resolution.

The process based on multiple views (**multi-look processing**) is a radar signal process, employed to reduce the speckle. It can be achieved either by processing the signal to create independent, single look images at reduced resolution, identifying them and then averaging the image power to form a multi-look image or it can be accomplished by processing the data to full resolution and spatially averaging the developed image. The image signal-to-noise ratio is preserved in multi-look processing. Multi-look processing requires special hardware and software, so it is usually performed at the data reception facilities.

The range of the pixel digital number "DN" depends on the dynamic range of radar signatures in the scene and on the digital coding used to create the image. Often SAR data are delivered in 32 or 16 bits per pixel, however many display and software packages only handle 8 bit range data. Ranges of 16 or 32 bits require high storage and processing capacities. Other conditions (human eye resolution, display and/or printing capacity, etc) make it more convenient to transform the final data to 8 bit range, thus these data are expressed in a range from 0 to 255 grey levels. The process of conversion to 8 bits is named "**scaling**".

Frequently additional radiometric enhancement is necessary in order to use the full range (0 to 255). This process, "**stretching**", increases the image contrast allowing the better detection of diverse features.

For **SAR images calibration** in particular, 2 types of radiometric processing can be applied:

- Absolute calibration: establishes a relationship between the DN in the SAR image and the target backscattering, independent of the time. It is used when DN should be compared between 2 or more images, for example for thickness (age) of sea ice, environmental effects, etc.

- Relative calibration: it establishes the same relationship between DN and backscattering, but only within the image. This results in a target having the same brightness regardless from where in the SAR image it is taken.

Generally radiometric calibration is carried out at the data acquisition facility.

3.2.7 Altimetry

Land and coastal altimetric information is of great assistance to the hydrographer. Description of the relief facilitates a clearer understanding of coastal topography, islands, port and signal infrastructure, etc. High resolution satellite systems allow the representation of relief by numerous diverse means. Presently the cartographic representation of relief has been generally via numeric modelling (Terrain Numeric Model TNM) and its digital versions (Digital Elevation Model DEM or Digital Terrain Model DTM).

Procedures have been developed to process various types of data (space photography, VIR sensors, SAR, altimeters), with different formats (analogical, digital) and for diverse methods (shadowing, stereoscopy, interferometry, polarimetry) taking advantage of the different characteristics of the sensors and the images (geometry, radiometry, phase), applying several types of technologies (analogical, analytic, digital) and of processing (interactive, automatic).

Among the methods, stereoscopic ones have been those which initially have spread more thoroughly for cartography due to the precursor of well-developed stereo air-photogrammetry (See 3.1).

Coming from the latest advances in the computer stereo vision, considerable advances have been achieved in the satellite stereoscopy; additionally radar image stereoscopy has had an important stimulus in the last 20 years.

From the launching of the ERS-1, interferometric techniques were extended using previously developed parametric models. With the inception of the RADARSAT-1 in 1995, radargrammetry was consolidated between the different methodologies for altimetric application, using it alone or complemented with VIR images (Toutin, 2000).

- **Stereoscopic methods**

Stereo methods are similar procedures to those used in air-photogrammetry (see 3.1.7), in which two images are used for the construction of the three-dimensional stereo model.

A digital stereo-plotter allows the measurement of features using two floating marks (one for each stereo pair image), which enable the views to be fused to give 3D cartographic co-ordinates (Toutin, 1995).

The processing of the stereo pair requires the use of digital restitution equipment and specific software. At the present time compact systems exist, based on PC computers which allow the stereo restitution of different digital images types (air, space, VIR, SAR). (Fig. 6.51)

Fig. 6.51 "Digital stereo-plotter scheme"

There are a variety of combinations to capture both images, which can be obtained in the same or contrary directional passes, diverse angles of incidence, etc.

The HRV-SPOT established system has a mobile device installed in the optic equipment, which facilitates the observation of the same area in successive passes (Fig. 6.52).

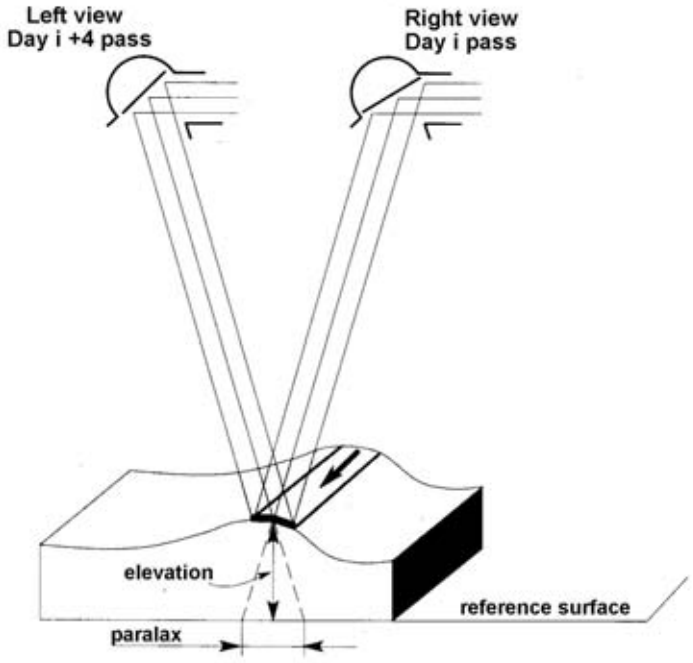

Fig. 6.52 "HRV SPOT stereo aptitude"

The MOMS system allows the capture of images in the same pass, by means of cameras in forward, after and nadir directions. The serial images are taken at intervals of 20 seconds, from three different viewing points (Fig. 6.53).

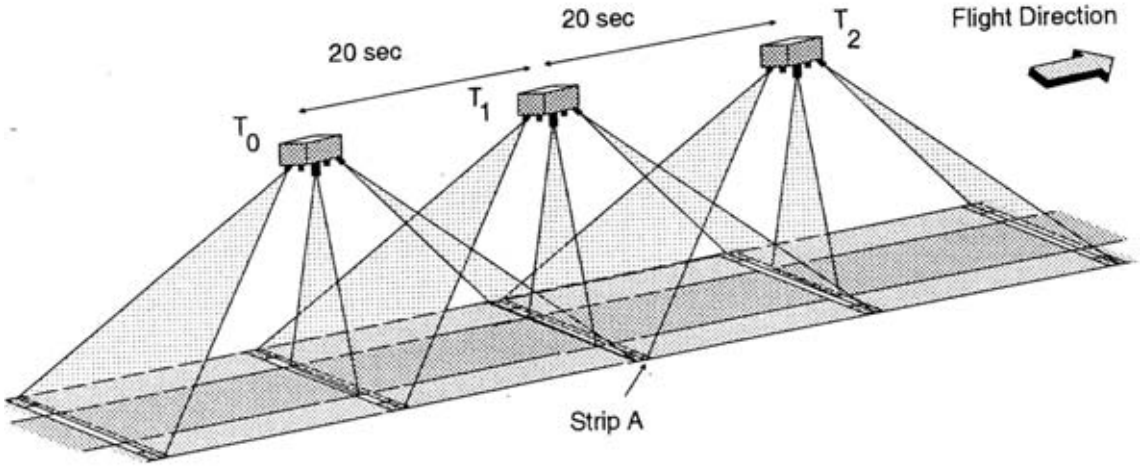

Fig. 6.53 "MOMS-02 stereo geometry (after DARA, 1994)"

Another system is the new HRS (High Resolution Stereoscopic) instrument in the SPOT-5 which has two telescopes looking forward and after in the direction of the orbital trajectory.

The forward-looking telescope captures images at a viewing angle of 20° ahead of the vertical. Ninety minutes later, the after-looking telescope acquires the same ground area at an angle of 20° behind the vertical (Fig. 6.54).

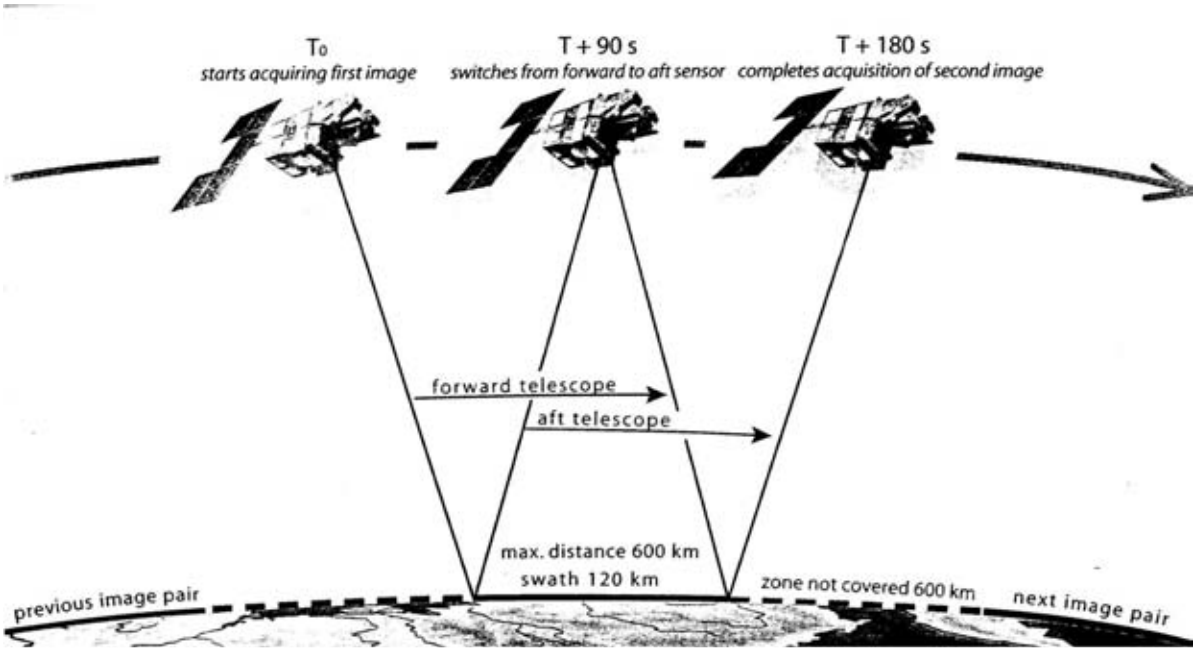

Fig. 6.54 "HRS SPOT-5 stereo geometry (after SPOT IMAGE, 2002)"

- **Radargrammetry**

Radargrammetry is a technique similar to photogrammetry which uses images obtained from the radar signal. A pair of images is acquired and using their correlation a DEM is generated. In this case, it should be noted that the angle of incidence is complementary to that corresponding to an optic image. The absolute precision is of the order of the pixel size. As with stereoscopy, diverse configurations exist (Fig. 6.55).

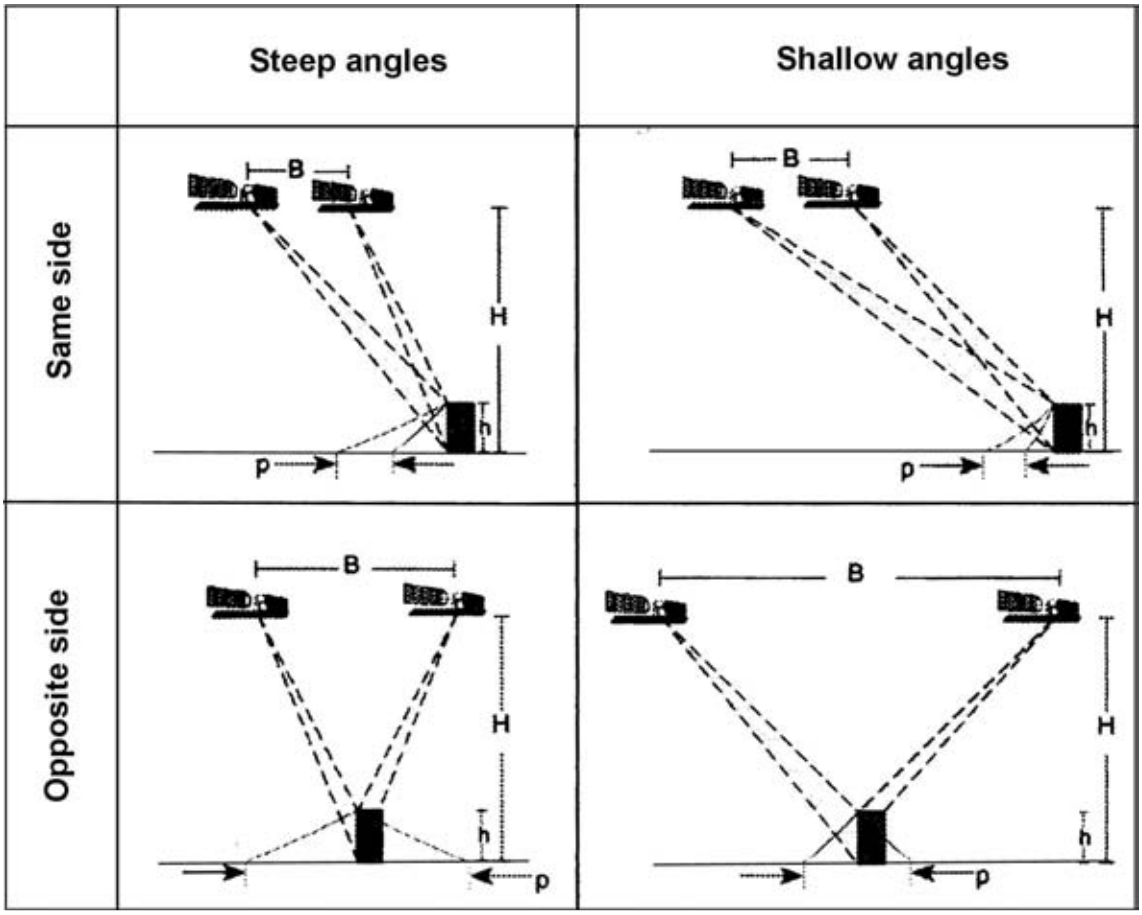

Fig. 6.55 "Diverse SAR stereo configurations (after Toutin, 2001)"

- **Interferometry**

With knowledge of phase of the radar signal, a channel of phase difference and a channel of phase coherence (constant phase angle) can be generated. They are useful in interpreting the interferometric information.

Two scenes, taken during two close passes of the satellite and at a distance called “base”, are required. The base should be less than the maximum value, depending on the frequency of the electromagnetic wave and between to 0.5-1 km. The environmental conditions (wind, rain, etc.) should be as similar possible as for both capture occasions.

One of the scenes, the primary, is used as the reference for the calculations. The other, the secondary, together with the primary is used to calculate a channel of phase difference, called an interferogram, and one of coherence, which is an indicator of the degree of dependability of the phase measurements. The phases should then be developed, adopting a resolution and transforming the fringes of the interferogram in terrain level curves.

The problems of this method:

a. The measurement is ambiguous; since the phase difference is know accurately but not the quantity (number) of complete wavelengths to the distance radar-target.

b. The phase depends on the radio-electric characteristics of the target. If they are modified between the scenes, coherence will not be achieved. However, if the fringes of the interferogram can be correctly built, it indicates that the target has remained unalterable.

3.2.8 Cartographic application

Over the last decades the considerable potential of satellite images, especially in the optic domain for cartographic updating, has been realised. According to the ISPRS, the mapping requirements utilising space images, can be divided in three categories:

- Planimetric precision;
- Altimetric precision;
- Detectability (Konecny, 1990).

The more demanding **planimetric precision** is linked with the cartographic resolution of +/- 0.2 mm, which generates requirements for the scales (1/D) the more frequent of which are (Table 6.6):

D	**Planimetric Precision**
25.000	+/- 5 m
50.000	+/- 10 m
100.000	+/- 20 m
200.000	+/- 40 m

Table 6.6

The **altimetric precision** requirement (**h**), knowing that the equidistance (contour interval "**e**") is e = +/- 5 · h, is shown in the Table 6.7.

E	**H**
20 m	+/- 4 m
50 m	+/- 10 m
100 m	+/- 20 m

Table 6.7 (Konecny, 1990)

The **detectability** refers to the possibility of detecting objects starting with the digital interpretation of the images. It is a requirement that the object covers at least 1.5 pixels, which creates to the following minimum dimensions for detectable objects (Table 6.8).

Object – Target	**Dimension**
Urban infrastructure	2 m
Land ways	2 m
Drainage network	5 m
Vial infrastructure	10 m

Table 6.8 (Konecny, 1990)

Taking into consideration the main commercial satellite systems and the most common cartographic scales, the following usage chart can be produced (Table 6.9):

Satellite sensor	**Ground resolution**	**Chart scale**
QUICK BIRD	0.7 m	1/3500
IKONOS	1 – 4 m	1/5000 – 1/20 000
SPOT PAN	10 m	1/50 000
Landsat 7 ETM	15 m	1/75 000
SPOT XS	20 m	1/50 000 – 1/100 000
RADARSAT 1 SAR	8 – 30 m	1/30 000 – 1/100 000
ERS SAR	30 m	1/100 000
Landsat TM	30 m	1/100 000
Landsat MSS	80 m	1/250 000
SAC-C MMRS	175 m	1/875 000

Table 6.9

MAIN PRESENT SATELLITE SYSTEMS AVAILABLE

The following systems list is not exhaustive. It details some of the most regularly used systems for mid-high scale cartography.

Satellite System/ Series **Country**	**Orbit type, Altitude, Recurrent period, Inclination**	**Scene area, Ground resolution, Modes**	**Sensors** **Spectral bands**
LANDSAT USA	Sun-synchronous 705 km 16 days 98.2°	185 x 185 km MSS: 80 m TM: 30 m ETM+:	 Multispectral Scanner (MSS) Band 1: 0.5 – 0.6 μm (green) Band 2: 0.6 – 0.7 μm (red) Band 3: 0.7 – 0.8 μm (near IR) Band 4: 0.8 – 1.1 μm (near IR) Thematic Mapper (TM) Band 1: 0.45 – 0.52 μm (blue) Band 2: 0.52 – 0.60 μm (green) Band 3: 0.63 – 0.69 μm (red) Band 4: 0.76 – 0.90 μm (near IR) Band 5: 1.55 – 1.75 μm (near IR) Band 6: 10.4 – 12.5μ m (thermal IR) Band 7: 2.08 – 2.35 μm (mid IR) Enhanced Thematic Mapper (ETM+)
SPOT France	Sun-synchronous 832 km 23 days 98.7°	60 x 60 km XS: 20 m P: 10 m	High Resolution Visible (HRV) Multi Band (XS) Band 1: 0.49 – 0.59 μm (green) Band 2: 0.61 – 0.68 μm (red) Band 3: 0.79 – 0.89 μm (near IR) Panchromatic (P) 0.51 – 0.73 μm
IRS India	Sun-synchronous 900 - 904 km 22 days 99.5°	148 x 148 km LISS-I: 73 m LISS-II: 36.5 m	Linear Imaging Self Scanning (LISS-I) Band 1: 0.45 – 0.52 μm (blue) Band 2: 0.52 – 0.569 μm (green) Band 3: 0.62 – 0.68 μm (red) Band 4: 0.77 – 0.86 μm (near IR) Linear Imaging Self Scanning (LISS-II) Consists of 2 cameras, same as above, with swath width 74 km per camera (145 km together)

Satellite System/ Series **Country**	**Orbit type, Altitude, Recurrent period, Inclination**	**Scene area, Ground resolution, Modes**	**Sensors** **Spectral bands**
MOS Japan	Sun-synchronous 909 km 17 days 99°	100 x 90 km MESSR: 50 m	MESSR Band 1: 0.51 – 0.59 μm (green) Band 2: 0.61 – 0.69 μm (red) Band 3: 0.72 – 0.80 μm (near IR) Band 4: 0.80 – 1.10 mμ (near IR)
JERS Japan	Sun-synchronous 568 km 44 days 97.7°	75 x 75 km OPS: 18 x 24 m SAR: 18 x 18 m	Optical Sensor (OPS) Visible and Near Infrared (VNIR) Band 1: 0.52 – 0.60 μm (green) Band 2: 0.63 – 0.69 μm (red) Band 3: 0.76 – 0.86 μm (near IR) Band 4: 0.76 – 0.86 μm (near IR) Short Wave Infrared (SWIR) Band 5: 1.60 – 1.71 μm Band 6: 2.01 – 2.12 μm Band 7: 2.13 – 2.15 μm Synthetic Aperture Radar (SAR) 1.275 GHz (L-Band) HH
ERS Europe	Sun-synchronous 777 km 3 - 35 days 98.5°	AMI works in three modes. In Image mode: 100 x 100 km 30 x 30 m (3 looks)	Active Microwave Instrument (AMI) Synthetic Aperture Radar (SAR) 5.3 GHz (C-Band) VV Incidence angle fix: 23°
RADARSAT Canada	Sun-synchronous 798 km 3 - 24 days 98.6°	Several modes In standard mode: 100 x 100 km 30 x 30 m (3 looks) In fine mode: 50 x 50 km 11 x 8 m (1 look)	Synthetic Aperture Radar (SAR) 5.3 GHz (C-Band) HH Incidence angle selectable: In standard mode: 20° – 50° In fine mode: 37° – 48°

Satellite System/ Series **Country**	**Orbit type, Altitude, Recurrent period, Inclination**	**Scene area, Ground resolution, Modes**	**Sensors** **Spectral bands**
IKONOS USA	Sun-synchronous 681 km 1-3 days 98.1°	Several incidence angles Multi-band: 4 m (with nominal angle 26°) Panchromatic:1 m (with nominal angle 26°)	Band 1: 0.45 – 0.52 μm (blue) Band 2: 0.52 – 0.60 μm (green) Band 3: 0.63 – 0.69 μm (red) Band 4: 0.76 – 0.90 μm (near IR) Panchromatic band: 0.45 – 0.90 μm

ACRONYMS

AIRSAR	AIRborne SAR sensor, (J P L)
ASPRS	American Society for Photogrammetry and Remote Sensing
AVHRR	Advanced Very High Resolution Radiometer
CCD	Charge Coupled Device
CCRS	Canadian Centre for Remote Sensing
DGPS	Differential GPS
DLR	German Aerospace Research Establishment
DN	Digital Number
DTM	Digital Terrain Model
EDM	Electronic Distance Measurement
EODM	Electro-Optic Distance Measurement
ERS	European Remote Sensing Satellite
ESA	European Space Agency
ETM	Enhanced Thematic Mapper
GALILEO	European (ESA) Global Positioning Satellite System
GBAS	Ground Based Augmentation System (Reference System for differential satellite positioning)
GCP	Ground Control Point
GIS	Geographic Information System
GLONASS	Global Navigation Satellite System (Russia)
GNSS	Global Navigation Satellite System (GPS + GALILEO + GLONASS)
GPS	Global Positioning System (USA)
HRV	High Resolution Visible
IFOV	Instantaneous Field Of View
IHO	International Hydrographic Organization
IHS	Intensity Hue Saturation
IR	InfraRed
IRS	Indian Remote Sensing satellite
ISPRS	International Society for Photogrammetry and Remote sensing
JERS	Japanese Earth Resources Satellite
JPL	Jet Propulsion Laboratory
KFA 1000	Kosmologisher Fotoapparat with 1000 mm focal length
LASER	Light Amplification by Stimulated Emission of Radiation
Lat	Latitude
Long	Longitude
LUT	Look-Up Table
MSS	MultiSpectral Scanner
NHO	National Hydrographic Office
NOAA	National Oceanic and Atmospheric Administration
pp.	Pages
PAN	Panchromatic
ppm	Part per million (1×10^{-6})
RBV	Return Beam Vidicon
RGB	Red Green Blue
RS	Remote Sensing
RSI	RadarSat International

RTK	Real Time Kinematic (Precise GNSS rapid method)
S-44	Special Publication 44 (IHO Standards for Hydrographic Surveying)
SAR	Synthetic Aperture Radar
SBAS	Satellite Based Augmentation System (Reference system for differential satellite positioning)
SPOT	Satellite Pour l-Observation de la Terre (France)
SSMI	Special Sensor Microwave Imager
TM	Thematic Mapper
USFAA	United States Federal Aviation Association
UTM	Universal Transverse Mercator
VIR	Visible and near InfraRed
WAAS	Wide Area Augmentation System
WGS	World Geodetic System
WGS 84	World Geodetic System 1984
XS	Multispectral

REFERENCES

(List intended to help the Chapter 6 reader in finding more information through printed matter or web pages)

ALBERZ J. KREILING W., (1989).	*"Photogrammetric Guide"*	Wichmann, Karlsruhe (Germany)
ASPRS ,(1980).	*"Manual of Photogrammetry"*	American Society for Photogrammetry and Remote Sensing. Bethesda, Maryland, (USA)
ASPRS ,(1983).	*"Manual of Remote Sensing. 2 Volumes"*	American Society for Photogrammetry and Remote Sensing. Bethesda, Maryland, (USA) The Sheridan Press.
ASPRS ,(1996).	*"Digital Photogrammetry"*	American Society for Photogrammetry and Remote Sensing. Bethesda, Maryland, (USA)
BOMFORD G. (1980).	*"Geodesy 4th Ed"*	Claredon Press, Oxford (UK).
CHUECA PAZOS Et. Al. (1996).	*"Tratado de Topografía (3 Volumes)"*	Paraninfo, Madrid (Spain)
Chuvieco E. **(**1995).	*"Fundamentos de Teledetección Espacial"*	Editorial RIALP, Madrid, Spain, 453 pp.
CNES**, (**2002).	*"HRS puts terrain into perspective"*	SPOT Magazine N°34, 1st semester 2002, pp 10-11.
FEDERAL GEODETIC CONTROL COMMITTEE (1984).	*"Standards and Specification for Geodetic Control Networks"*	NOAA Rockville Maryland (USA)
GDTA**, (**1995).	*"Aspects stéréoscopiques de SPOT, Cahier A2 MNT"*	Les Cahiers Pedagogiques du GDTA, France, 93 pp.
GERMAN SPACE AGENCY, (1994).	*"MOMS-02-D2 Data Catalogue"*	DARA, München, Germany.
HOFMANN WELLENHOF Et.Al. (2001).	*"GPS, Theory and Practice. 5th. Ed "*	Springer, Wien (Austria), New York (USA)

IHO (2008).	*"IHO Standards for Hydrographic Surveys. S-44 5th. Ed "*	IHB, Monaco. There will be French and Spanish versions available
IHO (1994).	*"Hydrographic Dictionary 5th Ed. S–32"*	IHB, Monaco. Also available are Spanish version (1997) and French version (1998).
JOECKEL R., STROBER M. (1995).	*"Elektronische Entfernungs und Richtungsmessung, 3th. Ed",*	Wittwer, Stuttgart (Germany).
KONECNY, G**.,** (1990).	*"Review of the latest technology in satellite mapping. Interim report, Inter-commission Working Group I/IV on International Mapping and Remote Sensing Satellite Systems of ISPRS, Vol.14"*	Hanover, Germany, pp. 11-21.
LANGERAAR W. (1984).	*"Surveying and Charting of the Seas"*	Elsevier. Amsterdam (The Netherlands), Oxford (UK) New York (USA) Tokyo (Japan)
LAURILA S. (1976).	*"Electronic Surveying and Navigation"*	J. Wiley & Sons, New York (USA)
LEICK A. (1995).	*"GPS Satellite Surveying. 2nd. Ed".*	Wiley Chichester, Brisbane. New York (USA) Toronto (Canada) Singapore.
LILLESAND, T.M. and KIEFER, R.W., (1987).	*"Remote sensing and image interpretation, 2nd edition"*	John Wiley and Sons, Inc., New York, 721 p.
MEISENHEIMER D. (1995).	*"Vermessungsinstrumente Aktuell"*	Wittwer, Stuttgart (Germany)
NASA, (1997).	*"The Remote Sensing Tutorial".*	Goddard Space Flight Centre, NASA Web Production. Written by: Nicholas M. Short, Sr.
OLLIVER F. (1995).	*"Instruments Topographiques"*	Eyrolles, Paris (France)
OLIVER C. and S. QUEGAN (1998).	*"Understanding Synthetic Aperture Radar Images"*	Artech House, Norwood, Massachuset (USA)
POHL, C., (1996).	*"Geometric aspects of multi-sensor image fusion for topographic map updating in the humid Tropics"*	ITC Publication Number 39, The Netherlands, 214 pp.
RANEY, R.K., (1992).	*"Course notes; unpublished notes"*	Canada Centre for Remote Sensing, Ottawa, Canada.
RICHARDUS P.	*"Project Surveying".*	Balkema. The Netherlands.

(1977).

SEEBER G. (1993). *"Satellite Geodesy"* W. de Gruyter Berlin (Germany) New York (USA)

SEEBER G. (2003). *"Satellite Geodesy 2nd. Ed "* Walter de Gruyter (Berlin - NY)

TORGE W. (2001). *"Geodesy"* W. de Gruyter Berlin (Germany) New York (USA)

TURNBULL D. (2001). *"The Evolution of an Object - Oriented Geospatial Information System Supporting Digital Nautical Chart Maintenance at the NIMA"* Bulletins Hydr. Int. Jul. Aug. - Sep; IHO, Monaco

TOUTIN, Th., (1998). *"Evaluation de la précision géométrique des images de RADARSAT"* Journal Canadien de télédétection, 23(1):80-88.

TOUTIN, Th., (1997). *"Single versus stereo ERS-1 SAR imagery for planimetric feature extraction"* International Journal of Remote Sensing, 18(18):3909-3914.

TOUTIN, Th. and B. RIVARD, (1997). *"Value-added RADARSAT Products for Geoscientific Applications"* Canadian Journal of Remote Sensing, 23(1):63-70.

TOUTIN, Th., (1995). *"Generating DEM from stereo images with a photogrammetric approach: Examples with VIR and SAR data"* EARSeL Journal Advances in Remote Sensing, 4(2):110-117.

WOLF R., BRINKER R.C. (1994). *"Elementary Surveying 9th. Ed. "* Harper Collins College Publishers New York (USA) There is available also a Spanish version "Topografía", Alfaomega, México (1998)

URL ADDRESSES

COUNTRY	INSTITUTION	WEB SITE
	European Space Agency	http://www.esa.int
	International Society on Photogrammetry and Remote Sensing	http://www.isprs.org
	Fédération Internationale de Géometres	http://www.Fig.net
	International Association of Geodesy	http://www.gfy.ku.dk/iag/
Argentina	Comisión Nacional de Actividades Espaciales	http://www.conae,gov.ar
Austr. – N.Z.	Australian - New Zealand Land Information Council	http://www.anzlic.org.au
Australia	Commonwealth Scientific & Industrial Research Organization	http://www.csiro.au
Australia	Surveying and Land Information Group	http://www.auslig.gov.au
Bolivia	Centro de Levantamientos Aeroespaciales y SIG	http://www.clas.unmss.edu.bo
Brazil	Instituto Nacional de Pesquisas Espaciais	http://www.inpe.br
Canada	Centre For Remote Sensing	http://www.ccrs.nrcan.ca
Canada	Radarsat International	http://www.rsi.ca
Canada	Geodetic Survey	http://www.geod.emr.ca
Chile	Agencia Chilena del Espacio	http://www.agenciaespacial.cl
China	China Academy of Space Technology	http://fas.org/nuke/guide/china/contractor/cast.htm
France	Centre National d'Etudes Spatiales	http://www.cnes
France	Group pour le Développement de la Téledetection Aerospatiale	http://www.gdta.fr
Germany	Institute für Erdmessung, Hanover University	http://www.ife.unihannover.de
Germany	Institute für Angewandte Geodäsie	http://www.gibs.leipzig.ifag
Germany	Karlsruhe University	http://www.ipfr.bau.verm.uni.karlsruhe.de
Germany	GPS Information Bulletin Board System	http://www.gibs.leipzig.ifag.de

COUNTRY	INSTITUTION	WEB SITE
Germany	Deutsches Zentrum für Luft und Raumfahrt	http://www.dlr.de
India	Indian Space Research Organization	http://www.isro.org
Italy	Agenzia Spaziale Italiana	http://www.asi.it
Japan	National Space Development Agency	http://www.nasda.go.jp
Russia	Russian Space Science Internet	http://www.rssi.ru
Spain	Instituto Nacional de Técnica Aeroespacial	http://www.inta.es
Spain	Org. for Cartography and Geodesy	http://www.cartesia.org
Spain	Valencia University	http://www.miranda.tel.uva.es
Switzerland	Astronomical Institute Berne University	http://www.aiub.unike.ch
UK	Nottingham University	http://www.ccc.nottingham.ac.uk
UK	British National Space Centre	http://www.bnsc.uk
USA	Ohio State University (Centre for Mapping)	http://www.cfm.ohio.state
USA	Maine University	http://www.spatial.maine.edu
USA	Geological Survey (EROS)	http://edc.usgs.gov
USA	Earth Observation Handbook	http://www.eohandbook.com
USA	Goddard Space Flight Centre (NASA)	http://www.gsfc.nasa.gov
USA	Nat. Ocean. And Atm. Adm. Central Library	http://www.lib.noaa
USA	Nat. Aeronautic and Space Adm.	http://www.nasa.gov
USA	National Oceanic and Atmospheric Adm.	http://www.noaa.gov
USA	Geological Survey	http://www.usgs.gov
USA	Professional Survey (review)	http://www.profsurvey.com
USA	Department of Defence	http://www.defenselink.mil
USA	National Geodetic Survey	http://www.ngs.noaa.gov
USA	Institute of Navigation	http://www.ion.org

COUNTRY	INSTITUTION	WEB SITE
USA	Jet Propulsion Laboratory	http://www.jpl.nasa.gov
USA	Naval Observatory	http://www.usno.navy.mil
USA	GPS Interface Control Document	http://www.navcen.usc.mil/gps
USA	Interagency GPS Executive Board	http://www.igeb.gov
USA	Texas University	http://www.host.cc.utean.edu
USA	GPS Nav. Inf.	http://www.navan.uscg.mil/gps
USA	California - Los Angeles University	http://www.cla.esc.edu
USA	American Society for Photogr. and R.S.	http://www.asprs.org
USA	National Imagery and Mapping Agency	http://www.164.214.2.59
USA	GPS issues	http://www.206.65.196

BIBLIOGRAPHY

(Edited or digital source information used in the preparation of Chapter 6).

ASPRS, (1983).	*"Manual of Remote Sensing"*	American Society of Photogrammetry and Remote Sensing. 2 volumes. The Sheridan Press, USA, 2420 pp.
CHUVIECO E. (1995).	*"Fundamentos de Teledetección Espacial"*	Editorial RIALP, Madrid, Spain, 453 pp.
CURAN P.J. (1985).	*"Principles of remote sensing"*	Longman, London, England.
CURLANDER J.C. and R.N. MCDONOUGH, (1991).	*"Synthetic Aperture Radar Systems and Signal Processing"*	John Wiley and Sons, Inc., Toronto
DRURY S.A., (1990).	*"A Guide to Remote Sensing"*	Oxford Science Publications, Oxford, USA, 199 pp.
ELACHI C. and F.T. ULABY, (1990).	*"Radar Polarimetry for Geoscience Applications"*	Artech House, Boston
ELACHI C. (1988).	*"Spaceborne Radar Remote Sensing: Applications and Techniques"*	IEEE Press, New York
FAO, (1990).	*"Remote sensing applications to land resources"*	FAO RSC Series 54, Rome, Italy.
FITCH J.P. (1988).	*"Synthetic Aperture Radar"*	Springer-Verlag, New York
HENDERSON F.M. and A.J. LEWIS, EDS. (1998).	*"Principles and Applications of Imaging Radar, Manual of Remote Sensing, Third Edition, Volume 2"*	John Wiley & Sons, Inc., Toronto
KNEISSL M. (1956).	*"Handbuch der Vermessungskunde Band III (Hohenmessung, Tachymetrie)"*	Metzer, Stuttgart (Germany)
KNEISSL M. (1958).	*"Handbuch der Vermessungskunde Band IV (Mathematische Geodäsie)"*	Metzer, Stuttgart (Germany)
KNEISSL M. (1963).	*"Handbuch der Vermessungskunde Band II (Feld und Land Messung, Abstekungsarbeiten)"*	Metzer, Stuttgart (Germany)
MAGUIRE D. et al (1991).	*Geographic Information System Principles and Applications"*	John Wiley & Sons N.Y.
NASA, (1997).	*"The Remote Sensing Tutorial"*	Goddard Space Flight Centre, NASA Web Production. Written by: Nicholas M. Short, Sr.

OLIVER C. and S. QUEGAN (1998).	*"Understanding Synthetic Aperture Radar Images"*	Artech House, Norwood, Mass.
RINNER K., BENZ F. (1966)	*"Handbuch der Vermessungskunde Band VI (Die Entfernunsmessung nit Elektromagnetische Wellen und ihre geodätische Anwendung)"*	Metzer, Stuttgart (Germany)
RINNER K., BENZ F. (1971).	*"Handbuch der Vermessungskunde Band III a,3 Volumes (Photogrammetrie)"*	Metzer, Stuttgart (Germany)
RUSSELL - WOLF (1984).	*"Elementary Surveying"*	Harper and Row Publishers, New York (USA)

The following texts of the REFERENCE LIST were also used:

ALBERZ J. KREILING W (1989)
ASPRS (1996)
BOMFORD G. (1980)
CHUECA PAZOS Et Al (1996)
HOFMANN WELLENHOF Et Al (2001)
IHO (1998)
IHO (1994)
LANGERAAR W. (1984)
MEISENHEIMER D. (1995)
SEEBER G. (1993)
TORGE W. (2001)
WOLF R, BRINKER R.C. (1994)

CHAPTER 6 – ANNEX A
ALGORITHMS FOR THE TRANSVERSE MERCATOR REPRESENTATION

1. PRESENTATION

The Mercator Transverse Representation (see chapter 2, 2.5.4 and 2.5.5) is a useful medium in which to transfer geodetic co-ordinates (latitude, longitude) to the plane. The use of plane co-ordinates (**x** & **y** or **N** & **E**) with small corrections related to the measured distances and angles is suitable for topographic survey purposes and also for some detailed hydrographic surveys.

2. GEOMETRIC GEODESY AND MATHEMATICAL CARTOGRAPHIC CONCEPTS

Before the study of these concepts, the reader should be familiar with Chapter 2: 2.4 and 2.5, with particular attention to subparagraphs 2.5.4 and 2.5.5.

Taking the earth rotation ellipsoid as the reference surface, with '**a**' semi-major (equatorial) axis and '**b**' semi-minor (polar) axis, it is possible to define:

$$f = \frac{a - b}{a}$$ (flattening, also described as "α" in chapter 2: 2.2.3)

$$\varepsilon = \frac{\sqrt{a^2 - b^2}}{a}$$ (first excentricity, also described as "**e**" in chapter 2: 2.1.1))

$$\varepsilon' = \frac{\sqrt{a^2 - b^2}}{b}$$ (2^{nd}. excentricity)

with elemental algebraic procedures it is feasible to verify the following relationships:

$$f(2 - f) = \varepsilon^2$$

$$(1 - f)^2 = 1 - \varepsilon^2$$

with the described constants, the computation of the curvature radius and arcs of lines on the ellipsoidal surface are possible:

$$M = a(1-f)^2\left[1 - f(2-f)\sin^2\varphi\right]^{-3/2} = a(1-\varepsilon^2)\left[1 - \varepsilon^2\sin^2\varphi\right]^{-3/2}$$
$$N = a\left[1 - f(2-f)\sin^2\varphi\right]^{-1/2} = a\left[1 - \varepsilon^2\sin^2\varphi\right]^{-1/2}$$
$$r = N\cos\varphi$$

$$\Delta p_{12} = r(\lambda_2 - \lambda_1)$$

$$B = \int_0^{\varphi} M d\varphi = \alpha\varphi + \beta \sin 2\varphi + \gamma \sin 4\varphi + \delta \sin 6\varphi + \ldots$$

where (see Fig 6A.1):

M - Meridian curvature radius
N - Normal (to the meridian) section curvature radius
R - Parallel curvature radius
φ - Geodetic (ellipsoidal) latitude
Δp_{12} - Parallel are between longitudes λ_1 and λ_2 at φ latitude, (λ_2 - λ_1) expressed in radians
B - Meridian arc from equator to the φ latitude (for the first term = αφ (alpha, phi), φ (phi) should be expressed in radians)

α = a (1- 1/4 ε^2 - 3/64 ε^4 - 5/256 ε^6) = a (1-f)² (1 + 3/2 f + 33/16 f² + 85/32 f^3)
β = -a (3/8 ε^2 + 3/32 ε^4 + 45/1024 ε^6) = -a/2(1-f)² (3/2 f + 3 f² + 285/64f^3)
γ = a (5/256 ε^4 + 45/1024 ε^6) = a/4(1-f)² (15/16 f² + 75/32 f^3)
δ = -a (35/3072 ε^6) = -a/6(1-f)² (35/64 f^3)

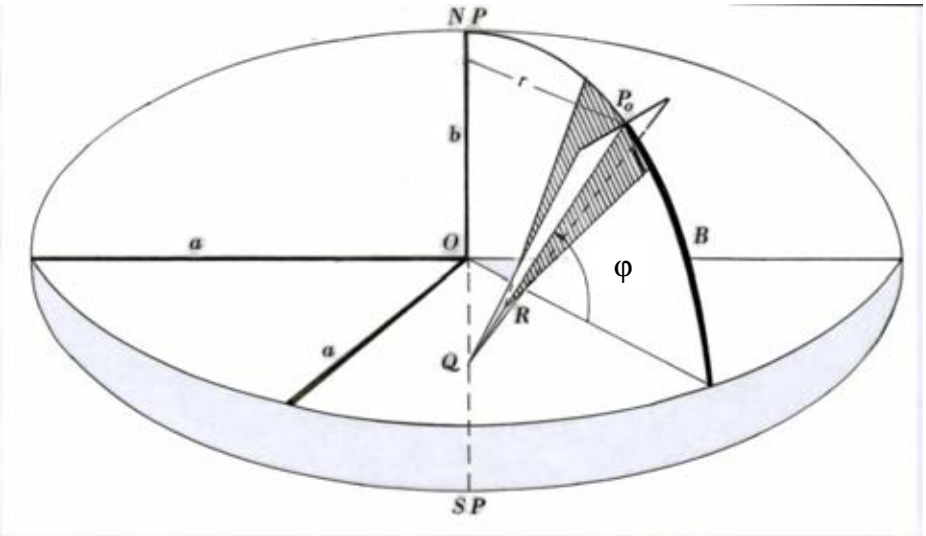

Po O = N
Po R = M
N ≥ M

Fig. 6A.1

The following table contains the described constants for two commonly used ellipsoids with the Q values (meridian arc, B, from equator to the pole) added

$$Q = \int_0^{\pi/2} M d\varphi$$

ELLIPSOID	MADRID 1924	WGS 84
A	6378388 m	6378137 m
F	1/297	1/298.2572236
$\varepsilon^2 = f\,(2 - f)$	0.0067226722	0.0066943800
α	6367654.500 m	6367449.146 m
β	-16107.035 m	-16038.509 m
γ	+ 16.976 m	+ 16.833 m
δ	- 0.022 m	- 0.022 m
Q	10002288.30 m	10001965.73 m

The mathematical form to generate a representation of the ellipsoid on the plane is:

$$x = x\,(\varphi, \lambda)$$
$$y = y\,(\varphi, \lambda)$$

and these formulae provide the properties for this transformation. For a conformal or othomorphic representation it is necessary to replace the latitude with a new variable called "isometric latitude" or "meridional part"

$$q = \int_0^{\varphi} \frac{M}{N \cos \varphi} d\varphi$$

The origin of this function is the MERCATOR representation of the earth ellipsoid on the plane, starting from a circular cylinder whose axis of orientation coincides with the semi-minor axis '**b**' of the rotation ellipse and the surface tangent to its respective equator (See Fig. 6A.2)

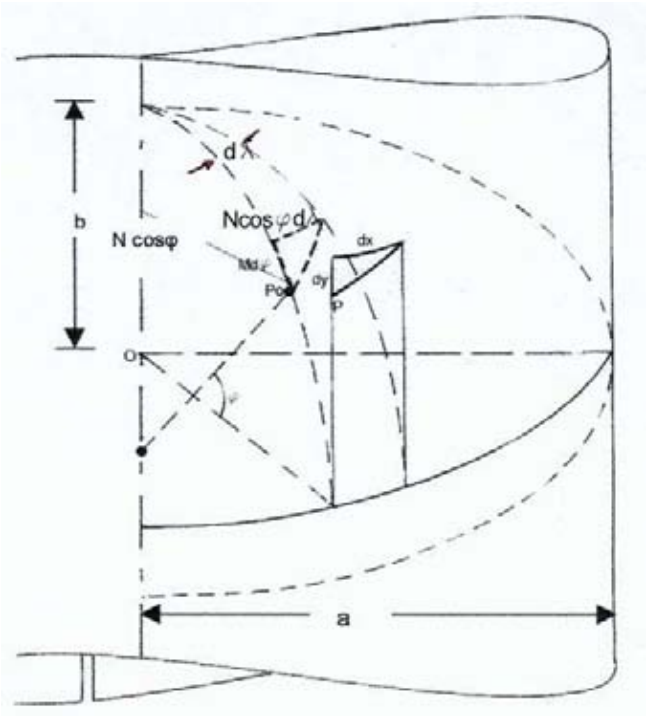

Fig. 6A.2

Taking the '**y**' axis with the projection of the longitudinal origin meridian ($\lambda = 0$) on the cylinder, with $y = 0$ for $\varphi = 0$ and the '**x**' axis representing the equator, with $x = 0$ for $\lambda = 0$, it is possible to show:

$$\mathbf{x = a\,\lambda}$$

(isometry on the tangent line = equator) but, in this case, the '**y**' should satisfy the following differential rate (see Fig. 6A.2)

$$\frac{dy}{Md\varphi} = \frac{dx}{N\cos\varphi d\lambda} = m$$

where **m** is coincident with $\mathbf{m_l}$ given in 2.4, chapter 2. Also:

$$\frac{dy}{Md\varphi} = \frac{ad\lambda}{N\cos\varphi d\lambda} = \frac{a}{N\cos\varphi} = m$$

and

$$y = a\int_0^{\varphi} \frac{M}{N\cos\varphi}\, d\varphi = aq$$

solving the integral it is possible to express:

$$q = \ln\left[\left(\frac{1-\varepsilon\sin\varphi}{1+\varepsilon\sin\varphi}\right)^{\varepsilon/2} tg\left(\frac{\pi}{4}+\frac{\varphi}{2}\right)\right]$$

Fig. 6A.3 shows a partial representation of the meridians and parallels grid and also of a geodetic line (minimum distance track over the ellipsoidal surface) among points A and B for this transformation ($x = a\lambda$, $y = aq$)

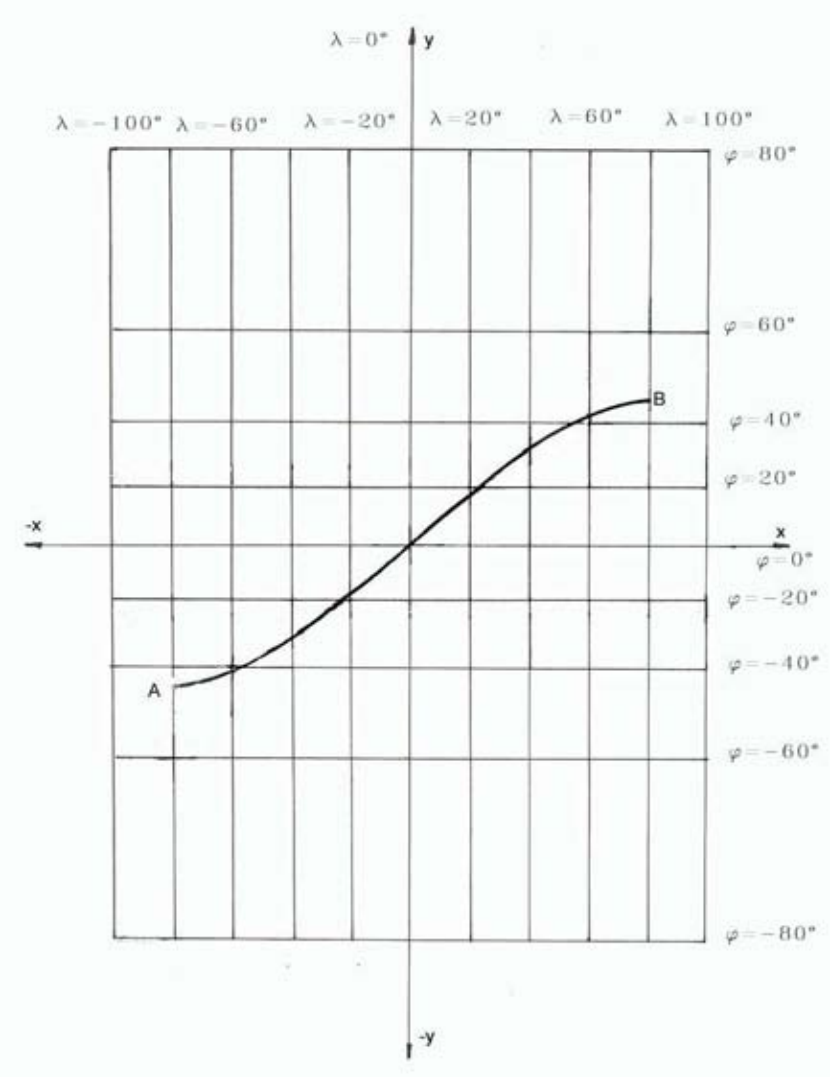

Fig. 6A.3

Algorithms based in these principals, but with other assumptions, are useful for nautical charting, but for further deliberations in this annex it is sufficient to remember that:

$$x = a\lambda$$

$$y = aq$$

$$q = \int_0^{\varphi} \frac{M}{N \cos \varphi} d\varphi$$

is a conform transform of the ellipsoid to the plane, in conclusion the principals of the analytical functions is applicable:

$$\mathbf{y + ix = f(q + i \lambda)} \qquad \mathbf{(2.1)}$$

(taking **y** to the north and **x** to de east) where $i = (-1)^{1/2}$ and the Cauchy - Riemann conditions should be satisfied:

$$\frac{\partial y}{\partial q} = \frac{\partial x}{\partial \lambda}$$

$$\frac{\partial x}{\partial q} = -\frac{\partial y}{\partial \lambda}$$

this is possible because **q**, **λ** and **x**, **y** are two plane co-ordinate pairs.

For a better comprehension of this subject, consultation of a mathematical text in complex variables and their application to conform transfer between two plane domains is recommended.

The general relation 2.1, the Cauchy - Riemann conditions and the following considerations are valid for all conformal transformations (not only for the described Mercator expressions).

Other mathematical formulae for the generic conformal representation come from differential expressions of $x = x(\varphi, \lambda)$ and $y = y(\varphi, \lambda)$:

$$dx = \left(\frac{\partial x}{\partial \varphi}\right) d\varphi + \left(\frac{\partial x}{\lambda}\right) d\lambda$$

$$dy = \left(\frac{\partial y}{\partial \varphi}\right) d\varphi + \left(\frac{\partial y}{\partial \lambda}\right) d\lambda$$

when φ = constant (parallel arc), the square of the plane differential distance $dx^2 + dy^2$ gives, with the correspondent ellipsoidal element ($N \cos \varphi \, d\lambda$) the square of linear deformation rate:

$$m^2 = \frac{\left(\frac{\partial x}{\partial \lambda}\right)^2 + \left(\frac{\partial y}{\partial \lambda}\right)^2}{N^2 \cos^2 \varphi}$$

and also for λ = constant and elementary meridian arc $M \, d\varphi$, issues:

$$m^2 = \frac{\left(\frac{\partial x}{\partial \varphi}\right)^2 + \left(\frac{\partial y}{\partial \varphi}\right)^2}{M^2}$$

is also valid:

$$m^2 = \frac{\left(\frac{\partial x}{\partial \varphi}\right)^2 + \left(\frac{\partial y}{\partial \varphi}\right)^2}{M^2} = \frac{\left(\frac{\partial x}{\partial \lambda}\right)^2 + \left(\frac{\partial y}{\partial \lambda}\right)^2}{N^2 \cos^2 \varphi} \qquad \textbf{(2.2)}$$

Arising from the same differential expressions and taking the rates:

$$\frac{dx}{dy} \quad \text{(for } \varphi = \text{constant)}$$

$$\frac{dy}{dx} \quad \text{(for } \lambda = \text{constant)}$$

it is possible to obtain the grid declination 'γ' formulas (γ is the angle between the cartesian axis and the lines of the respective meridians and parallels representation -see Fig. 6A.4)

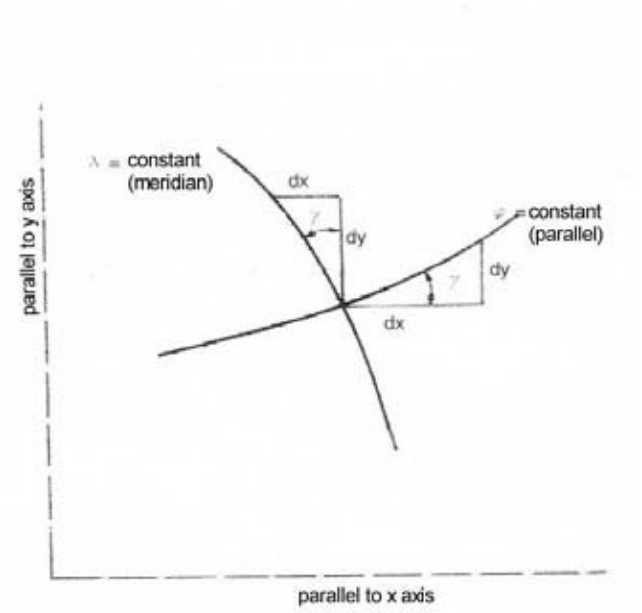

Fig. 6A.4

$$\operatorname{tg}\gamma = \frac{\left(\frac{\partial x}{\partial \varphi}\right)}{\left(\frac{\partial y}{\partial \varphi}\right)} = \frac{\left(\frac{\partial y}{\partial \lambda}\right)}{\left(\frac{\partial x}{\partial \lambda}\right)} \qquad \textbf{(2.3)}$$

in these formulae the sign of γ (or tgγ) is not considered.

3. GAUSS-KRÜGER FORMULAS

To start in the development of conformal representation with minimum deformation upon a NORTH - SOUTH strip, an elliptical cylinder tangent to a central meridian will be assumed (see Fig. 6A.5).

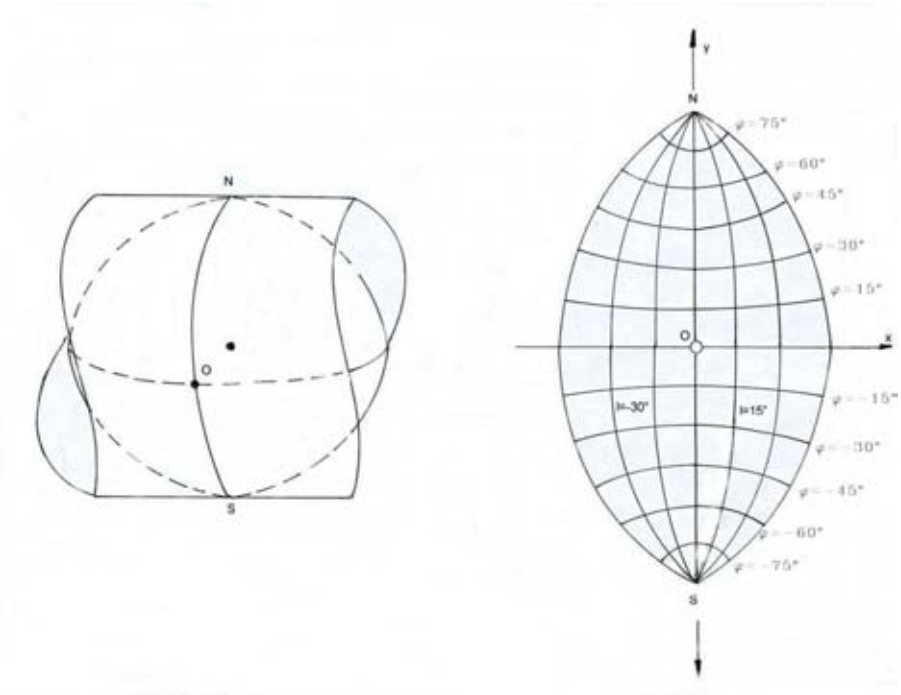

Fig. 6A.5

A more extensive representation of the meridians and parallels grid is given in Fig. 2.6 (2.5.4 Chapter 2), but for the following consideration we start from the former Fig. 6A.5.

For this case, the 2.1 formula will be transformed as follow:

$$\mathbf{f(q + il) = y + ix}$$

where **l** is the longitude referred to the central meridian:

$$\mathbf{l = \lambda - \lambda_0} \qquad \textbf{(2.4)}$$

Adopting a Taylor series development of the function issues:

$$f(q + il) = f(q) + \frac{df}{dq}(il) + \frac{d^2f}{dq^2}\frac{(il)^2}{2!} + \frac{d^3f}{dq^3}\frac{(il)^3}{3!} + \frac{d^4f}{dq^4}\frac{(il)^4}{4!} + \ldots$$

and separating the real and imaginary parts produces the generic expressions for the conformal representation of the described strip

$$x = f(q) \qquad -\left(\frac{d^2f}{dq^2}\right)\frac{l^2}{2} \qquad +\left(\frac{d^4f}{dq^4}\right)\frac{l^4}{24} + \ldots$$

$$\mathbf{y} = \qquad \left(\frac{df}{dq}\right)\cdot l \qquad +\left(\frac{d^3f}{dq^3}\right)\frac{l^3}{6} + \ldots$$

Taking the equidistance along the central meridian (l=0) it is correct to take:

$$y(l = 0) = f(q) = B = \int_0^{\varphi} M d\varphi$$

and then:

$$\frac{df}{d\varphi} = M$$

also, remembering that:

$$q = \int_0^{\varphi} \frac{M}{N\cos\varphi}\, d\varphi$$

it is possible to obtain:

$$\frac{d\varphi}{dq} = \frac{N\cos\varphi}{M}$$

and also:

$$\left(\frac{df}{dq}\right) = \left(\frac{df}{d\varphi}\right)\left(\frac{d\varphi}{dq}\right) = N\cos\varphi$$

Coming from these principals it is possible to obtain the following derivates

$$y = B + \frac{N \sin\varphi \cos\varphi}{2} l^2 + \frac{N \sin\varphi \cos^3\varphi}{24}\left(5 - tg^2\varphi + 9\eta^2 + 4\eta^4\right)\cdot l^2 + \ldots$$
$$x = N\cos\varphi l + \frac{N\cos^3\varphi}{6}\left(1 - tg^2\varphi + \eta^2\right)\cdot l^3 + \ldots$$

(2.5)

Where **B** and **N** are given in the formulae at beginning of 2 (in this Annex) and η^2 is:

$$\eta^2 = \varepsilon'^2 \cos^2\varphi = \frac{f(2-f)}{1-f(2-f)}\cos^2\varphi$$

l is given by (2.4) and for its application in (2.5) should be expressed in radians.

With the consideration of (2.2), (2.3) and (2.4) comes also:

$$\gamma = \sin\varphi l + \ldots$$
$$m = 1 + \frac{\cos^2\varphi\left(1+\eta^2\right)}{2} l^2 + \ldots = 1 + \frac{x^2}{2R^2} + \ldots \qquad \textbf{(2.6)}$$

Where:

$$R = \sqrt{MN} = \frac{a(1-f)}{\left[1 - f(2-f)\sin^2\varphi\right]}$$

(**R** is the best spherical radius suitable to the ellipsoid at **φ** latitude)

For the inverse computation (to obtain **φ**, **λ** arising from **x**, **y**) the following formulas are useful:

$$\varphi = \varphi_1 - \frac{tg^2\varphi_1}{2}\left(\frac{x^2}{M_1 N_1}\right) + \frac{tg\,\varphi_1}{24}\left(5 + 3\,tg^2\varphi_1 + \eta_1^2 - 9\eta_1^2\,tg^2\varphi_1\right)\left(\frac{x^4}{M_1 N_1^3}\right) + \ldots \qquad \textbf{(2.7)}$$

$$l = \frac{x}{N_1\cos^2\varphi_1} - \left(\frac{1 + 2\,tg^2\varphi_1 + \eta_1^2}{6\cos\varphi_1}\right)\left(\frac{x}{N_1}\right)^3 + \ldots$$

$$\lambda = \lambda_0 + l$$

where φ_1 is the latitude that made possible B(φ) = y

The representation with these algorithms was applied by GAUSS at beginning of the XIX century for the HANNOVER Kingdom. 100 years after this, Dr. L. KRÜGER made an explanatory analysis and

extension of the expressions applying several strips to Germany. Also similar criteria were extended to other countries.

With the tangent cylinder, where m = 1 by the central meridian of the strip, the zone width should be smaller than 200 km each side because in this case the linear deformation rate ($m = 1 + x^2/2R^2 + ...$) overcomes the 1.0005 value, this is 0.5 m in 1 km.

With this limitation, the use of these plane co-ordinates is very convenient for topographic charting purposes and also for many control networks computations. For better results, a correction to the measured elements should be made (see 2.2.5 a in Chapter 6).

4. GENERAL TRANSVERSES MERCATOR REPRESENTATIONS (See 2.5.4 and 2.5. at Chapter 2)

The Gauss-Krüger representation, after World War 2, was also called TRANSVERSE MERCATOR and it was utilised increasingly in many countries. For this reason, several constants and coefficients were adopted; for **N** (North co-ordinate) and **E** (East co-ordinate) are valid:

$$N = Y_0 + Ky$$

$$E = X_0 + Kx$$

and, consequently **(2.8)**

$$m = K\left(1 + \frac{x^2}{2R^2} + ...\right)$$

K is a coefficient (below 1) to reduce the linear deformation rate and allows the zone width extension (i.e. 300 km each side of central meridian), particularly for topographic charting in scales smaller than 1:100000 (1:200000 ...)

Y_0: is called FALSE NORTHING,
X_0: FALSE EASTING
K: SCALE FACTOR AT CENTRAL MERIDIAN

the application of **K** coefficient makes on the central meridian, it appear as a negative linear deformation, i.e. for K = 0.9998, the ellipsoidal distances contracts 20 cm/km and the isometric lines are transferred in two parallel lines to the described meridian image. This tangent surface is replaced by a secant elliptical cylinder.

For the U.S. world wide Universal Transverse Mercator Grid System (UTM) the following values are adopted:

K = 0.9996
Y_0 = 0 or 10000000 (for North or South Hemisphere respectively)
X_0= 500000 for each central meridian

and the zones are distributed at 6° longitude intervals, according to the following table

ZONE (Z)	CENTRAL MERIDIAN (LONGITUDE)	APPLICATION RANGE (LONGITUDE)
31	3°	0° to 6
32	9°	6° to 12°
.	.	.
.	.	.
.	.	.
50	117°	114° to 120°
.	.	.
.	.	.
.	.	.
60	177°	174° to 180°
1	183° (-177°)	180° to 186° (-174°)
.	.	.
.	.	.
.	.	.
20	297°(-63°)	294° (-66°)to 300° (-60°)
.	.	.
.	.	.
.	.	.
29	351° (-9°)	348° (-12°) to 354° (-6°)
30	357° (-3°)	354° (-6°) to 0°

The Zone number (Z) may be computed starting from the central meridian longitude with the following formulae:

$$Z = 30 + \frac{CM + 3}{6} \qquad \text{(East Hemisphere)}$$

$$Z = \frac{183 + CM}{6} \qquad \text{(West Hemisphere)}$$

in the second formula (West), the negative value of the longitude (of the central meridian) should be taken.

There are many software programs to solve the calculation of Transverse Mercator transformation, with the algorithms described in 3 and 4. of this Annex, or other alternative mode. However it is desirable to have good subject knowledge of the nature of the linear deformation rate.

In many cases it is suitable to select the general Transverse Mercator scheme adopted for the country representation but in particular cases there are chances to select the better plane representation procedure. For this purpose, it is important to remember that the Transverse Mercator representation is particularly suitable for application in a North - South strip, where the West - East width is less than 400 km (200 km to each side of the central meridian).

After the selection of the central meridian, taking into account the reduction of any distance for the selected area to this line, there is still the possibility of choosing a **K** coefficient (see formulas 2.8) for a better linear deformation rates distribution in the whole representation domain.

For topographic purposes, included coastal delineation, aids to navigation positioning, inshore feature descriptions and special harbour surveys, a linear deformation rate under 0.2m/km is better; this is '**m**' values between 0.9998 and 1.0002.

_____

CHAPTER 6 - ANNEX B
(COMMERCIAL EQUIPMENT EXAMPLES)

1. INTRODUCTION

In this Annex, is list of addresses, telephone numbers and web sites of some of the providers of equipment used in topographic and remote imagery surveying. However the analysis of commercial booklets or web pages is the recommended way of keeping abreast of the available technology, price information and future product launches.

In ground survey systems, there is a wide diversity of total stations (a combination of theodolite, distance measurement, data storage and computing) available, also of self aligning levels with digital reading of bar coded stadia and processing software. In photogrammetric data acquisition equipment there is a wide choice of cameras, both analogue, digital and including GNSS positioning, films, scanners, stereoplotters, image stations and specific software for digital processing and orthophoto elaboration. The Geospatial media gives a lot of possibility for product elaboration and access to images and image products through WEB servers.

2. ADDRESSES AND WEB PAGES

Below is a list set of companies or institutions that provide equipment, products and services related to the subjects covered in the CHAPTER 6, it is by no means exhaustive and it is hoped that in future versions of this manual a more comprehensive directory may be created.

INSTITUTION NAME	EQUIPMENT, PRODUCTS OR SERVICES	ADDRESS/COUNTRY	WEB SITE or E-MAIL
AGFA GEVAERT	Photogrammetric Films	B-2640 Mortsel BELGIUM	www.agfa.com
ANEBA, Geoinformatica	Topographic software (CARTOMAP)	Nicaragua 48. 2°, 6° 08029 - Barcelona SPAIN	www.aneba.com
ASAHI PRECISION	Theodolites, Levels, Total Stations (Pentax)	2-5-2 Higashi Oizumi Nerima-ku, Tokyo JAPAN	www.pentax.co.jp
CLARK LABS	Cartographic Software, GIS (IDRISI)	Clark University 950 Main Street Worcester, MA 01610-1477 USA	http://www.clarklabs.org
EARTH RESOURCE MAPPING (ERMAPPER)	imagery products and software for GIS database	4370 La Jolla Village Drive suite 900 San Diego CA USA	www.ermapper.com www.earthetc.com
ERDAS	Images Processing software	USA	www.esdas.com
ESRI	GIS (ArcInfo, ArcView)	USA	www.esri.com info@esri.com

INSTITUTION NAME	EQUIPMENT, PRODUCTS OR SERVICES	ADDRESS/COUNTRY	WEB SITE or E-MAIL
EURIMAGE	Imagery Products	Viale e. D'Onofrio 212, 00155 Rome, Italy	
GARMIN Int.	GPS Navigators	1200E 151 st., Street Olathe, KS 66062 – USA	www.garmin.com
GEOMATECH	Geomatics, GIS and cartography services and assistance	2, rue Philippe Lebon, BP 102, 44612, Saint Nazaire, FRANCE	geomatech@wanadoo.fr
GODDARD SPACE FLIGHT CENTER	Remote Sensing Assistance	USA	http://www.gsfc.nasa-gov
Hewlett-Packard	Hardware	USA	www.hp.com
Institute Cartografic de Catalunya	Cartographic, geomatics, photogrammetric and remote sensing services	Parc de Montjuic s/n, 08038 Barcelona, España	www.icc.es
INTERGRAPH CORPORATION	Soft/Hardware and images for Cartographic processing	P.O. Box 6695 Mailstop MD IW17A2 Huntsville Al 35894-6695 USA	http://imgs.intergraph.com www.intergraph.com
ISM Europe S.A.	Photogrammetric software and hardware, and services.	Passeig de Fabra i Piug 46, 08030, Barcelona, ESPAÑA	sales@ismeurope.com www.ismeurope.com
ITC	Photogrammetric and Cartographic assistance	Hengelostraat 99 P.O BOX 6 THE NETHERLANDS	www.itc.nl ilwis@itc.nl
KODAK, GR-OUPE ALTA	Films for Photogrammetry GIS, Cartography, Remote processing	Hant Monts Inc 3645, Boulevard Sainte-Anne Beauport (Quebec) CANADA G1E3L1	www.kodak.com www.mb-gepair.com www.groupealta.com
LEICA GEOSISTEMS AC	Total Stations Levels, Theodolites, GNSS, Photogramm. Cameras, Stereo plotters, Scanners	CH.9425 Heerbrugg SWITZERLAND	www.leica-geosistems.com
MAPINFO	Software for Cartography, Photogrammetry and GIS	USA	www.mapinfo.com
MicroImage, Inc	Software, Image processing TNT MIPS software	11th. Floor, The Sharp Tower 206 south 13th street Lincoln. NE 68508-2010 USA	www.microimages.com
OMNISTAR, INC.	Worldwide (satellite based) DGPS Service	8200 Westglen Dr. 77063-Houston, TX USA	www.omnistar.com
PCI GEOMATICS	Software for cartography and GIS	50 west Wilmon Street, Richmond Hill, Ontario CANADA L4B1M5	www.pci.on.ca sales@pci.on.ca

INSTITUTION NAME	EQUIPMENT, PRODUCTS OR SERVICES	ADDRESS/COUNTRY	WEB SITE or E-MAIL
P.GEERDERS Consultancy	Marine and coastal remote sensing applications services	Kobaltpad 18, 3402 JL, Ijsselstein, THE NETHERLANDS	pgcons@wxs.nl plaza.wxs.nl/pgconsult/
RADARSAT International	Images and Image Products.	CANADA	www.rsi.ca
RESEARCH SYSTEMS	ENVI Software	USA	www.rsinc.com
SITEM S.L.	Photography and satellite image processing, Digital Elevation Models cartography	Aragó 141-143, 08015 Barcelona, ESPAÑA	www.sitem-consulting.com
SOKKIA CO.LTD.	Total Stations Level, Theodolites	20-28, ASAHICHO 3-C HOME, MACHIDA,TOKIO,194-0023 JAPAN	www.sokkia.co.jp
SPOT Image	Remote Sensing Images, Products, etc.	FRANCE	http://www.spotimage.com
THALES NAVIGATION	GNSS (ASHTECHMAGUELLAN)	471 El Camino Real Santa Clara, CA 950050 – USA	www.ashtech.com
TRIMBLE NAVIGATION	GNSS, Total Stations, Theodolites, Levels, geodetic and topo-cartographic software	645 North Mary Ave. Sunnyvale, CA 94088-3642 USA	www.trimble.com
XYZ Sistemas Industriales S.A.	Cartographic and data base handling for their use with Internet Mapper application	Av. Infantes 105, 39005 Santander, Cantabria. ESPAÑA	www.imapper.com
Z/I Imaging Corporation	Cameras, Scanners, Stereo-plotters, GIS	301 Chochran Road, Suite 9 Huntsville AL USA 35824	www.ziimaging.com